Electronic Supplementary Information (ESI)

Control of the Stepwise Self-Assembly Process of a pH-Responsive Amphiphilic 4-Aminoquinoline-Tetraphenylethene Conjugate

Yosuke Hisamatsu,*[a] Fangzhou Cheng,[b] Katsuhiro Yamamoto,[c] Hiroshi Takase,[d] Naoki Umezawa,[a] and Tsunehiko Higuchi*[a]

[a]Graduate School of Pharmaceutical Sciences, Nagoya City University, 3-1 Tanabe-dori, Mizuho-ku, Nagoya 467-8603, Japan. E-mail: hisamatsu@phar.nagoya-cu.ac.jp; higuchi@phar.nagoya-cu.ac.jp

[b]Faculty of Pharmaceutical Sciences, Nagoya City University, 3-1 Tanabe-dori, Mizuho-ku, Nagoya 467-8603, Japan.

[c]Graduate School of Engineering, Nagoya Institute of Technology, Gokiso-cho, Showa-ku, Nagoya 466-8555, Japan

[d]Graduate School of Medical Sciences, Nagoya City University, 1 Kawasumi, Mizuho-cho, Mizuho-ku, Nagoya 467-8601, Japan

*Corresponding authors: E-mail: hisamatsu@phar.nagoya-cu.ac.jp; higuchi@phar.nagoya-cu.ac.jp

Table of Contents

1. General Information

All reagents and solvents were of the highest commercial quality and were used without further purification, unless otherwise noted. Anhydrous *N,N*-dimethylformamide (DMF) and anhydrous THF were purchased from Kanto Chemical Co., Inc. 1-(3-Dimethylaminopropyl)-3-ethylcarbodiimide hydrochloride, tetraethylene glycol monomethyl ether, *N*-hydroxysuccinimide (NHS) and sodium hydride (60%, dispersion in liquid paraffin) were purchased from Tokyo Chemical Industry (TCI) Co., Ltd. *tert*-Butyl acrylate and diethyl ether (for spectrochemical analysis) were purchased from FUJIFILM Wako Pure Chemical Corporation. CF_3COOH (TFA) was purchased from Watanabe Chemical Industries, Ltd. Dichloromethane (CH_2Cl_2) was distilled from calcium hydride (CaH_2). The compounds **S4**[S1] and **S6**[S2] were prepared according to the reported literature procedures.

Thin-layer chromatography (TLC) was performed using silica gel TLC plates (Merck, silica gel 60 F_{254}), amino silica gel TLC plates (Fuji Silysia Chemical Ltd., Chromatorex TLC plates NH), or aluminum oxide TLC plates (Merck, aluminum oxide 60 F_{254}). Column chromatography was performed on silica gel (Fuji Silysia Chemical Ltd., Chromatorex BW-300), amino silica gel (Fuji Silysia Chemical Ltd., Chromatorex NH-DM1020), or aluminum oxide (Merck, aluminum oxide 90 standardized). Milli-Q water was obtained from a Merck Millipore Milli-Q Integral 15 system.

^{1}H NMR spectra (500 MHz) were recorded on a JEOL JNM-ECZ-500R spectrometer (JEOL Ltd., Tokyo, Japan). Chemical shifts (δ) were determined relative to an internal reference of tetramethylsilane in $CDCl_3$ and the solvent peak in CD_3OD. Abbreviations for multiplicity are as follows: s, singlet; d, doublet; t, triplet; q, quartet; quin, quintet; m, multiplet; br, broad. ^{13}C NMR spectra (125 MHz) were recorded on JEOL JNM-ECZ-500R or Varian VNMRS 500 spectrometers. Chemical shifts (δ) were

determined relative to the solvent peaks or an internal reference of tetramethylsilane. Infrared (IR) spectra were recorded on a JASCO FT/IR-680 Fourier-transform infrared spectrophotometer (JASCO Corporation, Tokyo, Japan). Electrospray ionization mass spectrometry (ESI-MS) was done with a JEOL JMS-T100LP4G (JEOL Ltd., Tokyo, Japan). UV-Vis spectra were recorded on a JASCO V-550 UV-Vis spectrophotometer (JASCO Corporation, Ltd., Tokyo, Japan) equipped with a temperature controller unit. The pH values were measured using a pH meter and a pH electrode (LAQUA F–72 and 9618S–10D, Horiba, Kyoto, Japan). Fluorescence emission spectra were recorded on JASCO FP-8500 spectrofluorometer (JASCO Corporation, Ltd., Tokyo, Japan) (excitation bandwidth: 5 nm, emission bandwidth: 5 nm) equipped with a temperature controller unit. Quartz cuvettes (path length: 10 mm) were used for the measurements of UV-Vis and fluorescence spectra. DMSO (for spectrochemical analysis, FUJIFILM Wako Pure Chemical Corporation), MeOH (HPLC grade, FUJIFILM Wako Pure Chemical Corporation) and Milli-Q water were used for the measurements. The Good's buffer reagents were obtained from commercial sources: MES (2-morpholinoethanesulfonic acid) (TCI), HEPES (2-[4-(2-hydroxyethyl)-1-piperazinyl]ethanesulfonic acid) (Nacalai tesque), CHES (2-(cyclohexylamino)ethanesulfonic acid (Dojindo Laboratories), CAPS (*N*-cyclohexyl-3-aminopropanesulfonic acid) (TCI).

2. Synthesis

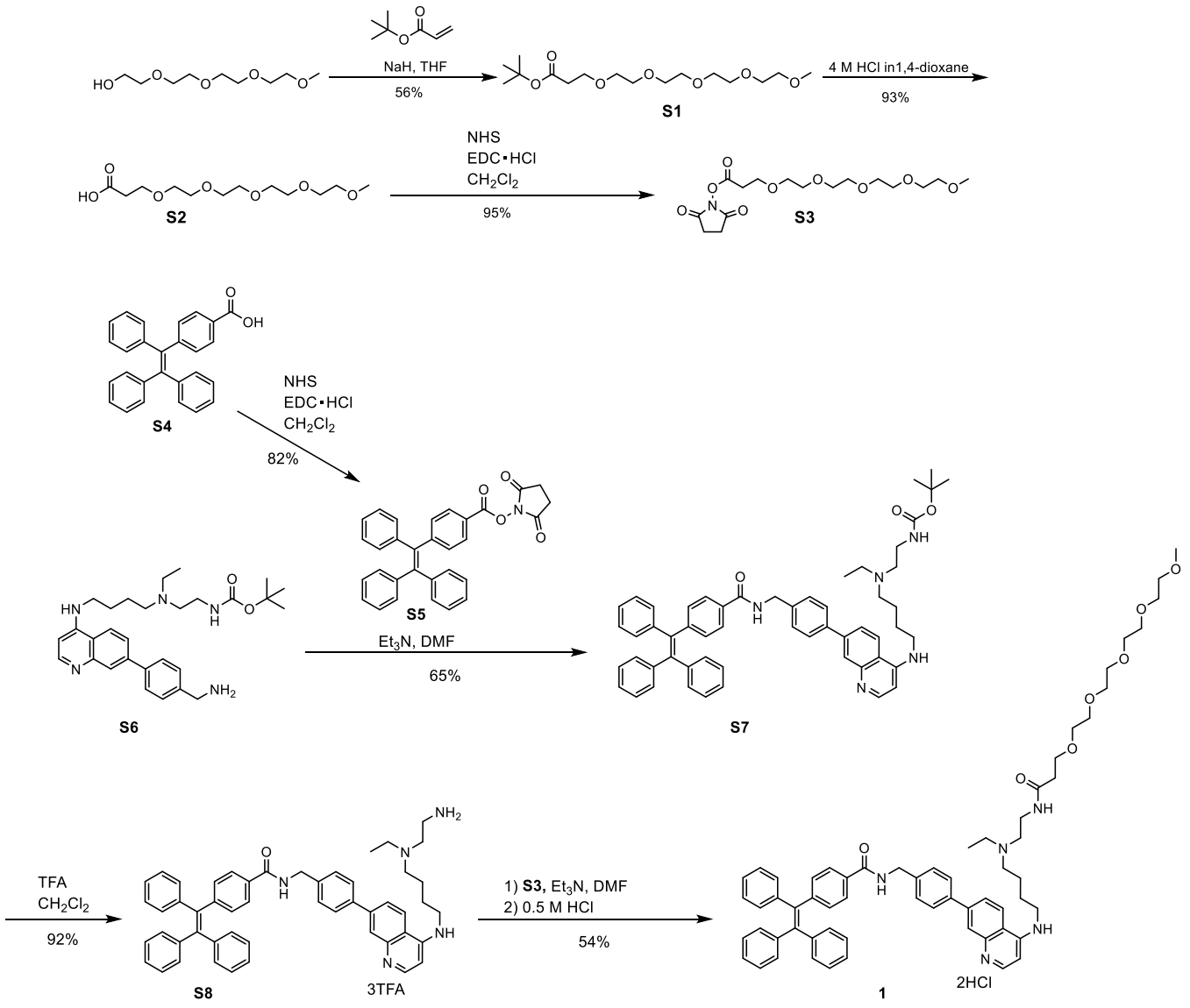

Scheme S1. Synthesis of compound **1**.

Synthesis of *tert*-butyl 3-[2-[2-[2-(2-methoxyethoxy)ethoxy]ethoxy]ethoxy]propanoate (S1)

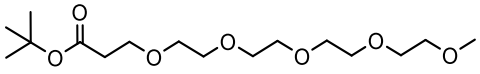

To a solution of tetraethylene glycol monomethyl ether (2.09 g, 10.0 mmol) in THF (20 mL), sodium hydride (60%, dispersion in liquid paraffin) (0.020 g, 0.50 mmol) and *tert*-butyl acrylate (1.54 g, 12.0

mmol) were added. The mixture was stirred for 4 h at 50 °C under an Ar atmosphere. After removing the solvent, the resulting crude was purified on a silica gel column chromatography (ethyl acetate) to give **S1** (1.90 g, 56%) as a colorless liquid. ^{1}H NMR (500 MHz, $CDCl_3$): δ 3.71 (t, J = 6.8 Hz, 2H), 3.67-3.60 (m, 14H), 3.56-3.54 (m, 2H), 3.38 (s, 3H) 2.50 (t, J = 6.6 Hz, 2H), 1.45 (s, 9H). ^{13}C NMR (125 MHz, $CDCl_3$): δ 170.92, 80.51, 71.95, 70.60, 70.52, 70.51, 70.38, 66.90, 59.05, 36.27, 28.10. IR (neat): cm^{-1} 2976, 2875, 1731. HRMS (ESI) *m/z* Calcd for $C_{16}H_{32}O_7Na$ $[M+Na]^+$: 359.2046 Found: 359.2073.

Synthesis of 3-[2-[2-[2-(2-methoxyethoxy)ethoxy]ethoxy]ethoxy]propanoic acid (S2)

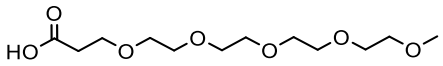

A solution of **S1** (1.40 g, 4.18 mmol) in 4 M HCl in dioxane (9.4 mL, 38 mmol) was stirred at room temperature. After stirring for 1.5 h, 4 M HCl in dioxane (4 mL, 16 mmol) was added to the solution again followed by stirring at room temperature for an additional 1 h under an Ar atmosphere. After removal of the solvent under reduced pressure, **S2** (1.08 g, 93%) was obtained as a colorless oil. ^{1}H NMR (500 MHz, $CDCl_3$): δ 3.78 (t, J = 6.0 Hz, 2H), 3.71-3.63 (m, 14H), 3.58-3.56 (m, 2H), 3.39 (s, 3H), 2.62 (t, J = 6.0 Hz, 2H). ^{1}H NMR data are in agreement with previously reported data.[S3]

Synthesis of compound S3

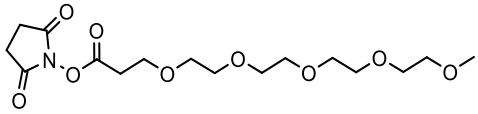

A mixture of **S2** (0.102 g, 0.362 mmol), *N*-hydroxysuccinimide (0.050 g, 0.44 mmol), 1-(3-dimethylaminopropyl)-3-ethylcarbodiimide hydrochloride (EDC·HCl) (0.104 g, 0.543 mmol) in dist. CH_2Cl_2 (2 mL) was stirred for 3 h at room temperature under an Ar atmosphere. After removing the solvent under reduced pressure, the crude material was dissolved in CH_2Cl_2 (15 mL) and washed with sat. NH_4Cl (15 mL) and water (15 mL). The organic layer was dried over Na_2SO_4 and then evaporated under reduced pressure to give **S3** as a pale yellow oil (0.130 g, 95%). ^{1}H NMR (500 MHz, $CDCl_3$): δ 3.85 (t, J

= 6.5 Hz, 2H), 3.66-3.63 (m, 14H), 3.56-3.54 (m, 2H), 3.38 (s, 3H), 2.90 (t, *J* = 6.5 Hz, 2H), 2.84 (br s, 4H), ^{13}C NMR (125 MHz, $CDCl_3$): δ 169.01, 166.74, 71.92, 70.70, 70.61, 70.59, 70.56, 70.54, 70.49, 65.71, 59.02, 32.13, 25.57. HRMS (ESI) *m/z* Calcd for $C_{16}H_{27}NO_9Na$ $[M+Na]^+$: 400.1584; Found: 400.1588.

Synthesis of compound S5

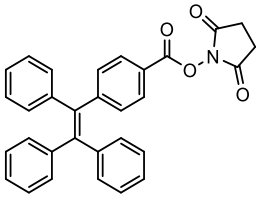

A mixture of 4-(1,2,2-triphenylvinyl)benzoic acid **S4**[S1] (0.309 g, 0.820 mmol), *N*-hydroxysuccinimide (0.142 g, 1.23 mmol), 1-(3-dimethylaminopropyl)-3-ethylcarbodiimide hydrochloride (EDC·HCl) (0.236 g, 1.23 mmol) in dist. CH_2Cl_2 (8 mL) was stirred for 6 h at room temperature under an Ar atmosphere. After removing the solvent under reduced pressure, the crude material was dissolved in CH_2Cl_2 (40 mL) and washed with sat. NH_4Cl (40 mL) and water (80 mL). The organic layer was dried over Na_2SO_4 and then evaporated and dried under reduced pressure to give **S5** as a pale yellow powder (0.317 g, 82%). ^{1}H NMR (500 MHz, $CDCl_3$): δ 7.86 (d, *J* = 8.6 Hz, 2H), 7.17-7.11 (m, 11H), 7.03-6.97 (m, 6H), 2.88 (br s, *J* = 8.0 Hz, 4H). ^{13}C NMR (125 MHz, $CDCl_3$): δ 169.48, 161.78, 151.32, 143.40, 143.14, 142.93, 139.57, 131.93, 131.44, 131.40, 131.37, 130.21, 128.22, 128.09, 127.89, 127.35, 127.07, 127.05, 122.65, 25.81. IR (neat): cm^{-1} 3086, 3055, 3024, 1770, 1741.

Synthesis of compound S7

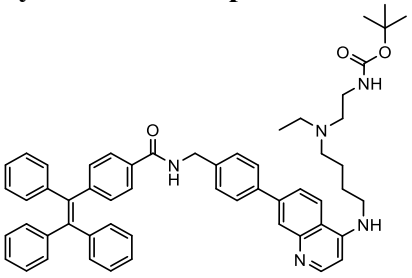

A mixture of **S5** (0.266 g, 0.562 mmol), **S6**[S2] (0.230 g, 0.468 mmol) and triethylamine (0.142 g, 1.40 mmol) in anhydrous DMF (5 mL) was stirred for 4 h at room temperature under an Ar atmosphere. After removing the solvent under reduced pressure, the resulting residue was purified by column chromatography using amino silica gel (*n*-hexane/$CHCl_3$ 1/1, $CHCl_3$) to give **S7** (0.256 g, 65%) as a colorless sticky solid. ^{1}H NMR (500 MHz, $CDCl_3$): δ 8.54 (d, *J* = 5.3 Hz, 1H), 8.16 (d, *J* = 1.8 Hz, 1H), 7.84 (br d, *J* = 8.4 Hz, 1H), 7.67 (d, *J* = 8.3 Hz, 2H), 7.63 (dd, *J* = 1.9, 8.7 Hz, 1H), 7.57 (d, *J* = 8.2 Hz, 2H), 7.42 (d, *J* = 8.2 Hz, 2H), 7.10-7.08 (m, 11H), 7.02-6.98 (m, 6H), 6.67 (br t, *J* = 5.4 Hz, 1H), 6.41 (d, *J* = 5.4 Hz, 1H), 5.36 (br s, 1H), 4.93 (br s, 1H), 4.65 (d, *J* = 5.7 Hz, 2H), 3.34 (q, *J* = 6.3 Hz, 2H), 3.20-3.18 (m, 2H), 2.57-2.49 (m, 6H), 1.80 (quin, *J* = 7.3 Hz, 2H), 1.62 (quin, *J* = 7.3 Hz, 2H), 1.42 (s, 9H), 1.02 (t, *J* = 7.1 Hz, 3H). ^{13}C NMR (125 MHz, $CDCl_3$): δ 167.22, 156.10, 151.43, 149.75, 148.65, 147.40, 143.28, 143.18, 143.15, 142.15, 141.09, 139.84, 139.53, 137.86, 131.99, 131.53, 131.26, 131.23, 128.51, 127.86, 127.78, 127.67, 127.62, 127.33, 126.79, 126.66, 126.48, 123.79, 120.20, 117.84, 98.77, 52.93, 52.61, 47.47, 43.73, 43.23, 38.27, 28.43, 26.77, 24.98, 11.57. IR (neat): cm^{-1} 3340, 2962, 2926, 1697, 1641, 1584, 1541. HRMS (ESI) *m/z* Calcd for $C_{56}H_{60}N_5O_3$ $[M+H]^+$: 850.4696; Found: 850.4698.

Synthesis of compound S8·3TFA

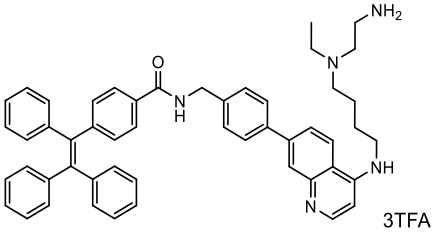

A solution of **S7** (0.233 g, 0.274 mmol) in CH_2Cl_2 (1 mL) and CF_3COOH (TFA) (0.5 mL) was stirred at room temperature for 1 h under an Ar atmosphere. After removing the solvent under reduced pressure, $CHCl_3$ was added and hexane was then added. The supernatant was decanted and the resulting product was dried under reduced pressure to give **S8** as a colorless solid (0.275 g, 92%, as 3TFA salt). ^{1}H NMR (500 MHz, CD_3OD): δ 8.45 (d, *J* = 9.2 Hz, 1H), 8.39 (d, *J* = 6.9 Hz, 1H), 8.01 (d, *J* = 1.7 Hz, 1H), 7.97

(dd, J = 1.7, 8.6 Hz, 1H), 7.76 (d, J = 8.6 Hz, 2H), 7.63 (d, J = 8.6 Hz, 2H), 7.51 (d, J = 8.6 Hz, 2H), 7.12-7.09 (m, 11H), 7.03-6.99 (m, 6H), 6.88 (d, J = 7.5 Hz, 1H), 4.62 (s, 2H), 3.68 (t, J = 6.6 Hz, 2H), 3.53-3.50 (m, 2H), 3.46-3.43 (m, 2H), 3.37-3.30 (m, 4H), 1.98-1.88 (m, 4H), 1.37 (t, J = 7.2 Hz, 3H). ^{13}C NMR (125 MHz, CD_3OD): δ 168.51, 160.82 (TFA), 156.16, 147.52, 145.90, 143.25, 143.20, 143.11, 142.34, 141.95, 140.33, 139.97, 138.40, 136.79, 131.85, 131.13, 130.90, 130.84, 127.98, 127.52, 127.37, 127.15, 126.49, 126.43, 126.39, 125.74, 123.17, 116.55, 116.36 (TFA), 97.82, 52.47, 48.63, 48.25, 42.69, 42.61, 33.69, 24.75, 21.11, 7.44. IR (neat): cm^{-1} 3445, 3335, 3039, 2927, 1675. HRMS (ESI) *m/z* Calcd for $C_{51}H_{52}N_5O$ $[M+H]^+$: 750.4172 Found: 750.4201.

Synthesis of compound 1·2HCl

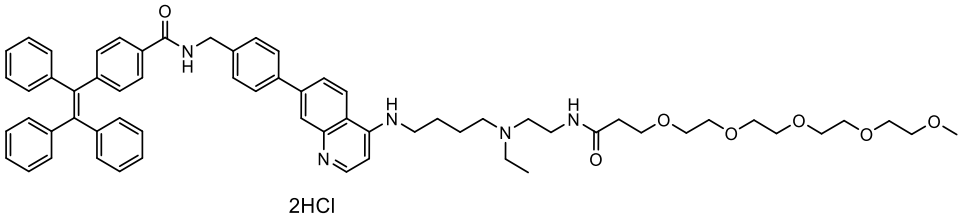

A mixture of **S3** (0.115 g, 0.305 mmol), **S8** (0.222 g, 0.203 mmol) and triethylamine (0.103 g, 1.02 mmol) in dehydrated DMF (2.5 mL) was stirred for 3 h at room temperature under an Ar atmosphere. After removing the solvent under reduced pressure, the resulting residue was purified by column chromatography using amino silica gel (hexane/$CHCl_3$ 2/3, 1/4, $CHCl_3$, $CHCl_3$/CH_3OH 50/1) to give **1** (free base) as a pale yellow amorphous solid. The obtained **1** was dissolved in methanol (2.5 mL), and 0.5 M HCl (20 mL) was then added. After lyophilization, product was dissolved in methanol (2 mL), and diethyl ether (25 mL) was then added. After centrifugation, the supernatant was decanted and the resulting product was dried under reduced pressure at 40 ºC to give **1** (0.118 g, 54% as 2HCl salt) as a colorless solid. ^{1}H NMR (500 MHz, CD_3OD): δ 8.49 (d, J = 9.2 Hz, 1H), 8.44 (d, J = 6.9 Hz, 1H), 8.04-8.02 (m, 2H), 7.79 (d, J = 8.6 Hz, 2H), 7.63 (d, J = 8.6 Hz, 2H), 7.53 (d, J = 8.0 Hz, 2H), 7.14-7.10 (m, 11H), 7.04-7.00 (m, 6H), 6.94 (d, J = 7.5 Hz, 1H), 4.62 (s, 2H), 3.71 (t, J = 6.0 Hz 4H), 3.60-3.57 (m, 14H), 3.51-

3.49 (m, 2H), 3.32-3.30 (m, 11H), 2.48 (t, J = 6.0 Hz, 2H), 1.95-1.90 (m, 4H), 1.36 (t, J = 7.2 Hz, 3H). ^{13}C NMR (125 MHz, CD_3OD): δ 174.55, 168.48, 156.14, 147.53, 146.01, 143.26, 143.20, 143.12, 142.35, 142.13, 140.45, 139.97, 138.50, 136.82, 131.83, 131.12, 130.91, 130.90, 130.84, 128.03, 127.52, 127.37, 127.18, 126.49, 126.40, 125.83, 123.33, 116.66, 115.88, 97.95, 71.50, 70.08, 70.05, 69.96, 69.88, 69.83, 66.46, 57.64, 52.69, 52.30, 48.56, 42.66, 42.61, 35.87, 34.81, 24.82, 21.35, 7.94. IR (neat): cm^{-1} 3430, 1636, 1614, 1549. HRMS (ESI) *m/z* Calcd for $C_{63}H_{74}N_5O_7$ $[M+H]^+$: 1012.5588; Found: 1012.5599.

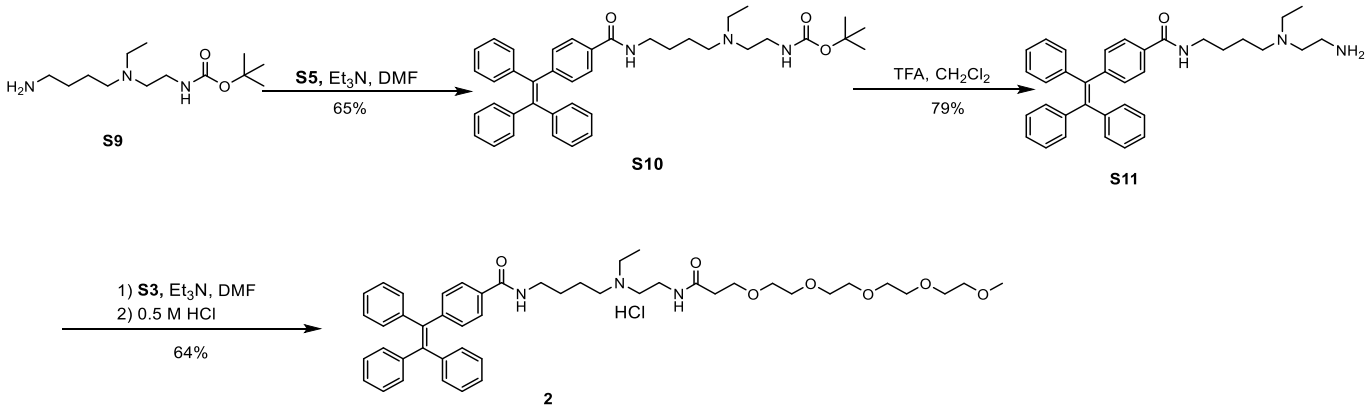

Scheme S2. Synthesis of compound **2**.

Synthesis of compound S10

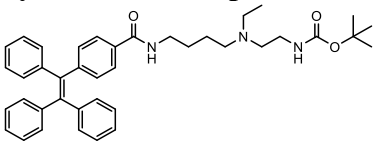

A mixture of **S9**[S2] (0.103 g, 0.395 mmol) and **S5** (0.206 g, 0.435 mmol), and triethylamine (0.200 g, 1.98 mmol) in anhydrous DMF (1 mL) was stirred for 3 h at room temperature under an Ar atmosphere. After removing the solvent under reduced pressure, the resulting residue was purified by column chromatography using silica gel (CH_2Cl_2/CH_3OH/Et_3N 200/2/1, 200/4/1 to 200/10/1) and aluminum oxide (CH_2Cl_2/Et_3N 200/1) to give **S10** (0.157 g, 65%) as a colorless amorphous solid. ^{1}H NMR (500 MHz, $CDCl_3$): δ 7.50 (d, J = 8.3 Hz, 2H), 7.11-7.08 (m, 11H), 7.03-6.98 (m, 6H), 6.30 (br s, 1H), 4.89 (br s, 1H), 3.42 (q, J = 6.6 Hz, 2H), 3.15 (d, J = 5.1 Hz, 2H), 2.51-2.43 (m, 6H) 1.60 (quin, J = 7.2 Hz, 2H),

1.50 (quin, J = 7.2 Hz, 2H), 1.43 (s, 9H), 0.98 (t, J = 7.1 Hz, 3H). ^{13}C NMR (125 MHz, $CDCl_3$): δ 167.37, 156.11, 147.11, 143.32, 143.25, 143.21, 142.06, 139.91, 132.50, 131.45, 131.28, 131.24, 127.85, 127.77, 127.69, 126.76, 126.66, 126.35, 79.07, 52.87, 52.53, 47.34, 39.88, 38.21, 28.44, 27.53, 24.67, 11.46. IR (neat): cm^{-1} 3332, 2972, 2934, 1699, 1639, 1542. HRMS (ESI) *m/z* Calcd for $C_{40}H_{48}N_3O_3$ $[M+H]^+$: 618.3696; Found: 618.3709.

Synthesis of compound S11

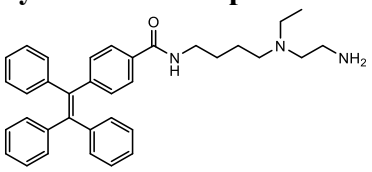

A solution of **S10** (0.123 g, 0.199 mmol) in CH_2Cl_2 (2 mL) and TFA (0.6 mL) was stirred at room temperature for 1 h under an Ar atmosphere. After removing the solvent under reduced pressure, the resulting residue was purified by column chromatography using amino silica gel (CH_2Cl_2, CH_2Cl_2/CH_3OH 100/1, 50/1, 30/1, 20/1) to give **S11** (0.0813 g, 79%) as a pale yellow amorphous solid. ^{1}H NMR (500 MHz, $CDCl_3$): δ 7.50 (d, J = 8.6 Hz, 2H), 7.11-7.07 (m, 11H), 7.03-6.98 (m, 6H), 6.48 (br t, J = 5.2 Hz, 1H), 3.42 (q, J = 6.5 Hz, 2H), 2.72 (t, J = 6.3 Hz, 2H), 2.50 (q, J = 7.3 Hz, 2H), 2.44 (q, J = 6.3 Hz, 4H), 1.62 (quin, J = 7.2 Hz, 2H), 1.55-1.51 (m, 2H), 0.99 (t, J = 7.2 Hz, 3H). ^{13}C NMR (125 MHz, CD_3OD): δ 167.44, 147.08, 143.33, 143.28, 143.22, 142.06, 139.94, 132.62, 131.44, 131.30, 131.25, 127.85, 127.78, 127.70, 126.75, 126.67, 126.36, 56.29, 53.23, 47.63, 39.95, 39.66, 27.53, 24.90, 11.59. IR (neat): cm^{-1} 3327, 2935, 1639. HRMS (ESI) *m/z* Calcd for $C_{35}H_{40}N_3O$ $[M+H]^+$: 518.3171 Found: 518.3184.

Synthesis of compound 2·HCl

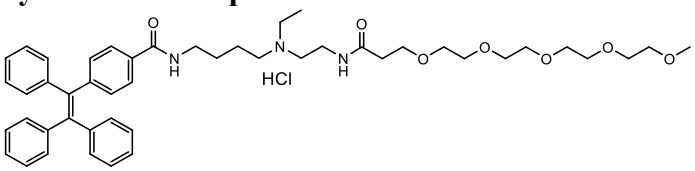

A mixture of compound **S3** (0.0787 g, 0.209 mmol), **S11** (0.0722 g, 0.139 mmol) and triethylamine (0.0706 g, 0.697 mmol) in anhydrous DMF (1.5 mL) was stirred for 14 h at room temperature under an Ar atmosphere. After removing the solvent under reduced pressure, the resulting residue was purified by column chromatography using amino silica gel (CH_2Cl_2/CH_3OH 200/1) to give **2** (free base) as a pale yellow amorphous solid. The obtained **2** was dissolved in methanol (1 mL), and 0.5 M HCl (20 mL) was then added. After lyophilization, the amorphous solid was dissolved in methanol (1 mL), and MilliQ water (20 mL) was then added. After lyophilization, **2** (0.0728 g, 64% as HCl salt) was obtained as a colorless sticky solid. ^{1}H NMR (500 MHz, CD_3OD): δ 7.59 (d, J = 8.6 Hz, 2H), 7.12-7.09 (m, 11H), 7.03-6.99 (m, 6H), 3.71 (t, J = 6.0 Hz, 2H), 3.64-3.55 (m, 16H), 3.53-3.51 (m, 2H), 3.42 (t, J = 6.6 Hz, 2H), 3.34 (s, 3H), 3.32-3.27 (m, 6H), 2.47 (t, J = 5.7 Hz, 2H), 1.77 (quin, J = 7.5 Hz, 2H), 1.68 (quin, J = 6.7 Hz, 2H), 1.33 (t, J = 7.2 Hz, 3H). ^{13}C NMR (125 MHz, CD_3OD): δ 174.65, 168.64, 147.44, 143.29, 143.16, 143.12, 142.34, 139.96, 131.92, 131.07, 130.91, 130.87, 130.82, 127.53, 127.37, 126.48, 126.41, 126.36, 71.53, 70.11, 70.08, 69.98, 69.90, 69.88, 66.46, 57.67, 52.77, 52.41, 48.39, 38.26, 35.89, 34.83, 26.22, 20.97, 7.86. IR (neat): cm^{-1} 3430, 1636, 1614. HRMS (ESI) *m/z* Calcd for $C_{47}H_{62}N_3O_7$ $[M+H]^+$: 780.4588; Found: 780.4565.

3. Measurements of UV-Vis absorption and fluorescence spectra

Stock solutions of **1** and **2** (2.0 mM) were prepared in DMSO (spectrophotometric grade) to avoid the possibility of pre-existing aggregates. The ^{1}H-NMR spectrum (DMSO-d_6) of **1** shows well-resolved sharp signals (Figure S41a). MES buffer (pH 5.0, 5.5, 6.0, 6.3, 6.5), HEPES buffer (pH 6.8, 7.1, 7.4, 7.8, 8.2), CHES buffer (pH 8.6, 9.5), and CAPS buffer (pH 10.4, 11.0) were used in this study. After mixing the sample solutions in 10 mM buffer containing NaCl (0 M or 0.10 M) and 0.5% (v/v) DMSO was carried out by gentle inversion (five times), UV-Vis absorption spectra measurements (scan speed: 1000 nm/min) were immediately performed at 25 ºC using quartz cuvettes (path length: 10 mm), and fluorescence measurements (scan speed: 1000 nm/min) were then performed at 25 ºC. In the fluorescence

measurements of the sample solutions in DMSO/water (HEPES buffer, pH 7.4) mixtures with varying water fraction, final concentrations of HEPES in the sample solutions were fixed at 10 mM.

Time-resolved UV-Vis absorption spectra were performed at 25 ºC. The sample solutions of **1** (50 μM) in 10 mM buffer (pH 5.5: MES, pH 7.4; HEPES) containing 0.10 M NaCl and 0.5% (v/v) MeOH were prepared from a stock solution of **1** (10 mM) in MeOH (HPLC grade) and the corresponding buffer. During the measurements, the sample solutions in the cuvettes were placed on UV-Vis spectrophotometer at 25 ºC or an incubator (i-CUBE FCI-280, AS-ONE, Japan) at 25 ºC.

When the UV-Vis absorption spectra of **1** at 0.40 mM were measured, a quartz cuvette with 1 mm path length was used. Sample solutions of **1** (0.40 mM) in 10 mM buffer containing 0.10 M NaCl and 0.5% (v/v) MeOH were prepared by measuring out the desired amount of **1**, adding MeOH (HPLC grade), and followed by the addition of 10 mM buffer containing 0.10 M NaCl.

4. Transmission electron microscopy (TEM) experiments

A stock solution of **1** (10 mM) was prepared in MeOH (HPLC grade). The ^{1}H-NMR spectrum of **1** (10 mM) in CD_3OD showed well-resolved sharp signals (Figure S41b). The buffers used in the TEM studies were filtered through a membrane filter (Millex LCR 0.45 μm, Merck Millipore Ltd., pore size: 0.45 μm) prior to use. Sample solutions of **1** (0.05 mM) in 10 mM buffer (pH 5.5: MES, pH 7.4; HEPES) containing NaCl (0 M or 0.10 M) and 0.5% (v/v) MeOH were prepared in glass vials and were then allowed to stand at room temperature (25±1 ºC) or at 25 ºC using aluminum block bath with cool thermo unit (CTU-mini, TAITEC, Japan). Sample solutions of **1** (0.4 mM or 0.5 mM) in 10 mM buffer containing 0.10 M NaCl and 0.5% (v/v) MeOH were prepared by measuring out the desired amount of **1**, adding MeOH (HPLC grade), followed by the addition of 10 mM buffer containing 0.10 M NaCl.

A hydrophilized carbon-coated copper grid was placed on the sample drop (10 μL) for ca. 5 s, and excess liquid was removed using a filter paper. The grid was placed on the drop of 2% phosphotungstic

acid (pH 7.0) for ca. 5 s, and excess liquid was removed using a filter paper. TEM observations were performed using JEM-1400Plus (JEOL, Tokyo, Japan) with an accelerating voltage of 100 kV.

Lengths of nanofibers were measured using the software ImageJ 1.53e (Wayne Rasband and contributors National Institutes of Health, USA). The histograms were prepared using KaleidaGraph version 4.5 (Synergy Software). The values of number-average length (L_n) and weight-average length (L_w) were calculated as follows:

$$L_n = \frac{\sum_{i=1}^{n} N_i L_i}{\sum_{i=1}^{n} N_i} \quad \text{(S1)}$$

$$L_w = \frac{\sum_{i=1}^{n} N_i L_i^2}{\sum_{i=1}^{n} N_i L_i} \quad \text{(S2)}$$

where N_i is the number of nanofibers of length L_i

The length distribution was characterized by the polydispersity index (PDI) according to:

$$PDI = \frac{L_w}{L_n} \quad \text{(S3)}$$

5. Dynamic light scattering (DLS) experiments

DLS measurements were carried out using the FDLS-3000 system (Otsuka Electronics Co., Ltd., Osaka, Japan), equipped with a solid-state laser (wavelength: 532 nm) at 25 ºC. The detection angle used was 90º. Stock solution of **1** (10 mM or 16 mM) in MeOH (HPLC grade) was prepared. HEPES buffer (10 mM, pH 7.4) was filtered through a membrane filter (Millex LG 0.20 μm, Merck Millipore Ltd., pore size: 0.20 μm) prior to use. The prepared sample solutions were filtered through a membrane filter (Millex LCR 0.45 μm, Merck Millipore Ltd., pore size: 0.45 μm) again. The filtered sample solutions in a

cylindrical glass cell (DL-20-12A, Otsuka Electronics Co., Ltd., Osaka, Japan) were allowed to age at 25 ºC. Hydrodynamic diameters were calculated by means of the NNLS method. The average hydrodynamic diameter was reported as the average of the peak average of three or four independent measurements ± standard deviation.

6. Small-angle X-ray scattering (SAXS) experiments

SAXS experiments were carried out at the BL10C station or the BL15A2 station at the Photon Factory of High Energy Accelerator Organization (KEK) in Japan. SAXS intensity, two-dimensional scattering intensity was obtained with a PILATUS 2M (DECTRIS) detector. Two-dimensional SAXS patterns were converted by circular averaging to get one-dimensional SAXS profiles $I(q)$. The magnitude of the scattering vector q is defined as $q = \frac{4\pi\sin\theta}{\lambda}$, where 2θ is the scattering angle, and λ is the wavelength of X-rays (0.1 nm). The distances from the sample to the detector for SAXS were 3,000 and 3,500 mm at the BL10C and the BL15A2, respectively. The X-ray transmittance of the sample was monitored with a photodiode located on the beam stopper. The sample solution was packed in a 2 mm diameter quartz capillary (Hilgenberg GmbH, Germany). The excess scattering intensity $I(q)$ of the solutes (buffer solution) was obtained by subtracting the background scattering from the raw SAXS profile with an appropriate correction for X-ray transmittance.

Sample solutions of **1** (0.5 mM) in 10 mM buffer containing 0.10 M NaCl and 0.5% (v/v) MeOH were prepared by measuring out the desired amount of **1**, addition of MeOH (HPLC grade), and then addition of 10 mM buffer containing 0.10 M NaCl. The sample solution of **1** (0.5 mM) in 10 mM MES buffer (pH 5.5, 0.10 M NaCl) containing 0.5% (v/v) MeOH was allowed to stand at room temperature (24±1 ºC) for about 2 h prior to the measurements. The sample of **1** was prepared (0.5 mM) in 10 mM HEPES buffer (pH 7.4, 0.10 M NaCl, 0.5% (v/v) MeOH were carried out by sonication for 30 s using ultrasonic water bath and then heating at 60 ºC for 5 min by water bath, followed by cooling down to room temperature for about 1.5 h. SAXS measurements were conducted at the BL10C station (exposure time: 300 s).

Time-resolved SAXS measurements was carried out at room temperature (24±1 ºC). Sample solutions of **1** (0.4 mM) in 10 mM buffer containing 0.10 M NaCl and 0.5% (v/v) MeOH were prepared by measuring out the desired amount of **1**, adding MeOH (HPLC grade), followed by the addition of 10 mM buffer containing 0.10 M NaCl. The sample solution of **1** in 10 mM HEPES buffer (pH 7.4, 0.10 M NaCl) containing 0.5% (v/v) MeOH was packed in a 2 mm diameter quartz capillary, and SAXS measurements were started each time at the BL10C station (exposure time for each measurement: 300 s). The sample solution of **1** in 10 mM MES buffer (pH 5.5, 0.10 M NaCl) containing 0.5% (v/v) MeOH was packed in a 2 mm diameter quartz capillary, and time-resolved SAXS measurements were performed at the BL15A2 station (exposure time for each measurement: 60 s).

Model Calculation

No appreciable concentration effect was observed in the scattering intensity at the experimental concentration. For q < 1 nm^{-1}, $I(q)$ follows the relation $I(q) \propto q^{-1}$, indicating the presence of a rod-like scattering object. To fit the data, we applied the following form factor for a solid cylinder (the length of the cylinder is long enough in the observed q-range) with the radius of R for simplicity:

$$I(q) \propto \frac{1}{q}\left[\frac{J_1(qR)}{qR}\right]^2$$

Here, J_1 is a Bessel function of the first kind.

In numerical analyses, the distribution function of a cross-sectional radius $W(R)$ was taken into account using Gaussian distribution

$$W(R) \sim \exp\left[-\frac{(R-\bar{R})^2}{2\sigma}\right]$$

where $\bar{R}$ and σ are the mean radius and a standard deviation of R from $\bar{R}$, respectively.

For the spherical model, the form factor is given by the following equation:

$$I(q) \propto \left[\frac{3\sin(qR) - qR\cos(qR)}{(qR)^3}\right]^2$$

Here, *R* is the radius of the spherical particle. The spherical core should have a finite distribution particle size assuming the Gaussian distribution (above equation).

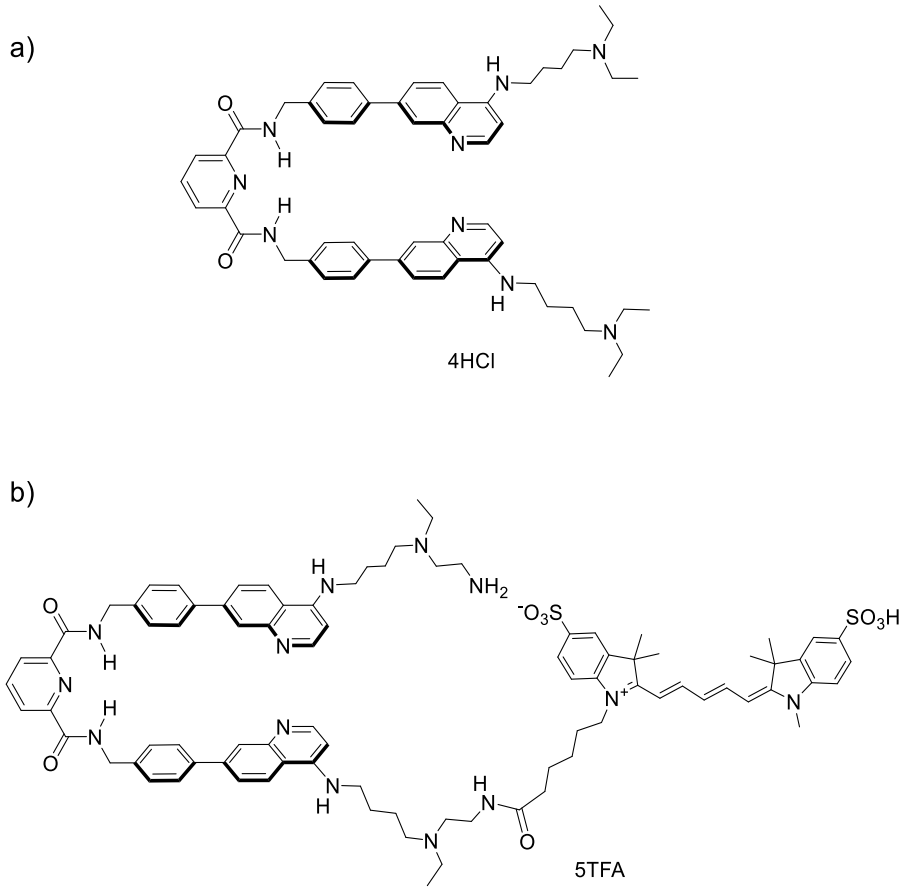

Figure S1. Structures of a) 4-aminoqinoline-based tweezer-type synthetic receptor for heme[S4] and b) synthetic receptor with sulfo-Cy5.[S2]

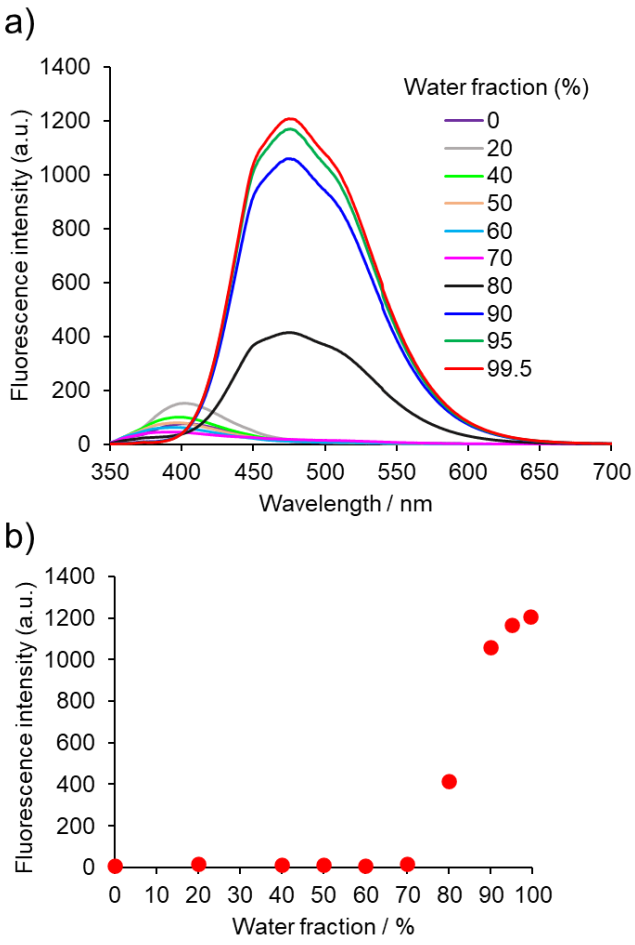

Figure S2. a) Fluorescence spectra of **1** (10 μM) in DMSO/water (HEPES buffer, pH 7.4) mixtures at 25 ºC. Ex. 330 nm. b) Fluorescence intensity of **1** at 474 nm in different fractions of water (v/v%).

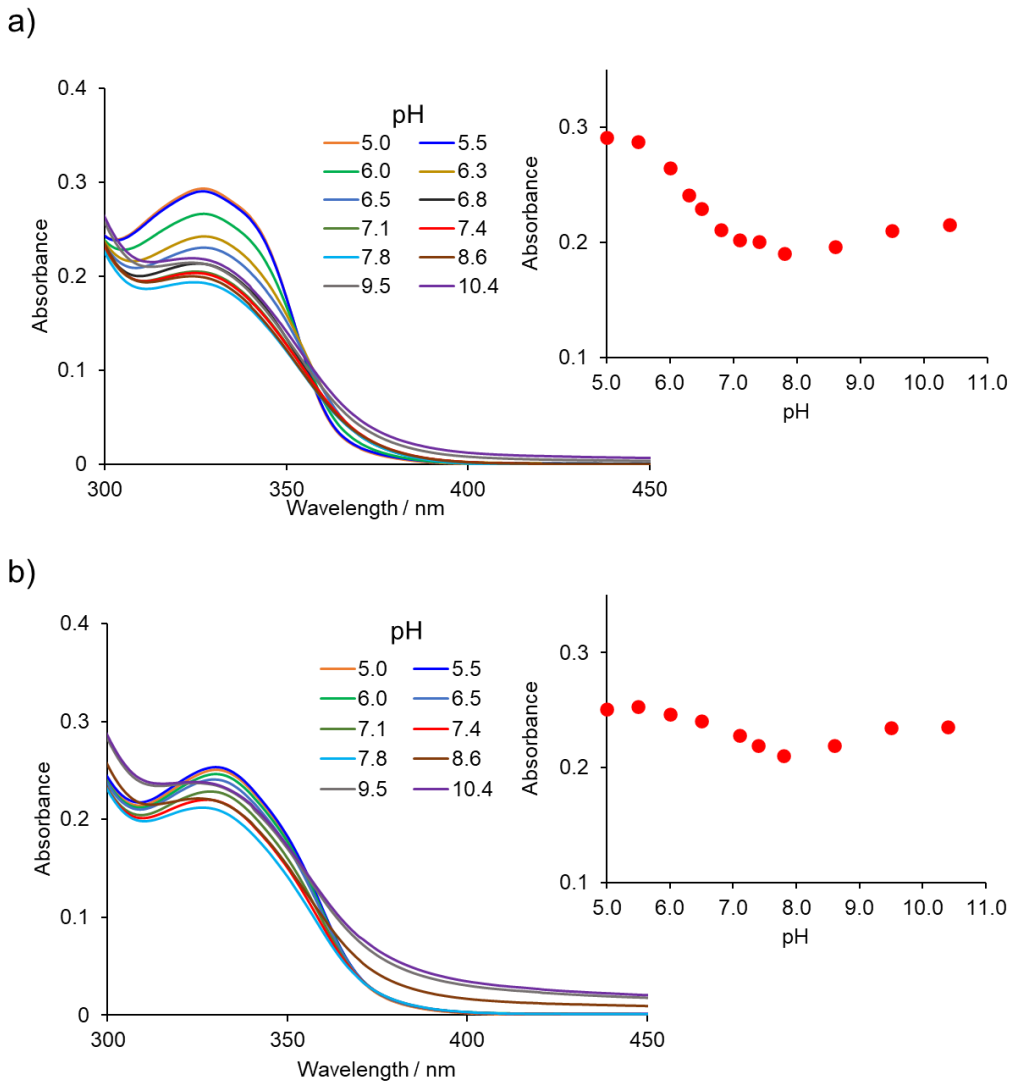

Figure S3. pH-Dependent change in UV-Vis absorption spectra of a) **1** and b) **1** in the presence of 0.10 M NaCl. Conditions: [**1**] = 10 μM, 10 mM Good's buffer (from pH 5.0 to 10.4) containing 0.5% (v/v) DMSO, 25 °C, Insets: plot of the pH-dependent change in absorbance of **1** at 330 nm.

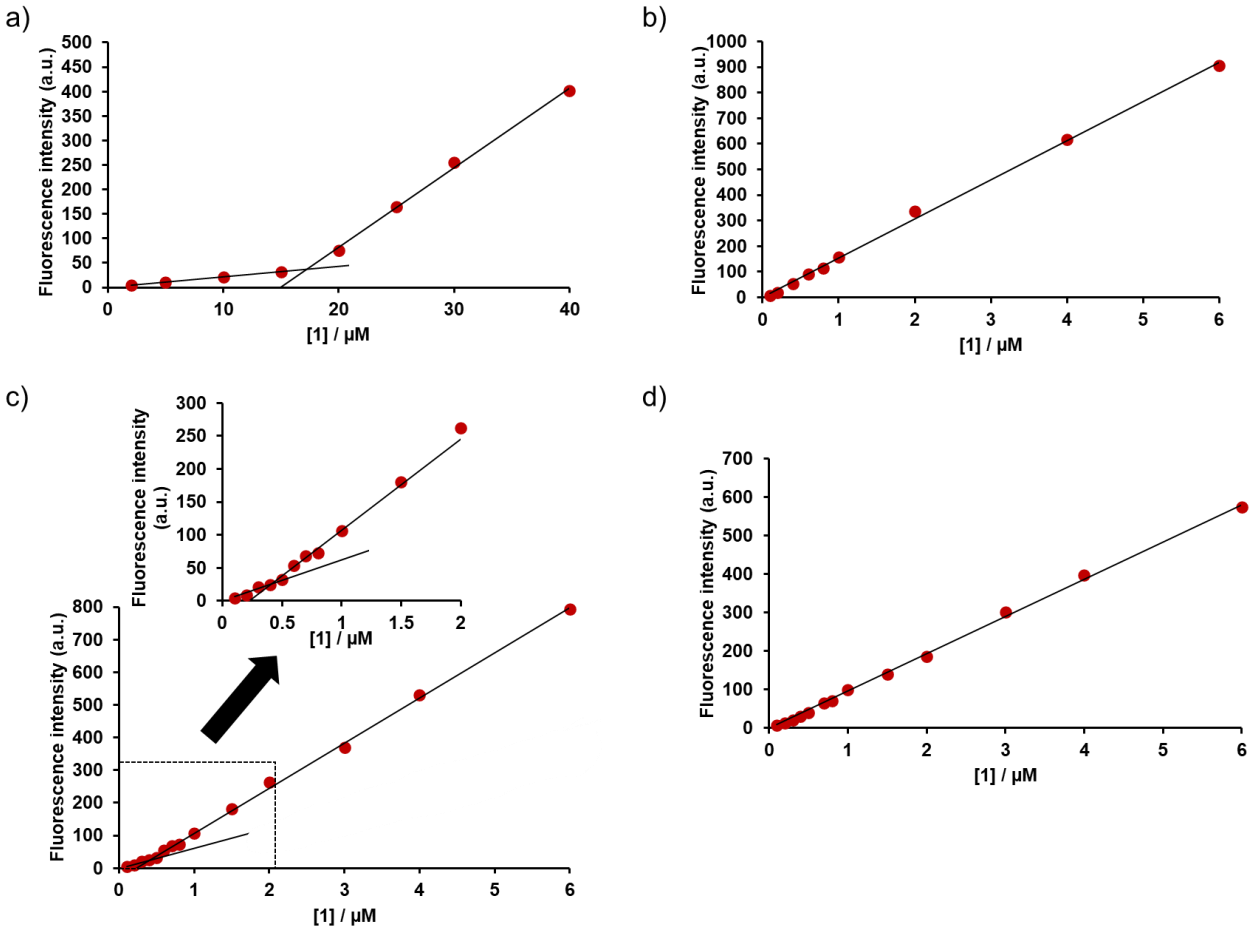

Figure S4. Determination of CAC values of **1**. Fluorescence intensity (474 nm) of **1** at different concentrations in 10 mM buffer containing 0.5% (v/v) DMSO at 25 ºC. a) MES buffer (pH 5.5), b) MES buffer (pH 5.5, 0.10 M NaCl), c) HEPES buffer (pH 7.4) and d) HEPES buffer (pH 7.4, 0.10 M NaCl). Ex. 330 nm.

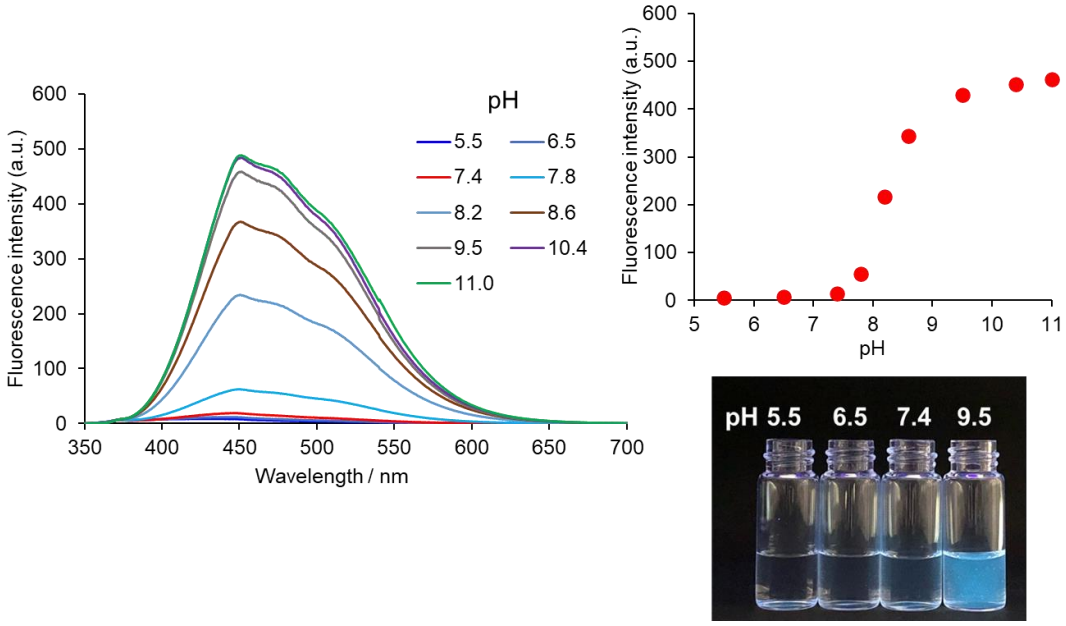

Figure S5. pH-Dependent change in fluorescence spectra of **2**. Inset: Plot of pH-dependent change in fluorescence intensity of **2** at 450 nm. Conditions: [**2**] = 10 μM, 10 mM Good's buffer (from pH 5.5 to 11) containing 0.5% (v/v) DMSO, 25 ºC, Ex. 330 nm. Photograph shows fluorescence emission of **2** at various pH. Ex. 365 nm.

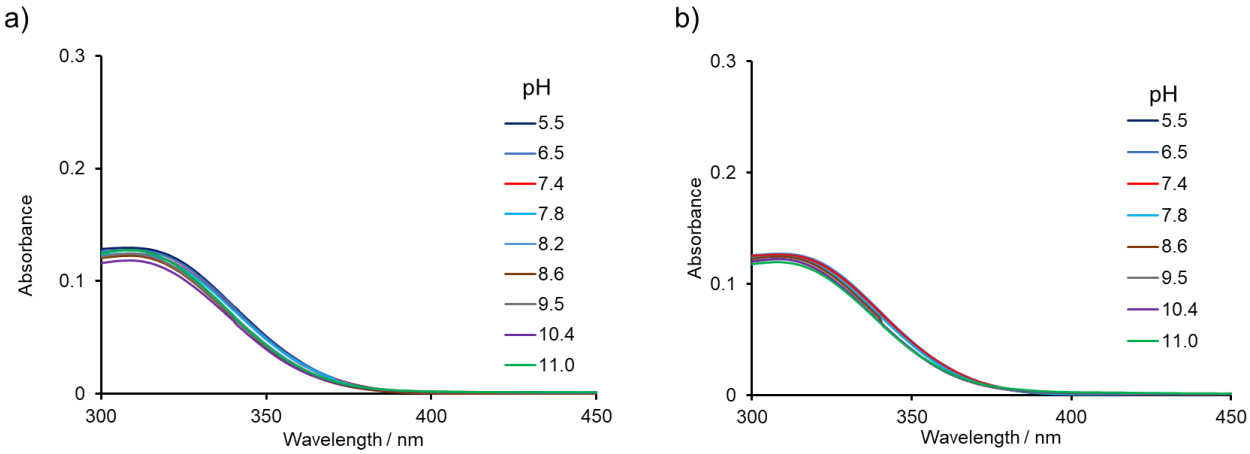

Figure S6. pH-Dependent change in UV-Vis absorption spectra of a) **2** and b) **2** in the presence of 0.10 M NaCl. Conditions: [**2**] = 10 μM, 10 mM Good's buffer (from pH 5.5 to 11.0) containing 0.5% (v/v) DMSO, 25 ºC.

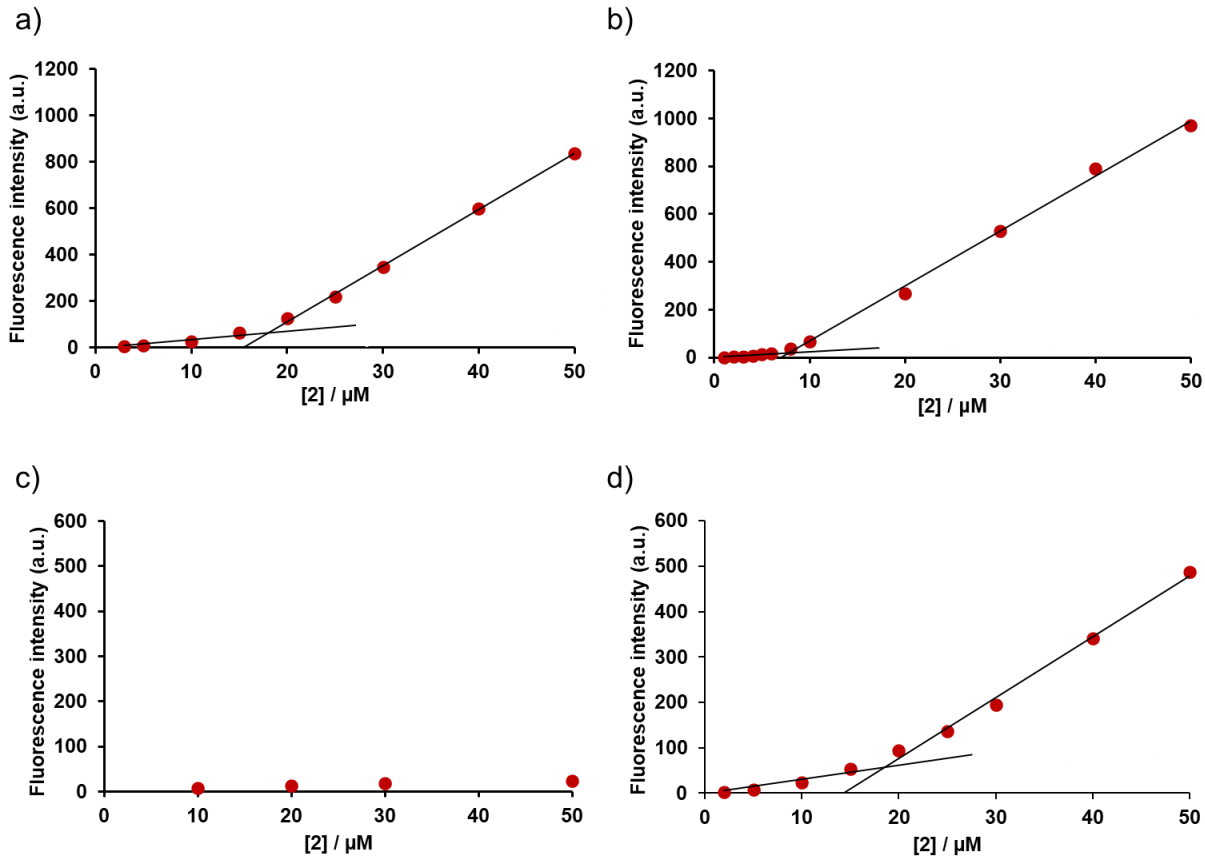

Figure S7. Determination of CAC values of **2**. Fluorescence intensity (450 nm) of **2** at different concentrations in 10 mM buffer containing 0.5% (v/v) DMSO at 25 ºC. a) HEPES buffer (pH 7.4), b) HEPES buffer (pH 7.4, 0.10 M NaCl), c) MES buffer (pH 5.5), and d) MES buffer (pH 5.5, 0.10 M NaCl). Ex. 330 nm.

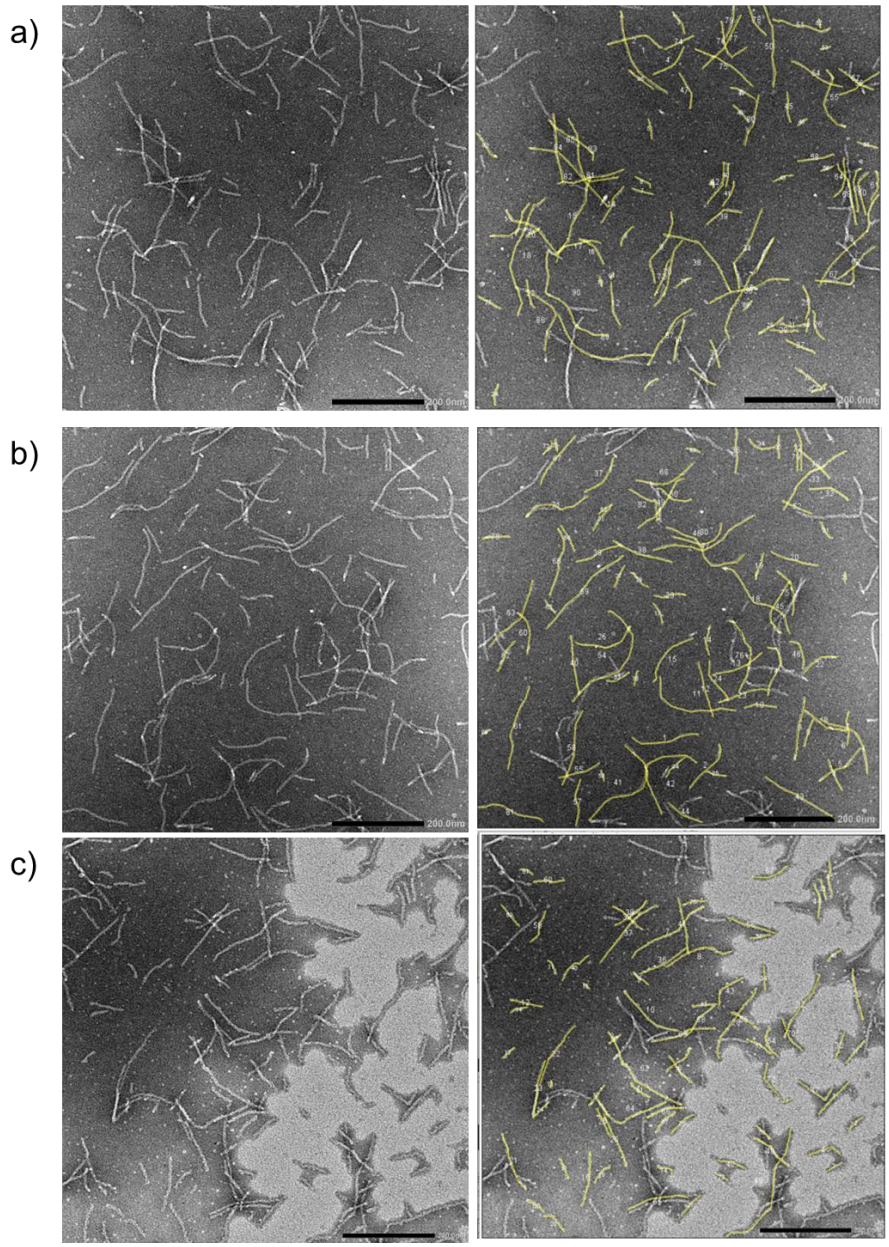

Figure S8. a)-c) Three representative TEM images (left) of **1** (0.05 mM) at pH 5.5 in the presence of 0.10 M NaCl after aging for 1 h at room temperature (25±1 °C), and the corresponding images were analyzed with the ImageJ software (right). Scale bars: 200 nm. d) The histogram of lengths was prepared using three TEM images (number of measured nanofibers: 254). Conditions: [**1**] = 0.05 mM, 10 mM MES buffer pH 5.5 containing 0.10 M NaCl and 0.5% (v/v) MeOH.

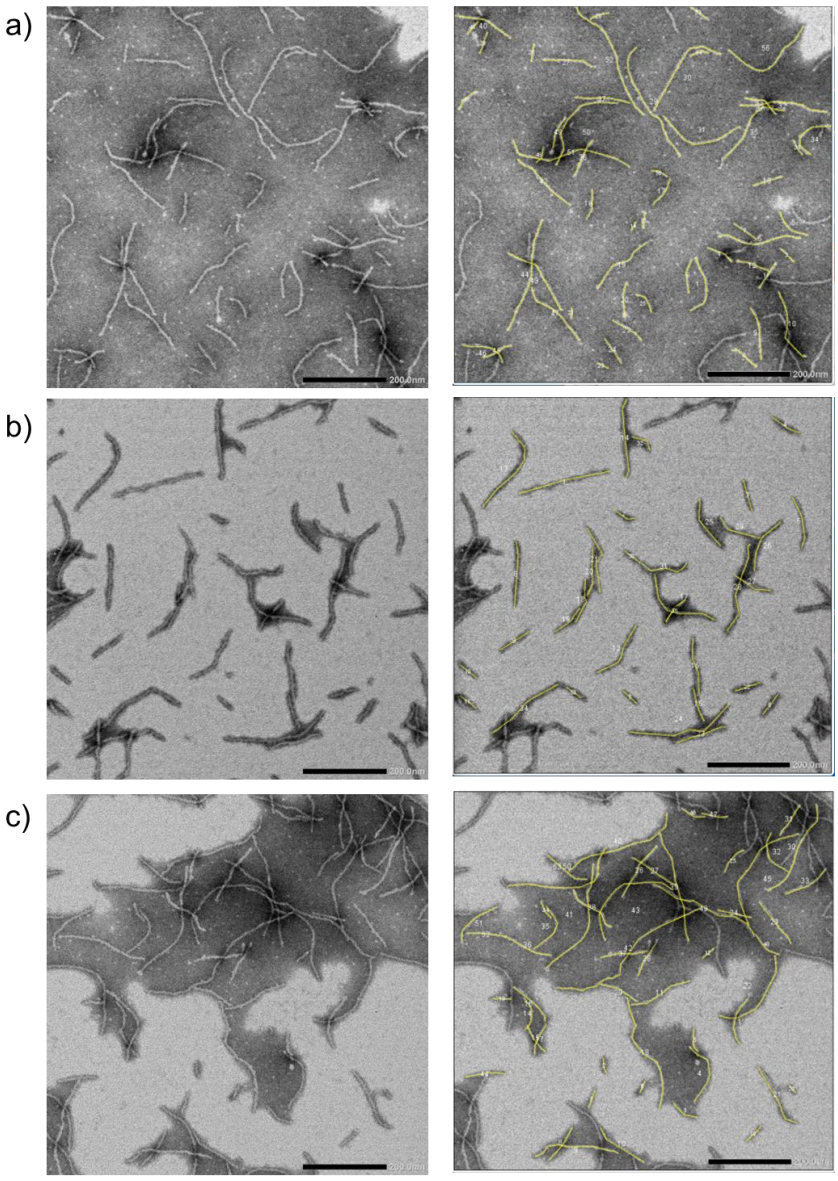

Figure S9. a)-c) Three representative TEM images (left) of **1** (0.05 mM) at pH 5.5 in the presence of 0.10 M NaCl after aging for 24 h at room temperature (25±1 ºC), and the corresponding images were analyzed with the ImageJ software (right). Scale bars: 200 nm. d) The histogram of lengths was prepared using five TEM images (number of measured nanofibers: 230). Conditions: [**1**] = 0.05 mM, 10 mM MES buffer pH 5.5 containing 0.10 M NaCl and 0.5% (v/v) MeOH.

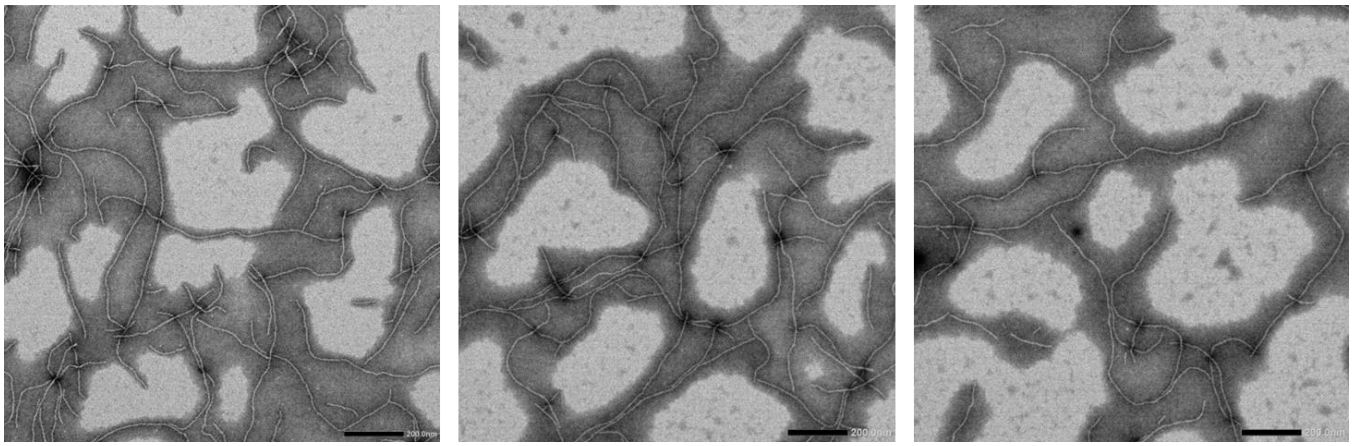

Figure S10. Representative negative stain TEM images of **1** at pH 5.5 in the presence of 0.10 M NaCl after aging for 7 days at room temperature (25±1 ºC) Conditions: [**1**] = 0.05 mM, 10 mM MES buffer pH 5.5 containing 0.10 M NaCl and 0.5% (v/v) MeOH. Scale bars: 200 nm.

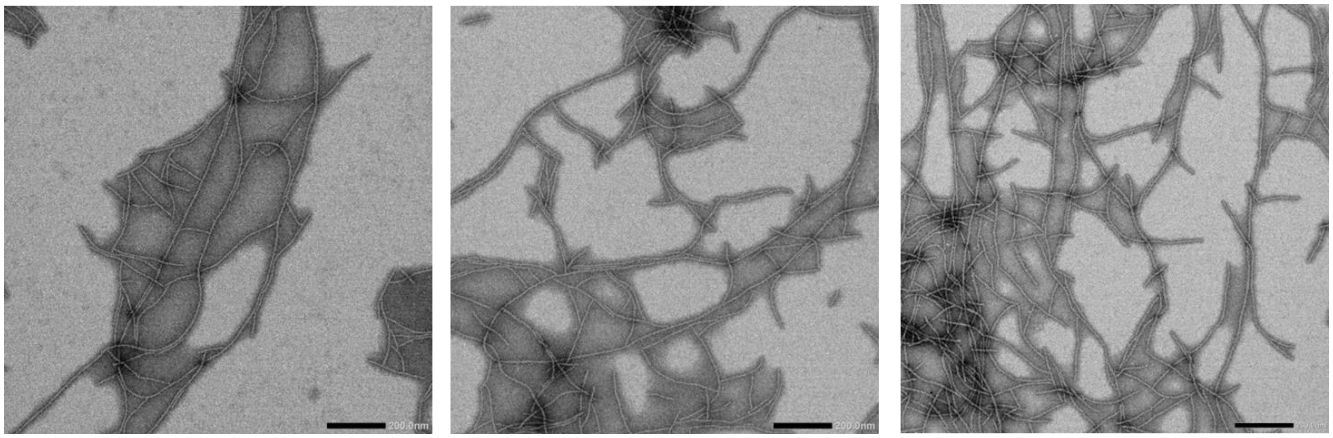

Figure S11. Representative negative stain TEM images of **1** at pH 5.5 in the presence of 0.10 M NaCl after heating at 80 ºC (CTU-Mini, TAITEC) for 30 min then cooling to room temperature. Conditions: [**1**] = 0.05 mM, 10 mM MES buffer pH 5.5 containing 0.10 M NaCl and 0.5% (v/v) MeOH. Scale bars: 200 nm.

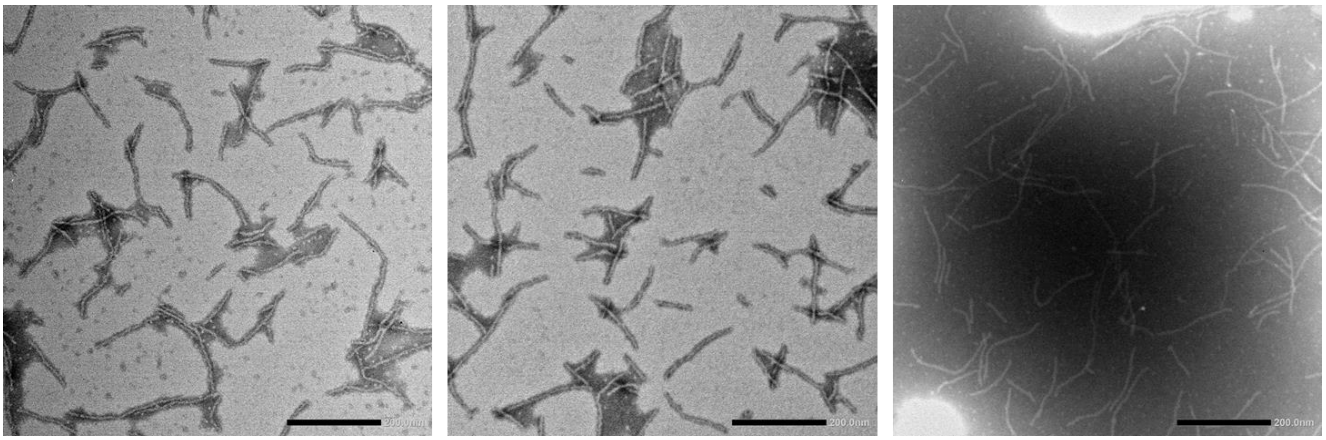

Figure S12. Representative negative stain TEM images of **1** at pH 5.5 in the presence of 0.10 M NaCl after heating at 60 ºC (water bath) for 5 min followed by cooling to room temperature for 1 h. Conditions: [**1**] = 0.05 mM, 10 mM MES buffer pH 5.5 containing 0.10 M NaCl and 0.5% (v/v) MeOH. Scale bars: 200 nm.

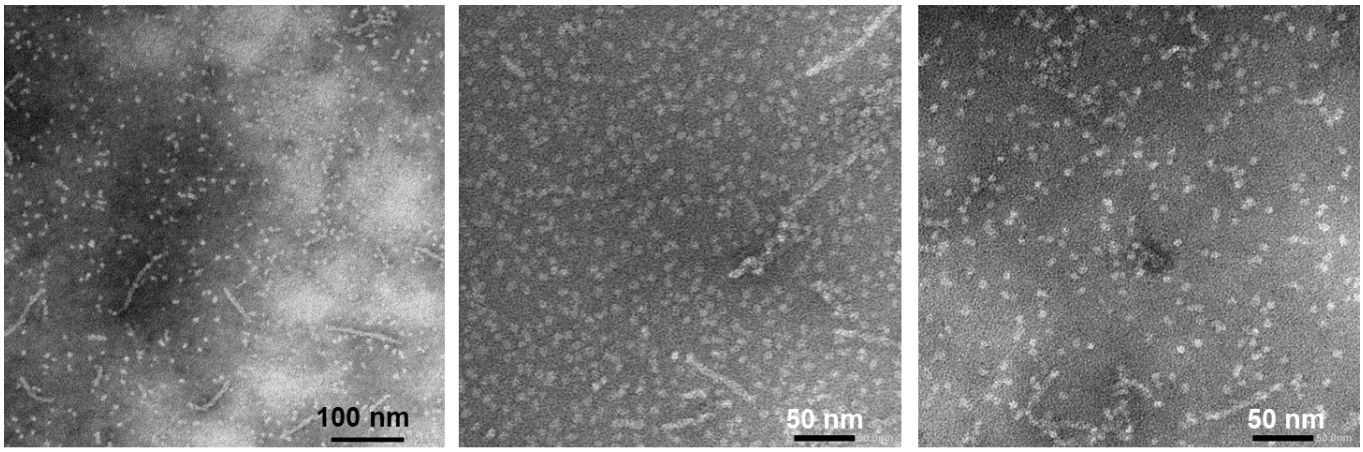

Figure S13. a) Representative negative stain TEM images of **1** at pH 5.5 in the presence of 0.10 M NaCl after aging for 2 min at room temperature (25±1 ºC). Conditions: [**1**] = 0.05 mM, 10 mM MES buffer (pH 5.5, 0.10 M NaCl) containing 0.5% (v/v) MeOH.

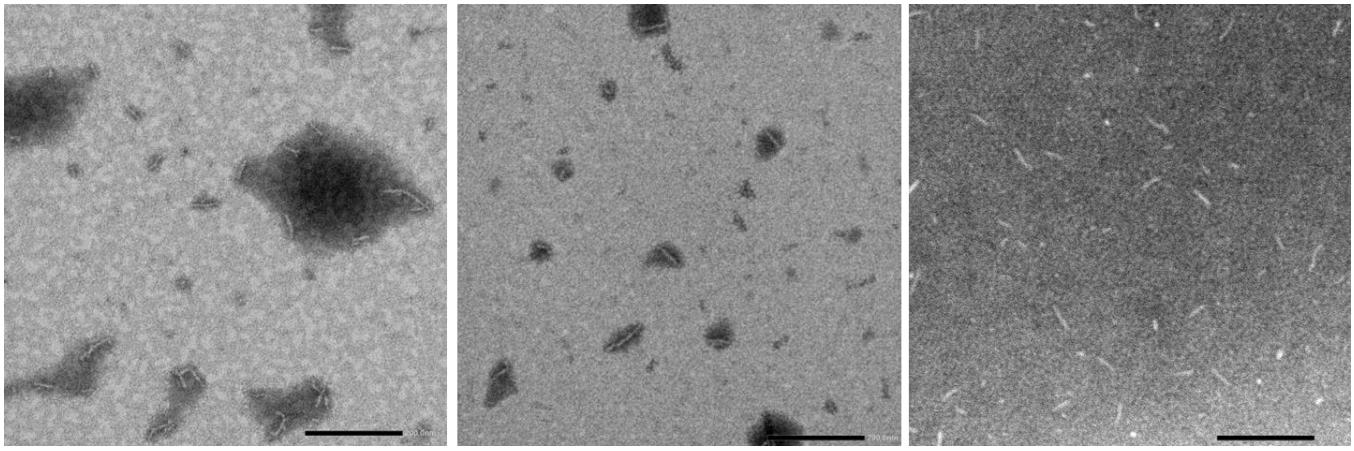

Figure S14. Representative three TEM images (left) of **1** (0.05 mM) at pH 5.5 after aging for 1 h at room temperature (25±1 ºC). Conditions: [**1**] = 0.05 mM, 10 mM MES buffer pH 5.5 containing 0.5% (v/v) MeOH. Scale bars: 200 nm. Short nanorod-like aggregates were observed after aging for 1 h, although the frequency on the grids was low probably due to the high CAC value.

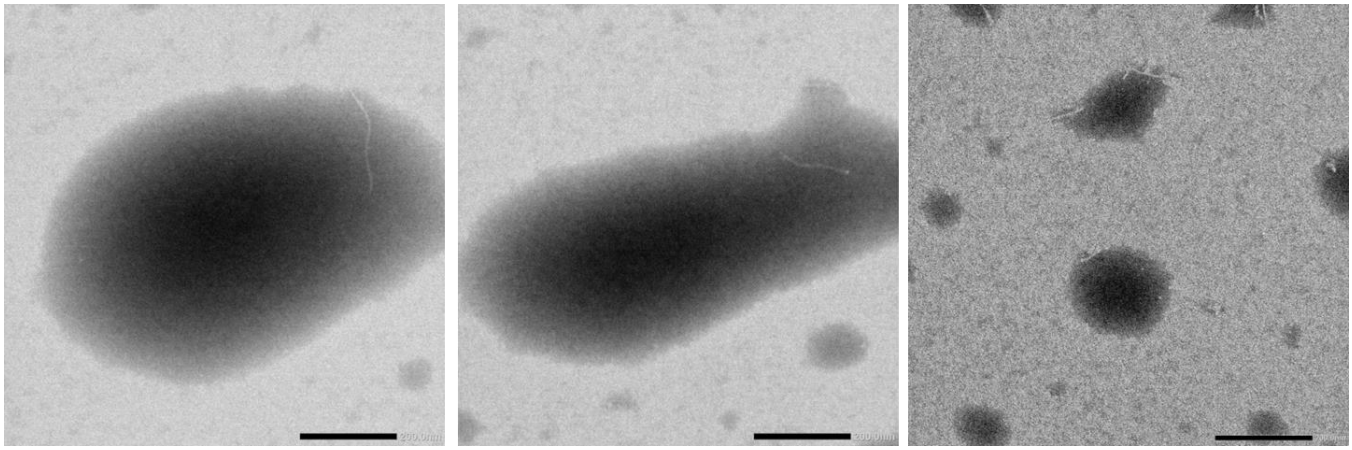

Figure S15. a) Representative negative stain TEM images of **2** at pH 5.5 in the presence of 0.10 M NaCl after aging for 1 h at room temperature (25±1 ºC). Conditions: [**2**] = 0.05 mM, 10 mM MES buffer (pH 5.5, 0.10 M NaCl) containing 0.5% (v/v) MeOH. Scale bars: 200 nm. Although it was not easy to find the nanostructures as the frequency of the objects on the TEM grids was very low, nanofiber-like aggregates may be formed after aging for 1 h.

a)

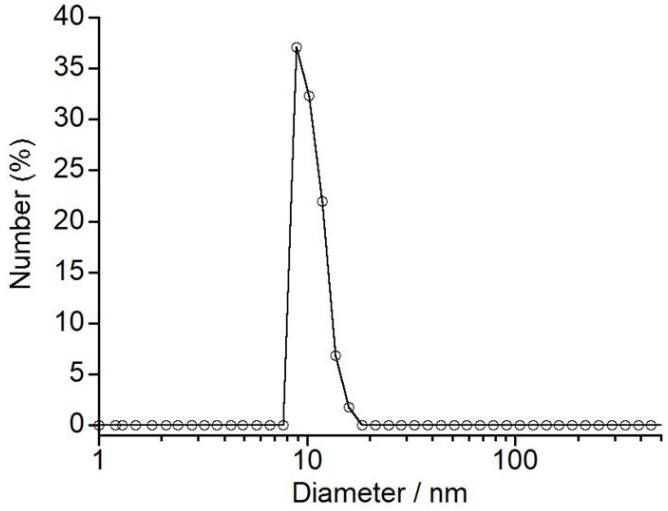

b)

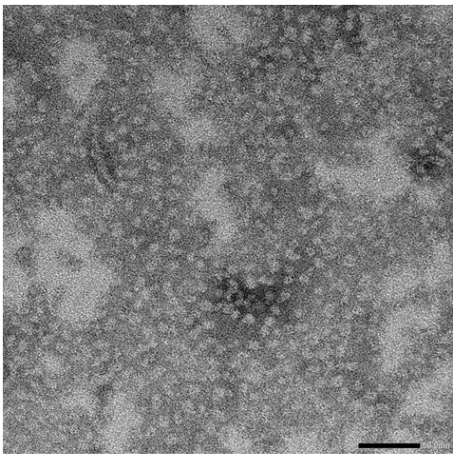

	Peak average (S.D.)
Exp. 1	10.8±1.8 nm
Exp. 2	10.4±1.6 nm
Exp. 3	8.6±1.3 nm
Exp. 4	7.7±0.9 nm

Average hydrodynamic diameter ± S.D. (Average of peak average ± S.D.)	9.4±1.5 nm

Figure S16. a) Representative size distribution of **1** in 10 mM HEPES buffer (pH 7.4, 0.10 M NaCl) after aging for 30 min at 25 ºC, measured by DLS. The average hydrodynamic diameter was determined by average of the peak average of four independent experiments. Conditions: [**1**] = 0.05 mM, 10 mM HEPES buffer pH 7.4 containing 0.10 M NaCl and 0.5% (v/v) MeOH. b) Representative negative stain TEM images of **1** (0.05 mM) in 10 mM HEPES buffer (pH 7.4, 0.10 M NaCl) after aging for 30 min at room temperature (25±1 ºC). Scale bar: 50 nm.

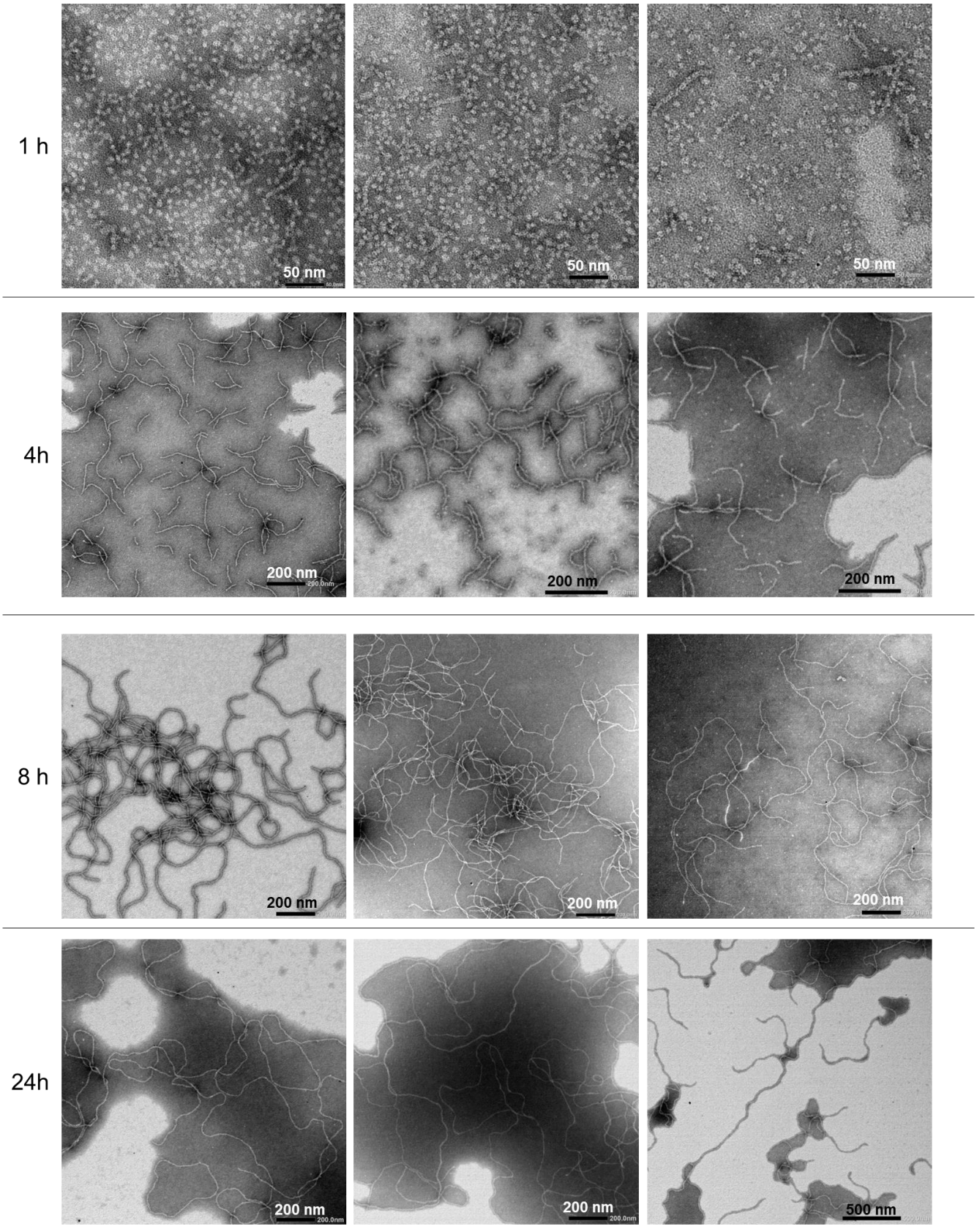
1 h
50 nm
50 nm
50 nm
4h
200 nm
200 nm
200 nm
8 h
200 nm
200 nm
200 nm
24h
200 nm
200 nm
500 nm

Figure S17. Representative negative stain TEM images of **1** at pH 7.4 in the presence of 0.10 M NaCl after aging for 1, 4, 8, 24 h at room temperature (25±1 ºC). Conditions: [**1**] = 0.05 mM, 10 mM HEPES buffer pH 7.4 containing 0.10 M NaCl and 0.5% (v/v) MeOH.

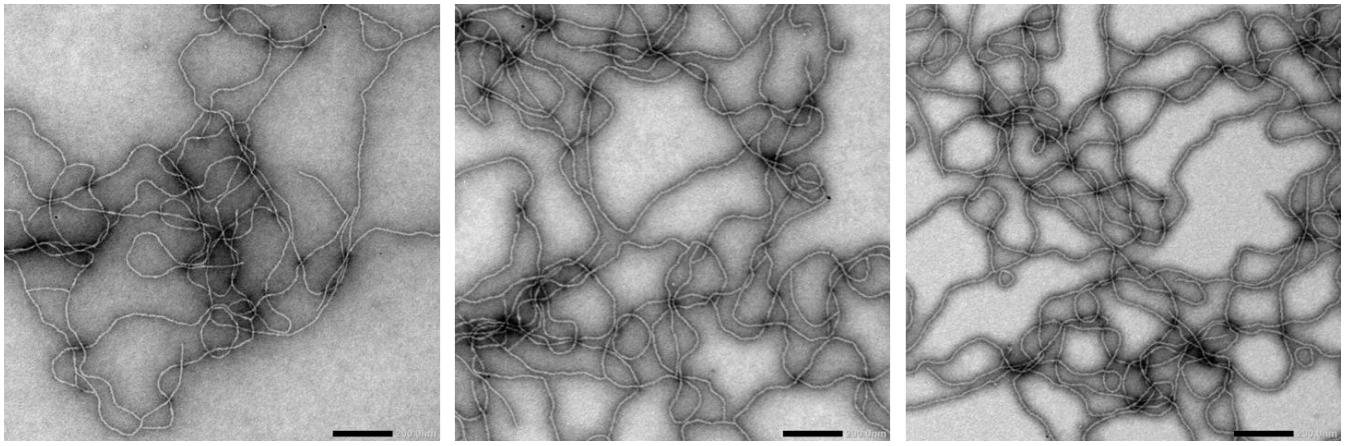

Figure S18. Representative negative stain TEM images of **1** at pH 7.4 in the presence of 0.10 M NaCl after heating at 60 ºC (water bath) for 5 min then cooling to room temperature for 1 h. Conditions: [**1**] = 0.05 mM, 10 mM HEPES buffer pH 7.4 containing 0.10 M NaCl and 0.5% (v/v) MeOH. Scale bars: 200 nm.

a) b)

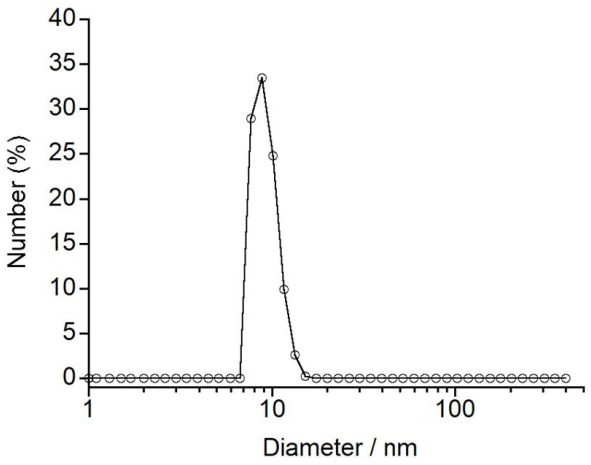

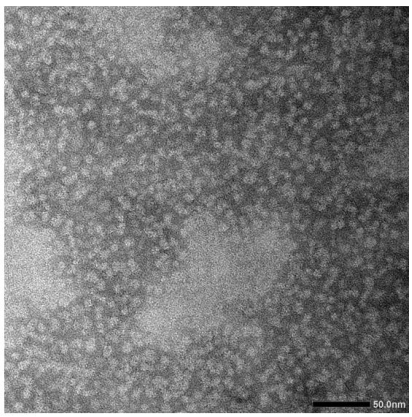

	Peak average (S.D.)
Exp. 1	10.5 ± 1.8 nm
Exp. 2	9.2 ± 1.4nm
Exp. 3	8.8 ± 1.5nm

Average hydrodynamic diameter ± S.D. （Average of peak average ± S.D.）	9.5 ± 0.9 nm

Figure S19. a) Representative size distribution of **1** at pH 7.4 after aging for 1 h at 25 °C, measured by DLS. The average hydrodynamic diameter was determined by average of the peak average of three independent experiments. Conditions: [**1**] = 0.08 mM, 10 mM HEPES buffer pH 7.4 containing 0.5% (v/v) MeOH at 25 °C. b) Representative negative stain TEM images of **1** (0.08 mM) in 10 mM HEPES buffer (pH 7.4) after aging for 1 h at room temperature (25±1 °C). Scale bar: 50 nm.

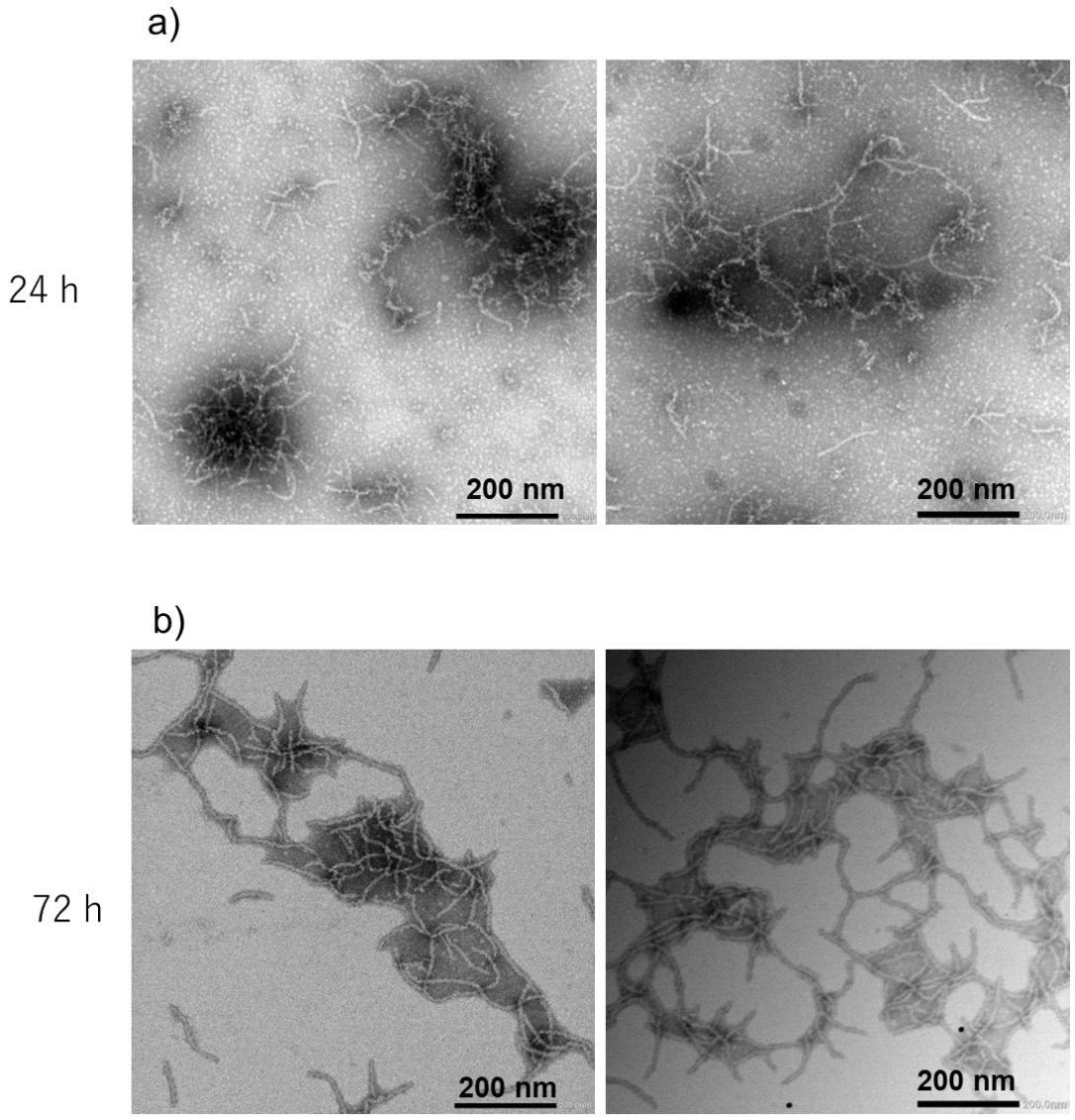

Figure S20. Representative TEM images of **1** (0.05 mM) at pH 7.4 after aging for a) 24 h and b) 72 h at room temperature (25±1 ºC). Conditions: [**1**] = 0.05 mM, 10 mM HEPES buffer pH 7.4 containing 0.5% (v/v) MeOH. Scale bars: 200 nm.

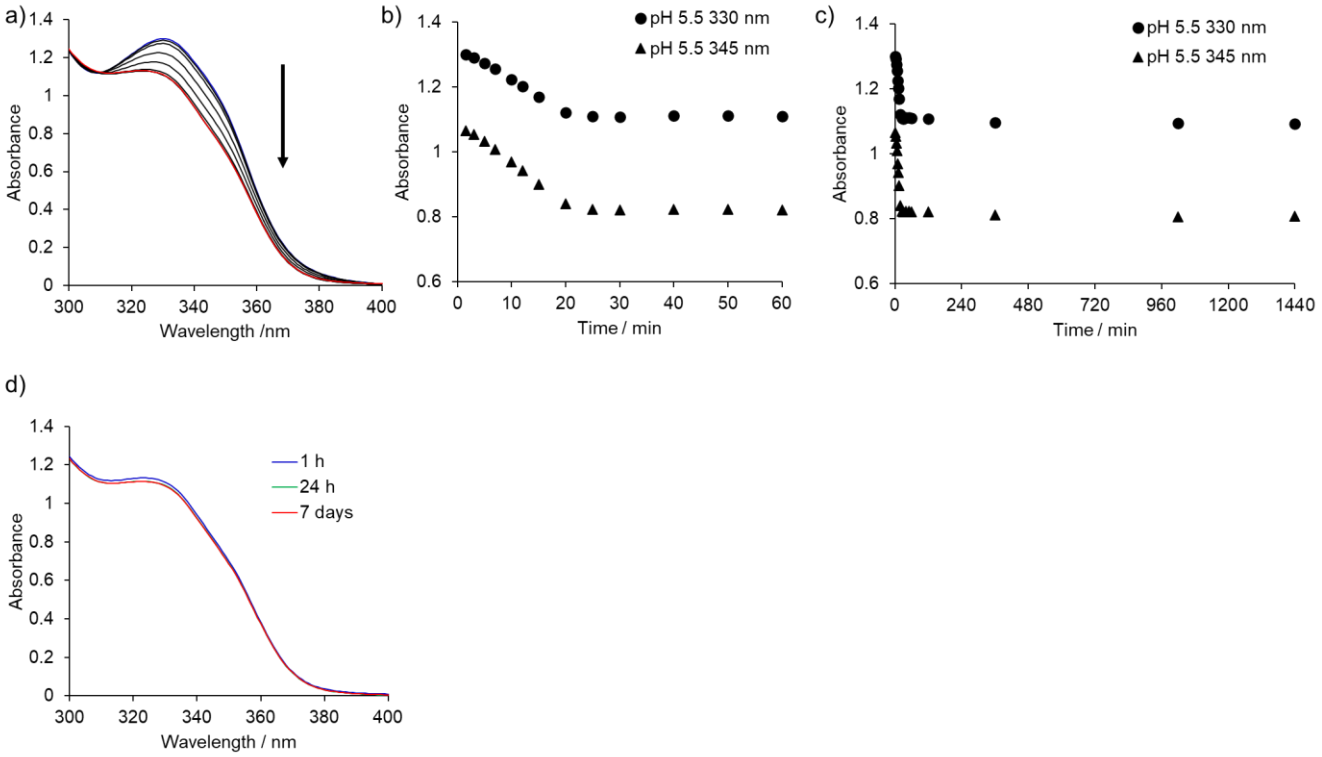

Figure S21. a) Time-resolved UV-Vis absorption spectra of **1** in the presence of 0.10 M NaCl at pH 5.5 from 1.5 min (blue line) to 60 min (red line). Time-dependent change in absorbance at 330 nm (closed circles) and 345 nm (closed triangles) of **1** from b) 1.5 min to 60 min and c) from 1.5 min to 1440 min (24 h). d) UV-Vis spectra of **1** after aging for 1 h, 24 h, and 7 days. The change in the spectra was negligible. Conditions: [**1**] = 50 μM, 10 mM MES buffer (pH 5.5, 0.10 M) containing 0.5% (v/v) MeOH at 25 °C.

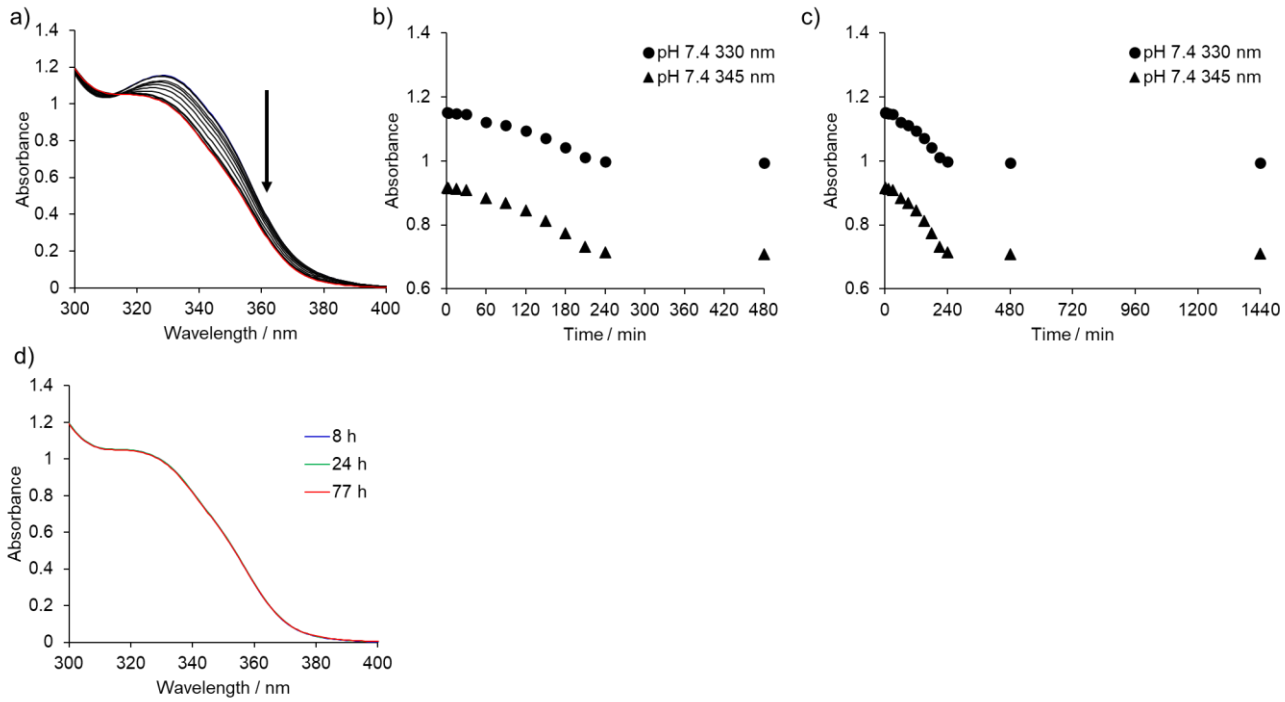

Figure S22. a) Time-resolved UV-Vis absorption spectra of **1** in the presence of 0.10 M NaCl at pH 7.4 from 1.5 min (blue line) to 480 min (red line). Time-dependent change in absorbance at 330 nm (closed circles) and 345 nm (closed triangles) of **1** from b) 1.5 min to 480 min (8 h) and c) from 1.5 min to 1440 min (24 h). d) UV-Vis spectra of **1** after aging for 8 h, 24 h, and 77 h. The change in the spectra was negligible. Conditions: [**1**] = 50 μM, 10 mM HEPES buffer (pH 7.4, 0.10 M NaCl) containing 0.5% (v/v) MeOH at 25 ºC.

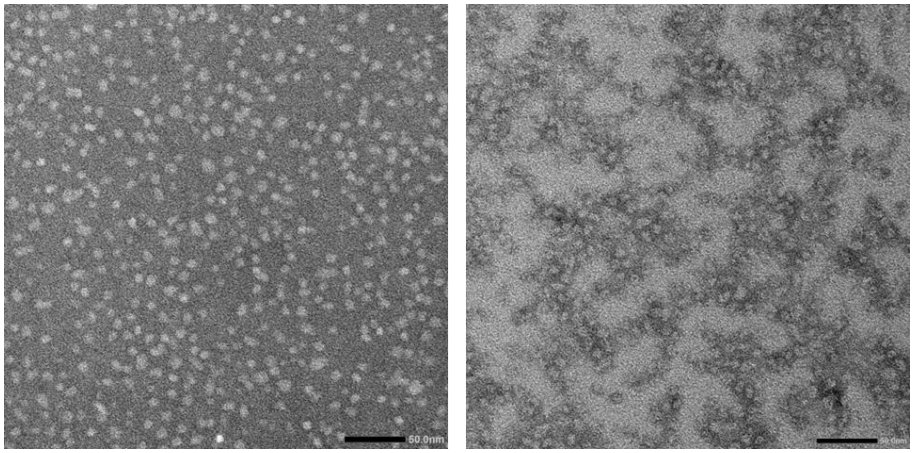

Figure S23. a) Representative negative stain TEM images of **1** at pH 7.4 in the presence of 0.10 M NaCl after aging for 2 min at room temperature (25±1 °C). Conditions: [**1**] = 0.05 mM, 10 mM HEPES buffer (pH 7.4, 0.10 M NaCl) containing 0.5% (v/v) MeOH. Scale bars: 50 nm.

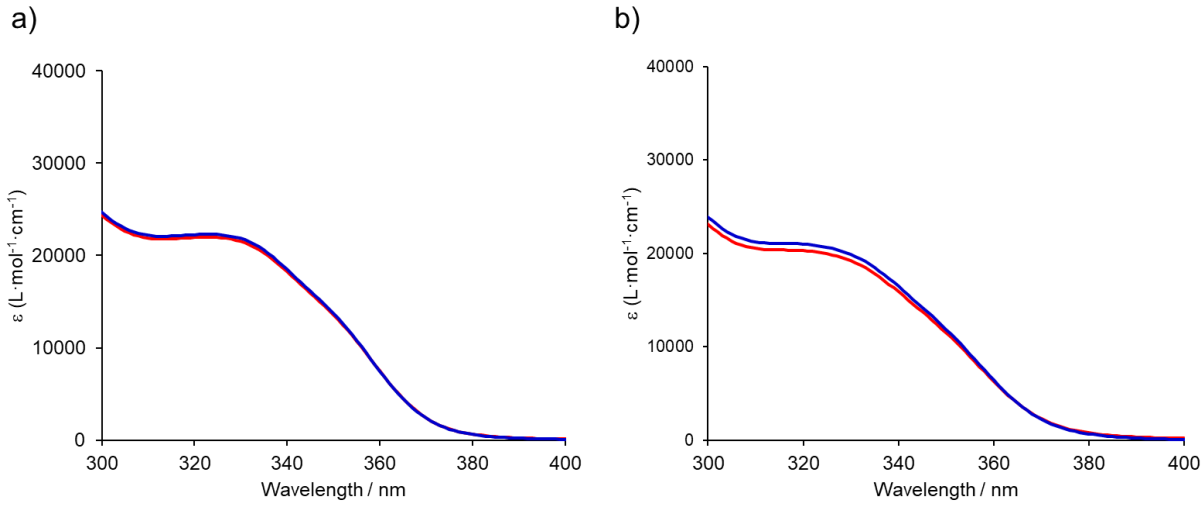

Figure S24. UV-vis spectra of **1** (50 μM (blue line) and 0.40 mM (red line)). a) At pH 5.5 in the presence of 0.10 M NaCl after aging for 24 h. b) At pH 7.4 in the presence of 0.10 M NaCl after aging for 24 h. Conditions: 10 mM buffer (pH 5.5: MES, pH 7.4: HEPES) containing 0.10 M NaCl and 0.5% (v/v) MeOH at 25 °C.

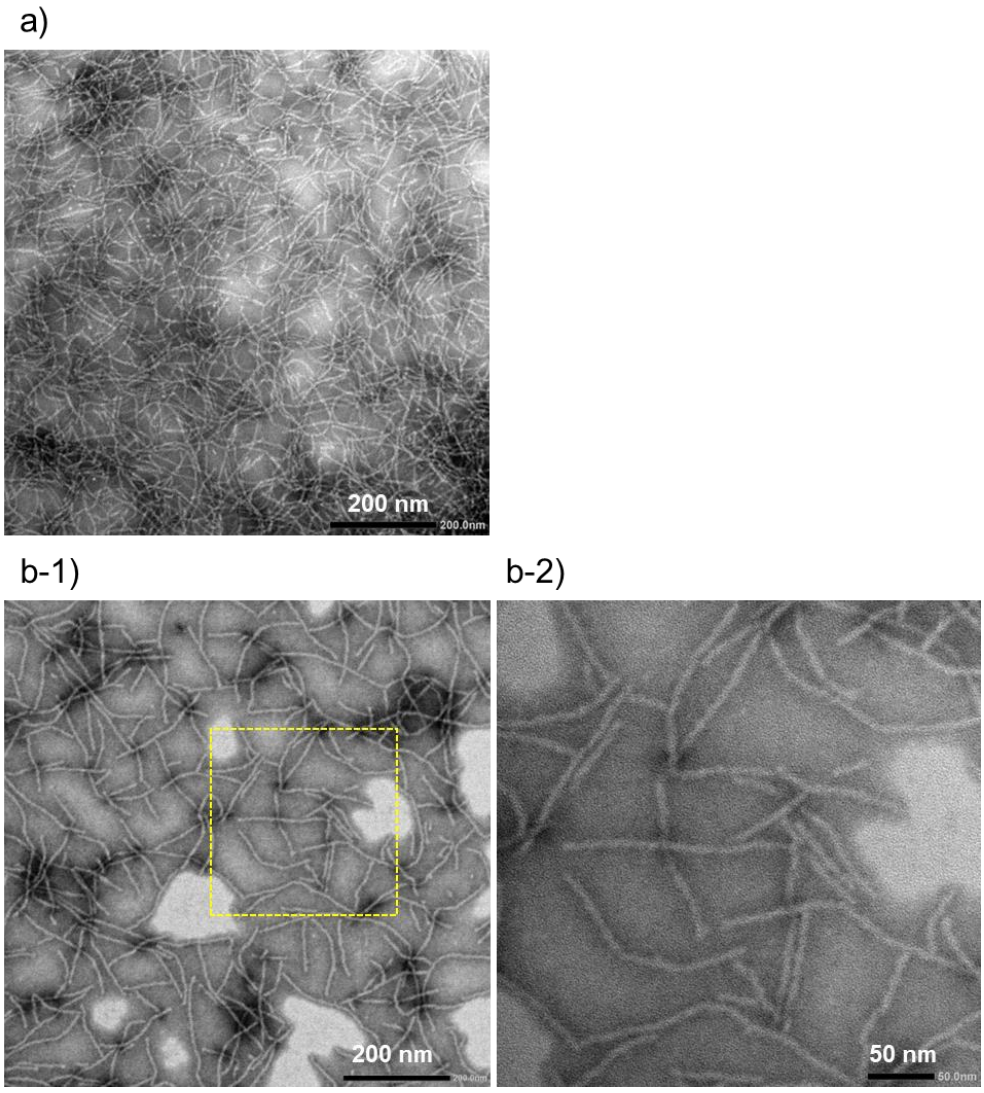

Figure S25. a) and b-1) Representative negative stain TEM images of **1** (0.5 mM) at pH 5.5 in the presence of 0.10 M NaCl after aging for 1 h at room temperature (25±1 ºC). b-2) Expanded image of the region of yellow dashed square in b-1). Conditions: [**1**] = 0.5 mM, 10 mM MES buffer pH 5.5 containing 0.10 M NaCl and 0.5% (v/v) MeOH.

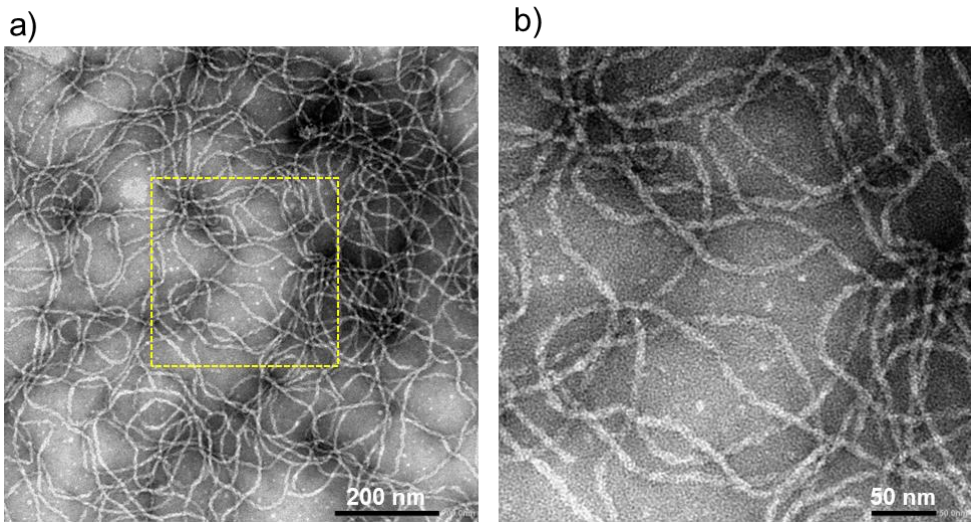

Figure S26. a) Representative negative stain TEM images of **1** (0.50 mM) at pH 7.4 in the presence of 0.10 M NaCl. The sample was prepared by sonication for 30 s (water bath), heating at 60 ºC (water bath) for 5min, and then cooling to room temperature. b) Expanded image of the region of yellow dashed square in a). Conditions: [**1**] = 0.5 mM, 10 mM HEPES buffer pH 7.4 containing 0.10 M NaCl and 0.5% (v/v) MeOH.

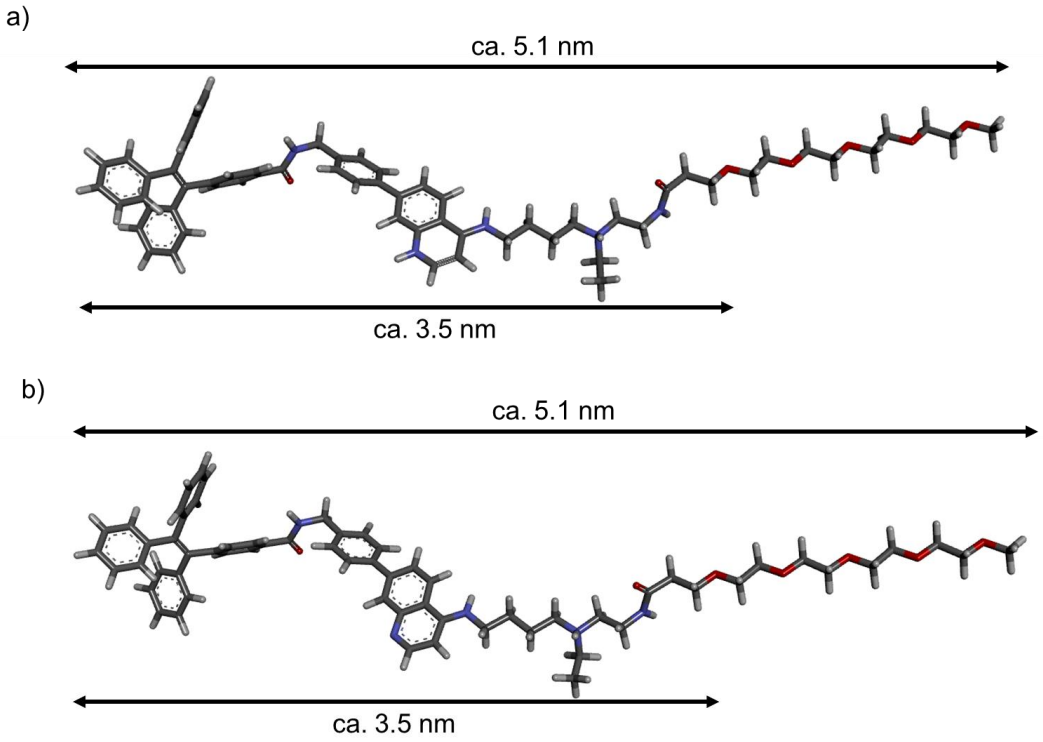

Figure S27. The geometry optimization of a) diprotonated form (-3245.055947 hartree) and b) monoprotonated form (-3244.590736 hartree) of **1** were carried out by density functional theory calculations (ωB97X-D/6-31+G*, solvent: water) using SPARTAN'18.

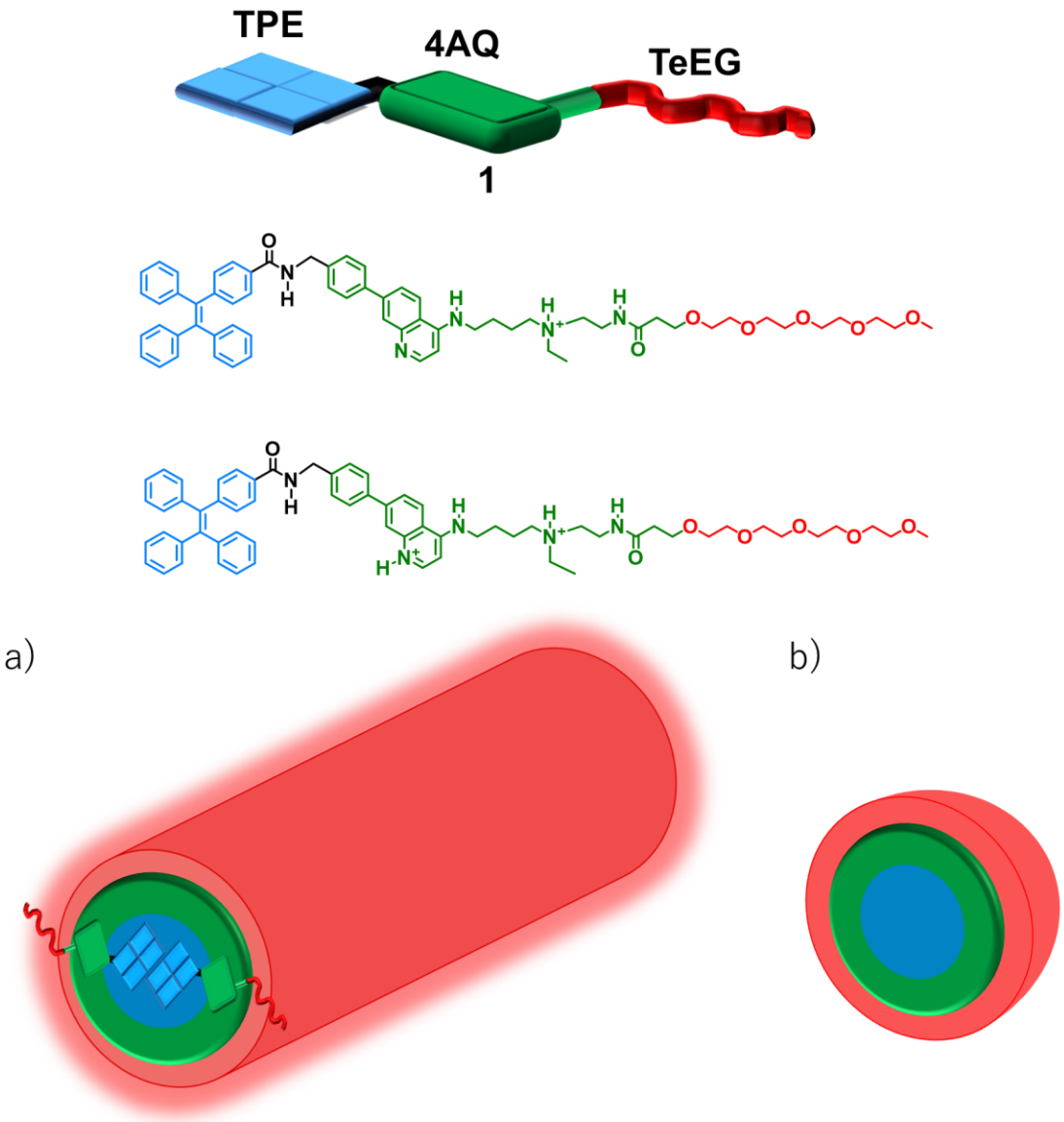

Figure S28. The proposed structures of a) nanofiber and b) sphere-like nanoparticle (sphere-like micelle) formed from **1**

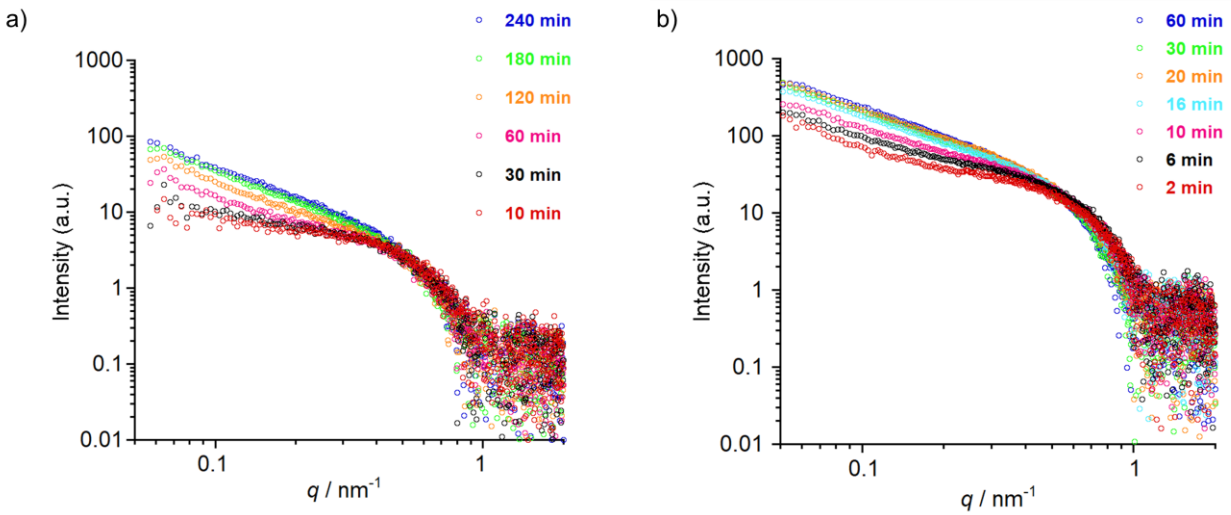

Figure S29. a) Time-resolved SAXS profiles (open circles) of **1** (0.4 mM) in 10 mM HEPES buffer (pH 7.4, 0.10 M NaCl) containing 0.5% MeOH (v/v) at 10 min (red), 30 min (black), 60 min (pink), 120 min (orange), 180 min (yellow-green) and 240 min (blue). b) Time-resolved SAXS profiles (open circles) of **1** (0.4 mM) in 10 mM MES buffer (pH 5.5, 0.10 M NaCl) containing 0.5% MeOH (v/v) at 2 min (red), 6 min (black), 10 min (pink), 16 min (sky blue), 20 min (orange), 30 min (yellow-green) and 60 min (blue).

The timescale of the transition process monitored by SAXS appeared to be somewhat faster than that monitored by the corresponding TEM study (Figures S30 and S32). The production of larger size aggregates (e.g., aggregates of sphere-like nanoparticles[S5] and/or nanofibers) observed in TEM images may exhibit strong scattering intensity and tend to become dominant for the SAXS profile.

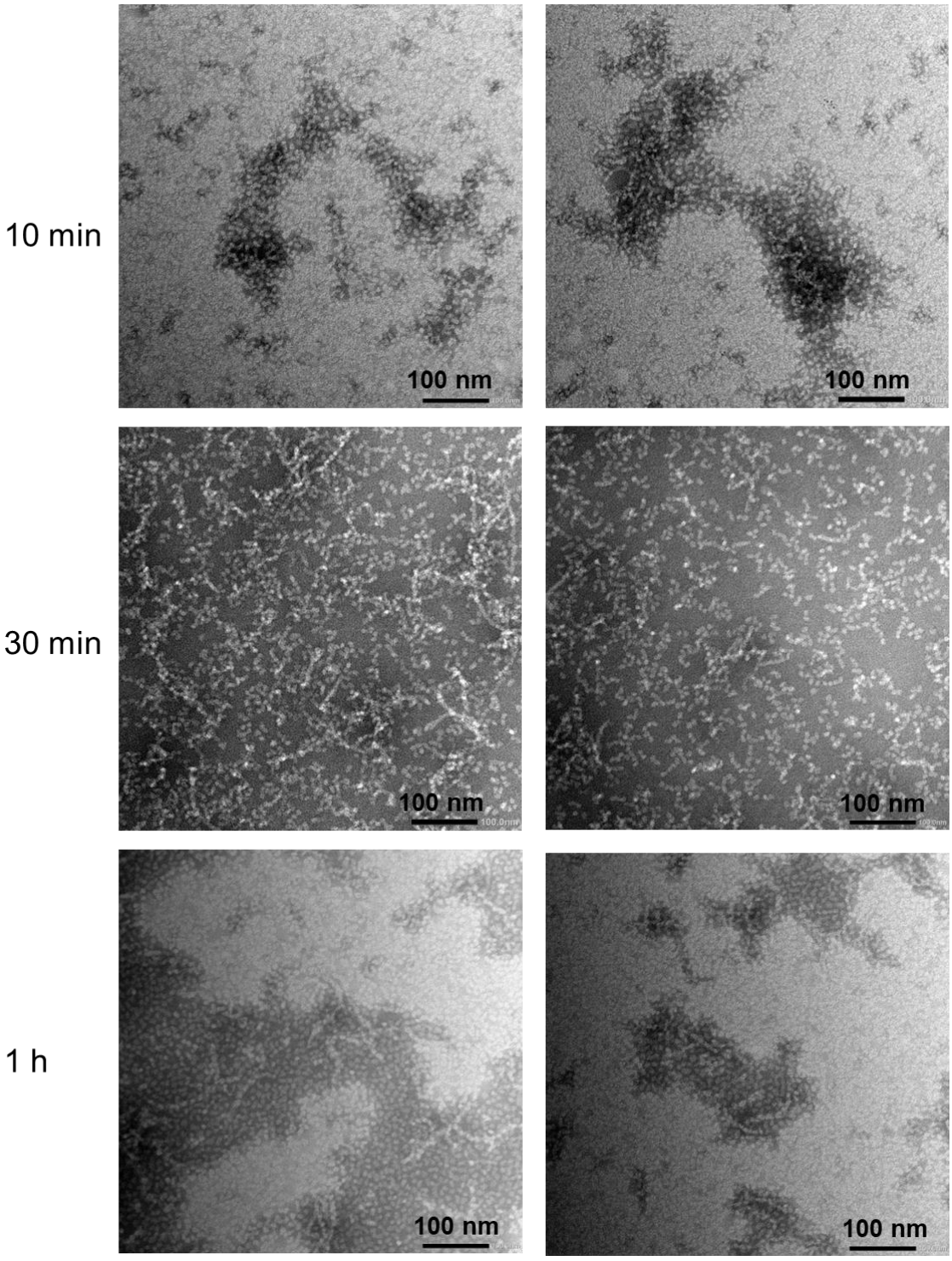
10 min
30 min
1 h
100 nm
100 nm
100 nm
100 nm
100 nm
100 nm

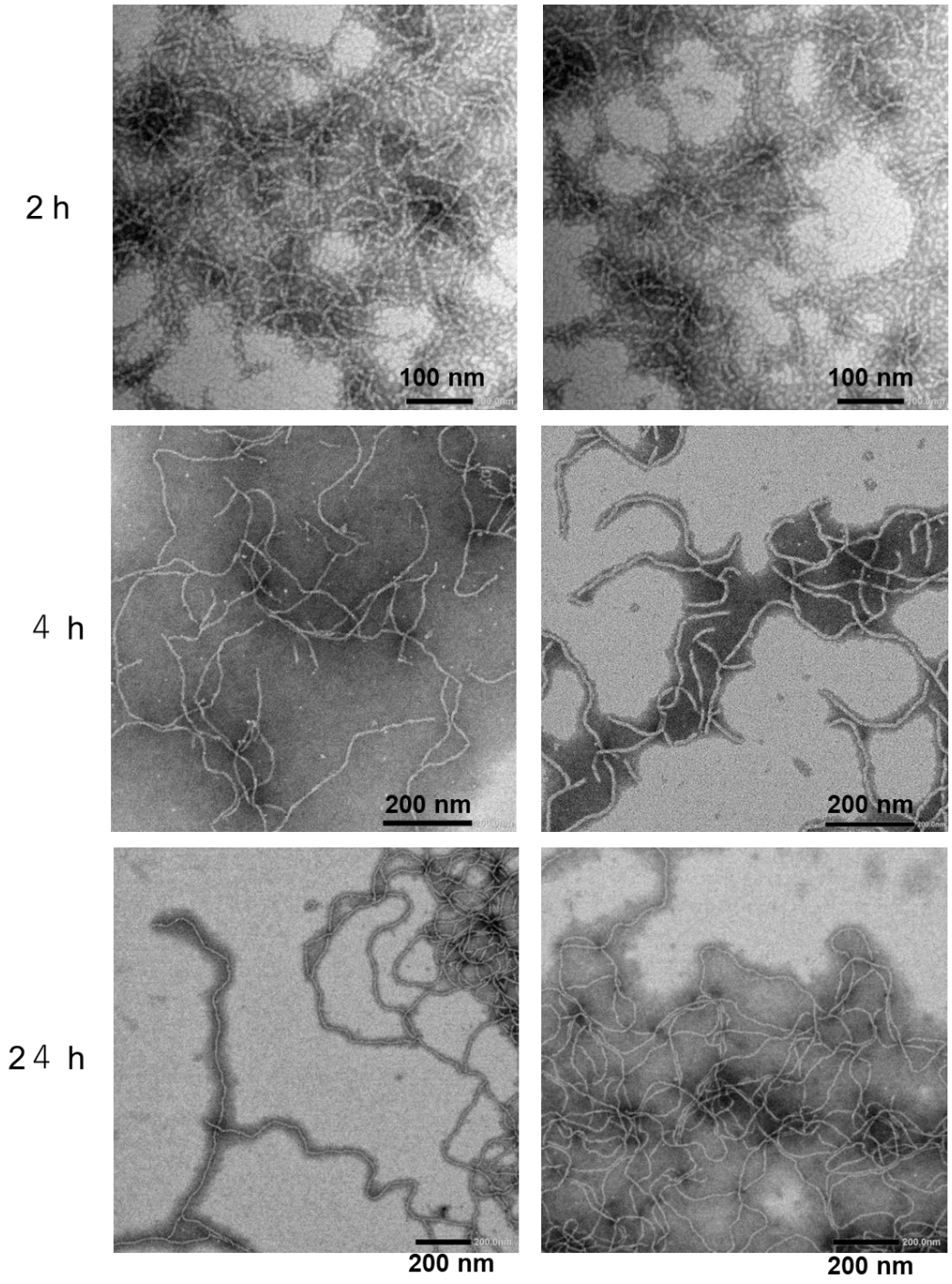

Figure S30. Representative negative stain TEM images of **1** at pH 7.4 in the presence of 0.10 M NaCl after aging for 10 min, 30 min, 1 h, 2 h, 4 h, 24 h at room temperature (25±1 ^{o}C). Conditions: [**1**] = 0.4 mM, 10 mM HEPES buffer pH 7.4 containing 0.10 M NaCl and 0.5% (v/v) MeOH.

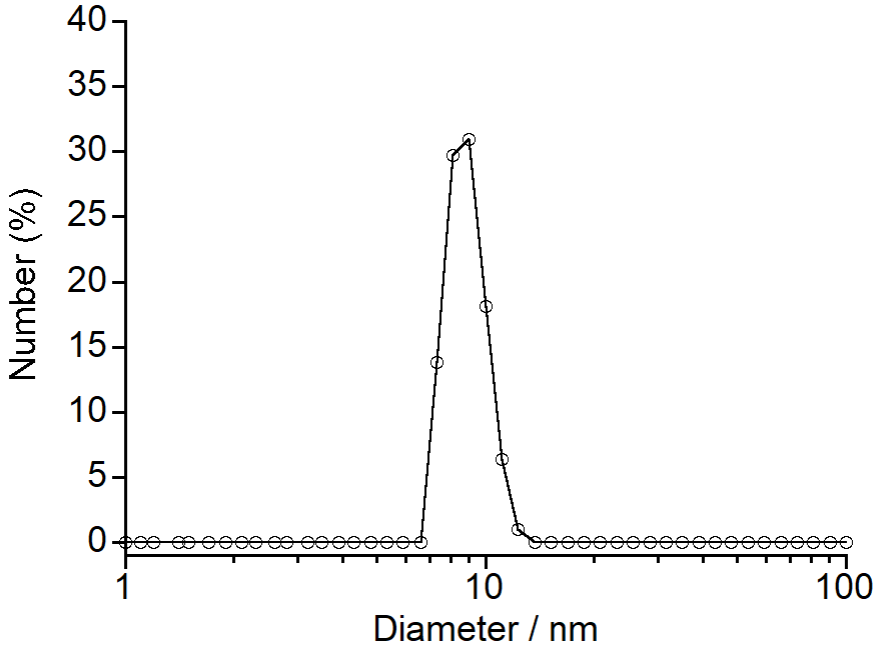

	Peak average (S.D.)
Exp. 1	10.3 ± 1.2 nm
Exp. 2	8.9 ± 1.1nm
Exp. 3	8.3 ± 1.2nm

Average hydrodynamic diameter ± S.D. （Average of peak average ± S.D.）	9.2 ± 1.0 nm

Figure S31. Representative size distribution of **1** (0.4 mM) with 0.10 M NaCl at pH 7.4 after aging for 10 min at 25 °C, measured by DLS. The average hydrodynamic diameter was determined by average of the peak average of three independent experiments. Conditions: [**1**] = 0.4 mM, 10 mM HEPES buffer pH 7.4 containing 0.5% (v/v) MeOH at 25 °C.

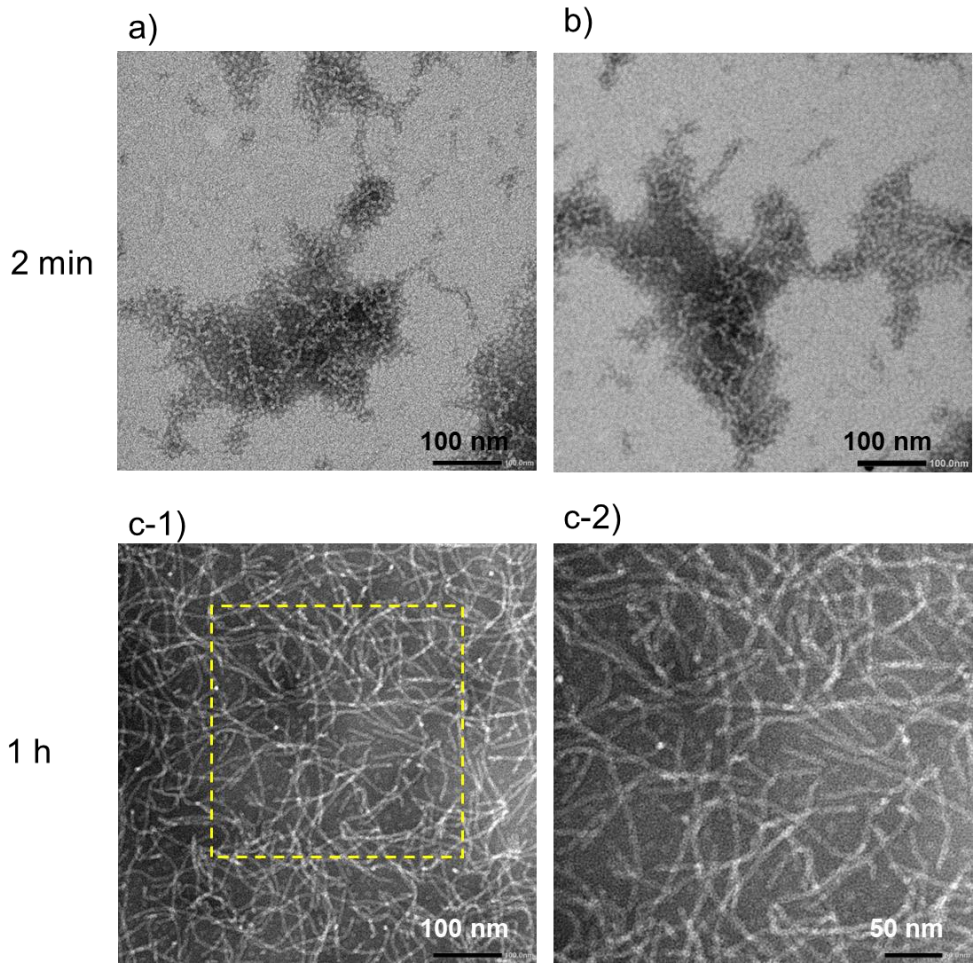

Figure S32. Representative negative stain TEM images of **1** at pH 5.5 in the presence of 0.10 M NaCl after aging for a), b) 2 min and c-1) 1 h at room temperature (25±1 °C). c-2) Expanded image of the region of yellow dashed square in c-1). Conditions: [**1**] = 0.4 mM, 10 mM MES buffer pH 5.5 containing 0.10 M NaCl and 0.5% (v/v) MeOH.

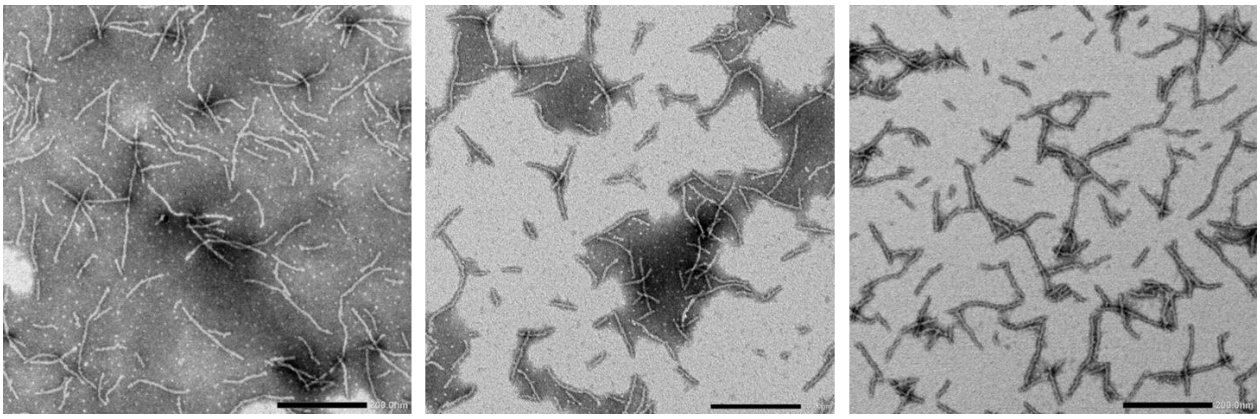

Figure S33. Representative TEM images of **1** (0.05 mM) in 10 mM HEPES buffer (pH 5.5, 0.10 M NaCl) containing 0.5 % (v/v) MeOH. Scale bars: 200 nm.

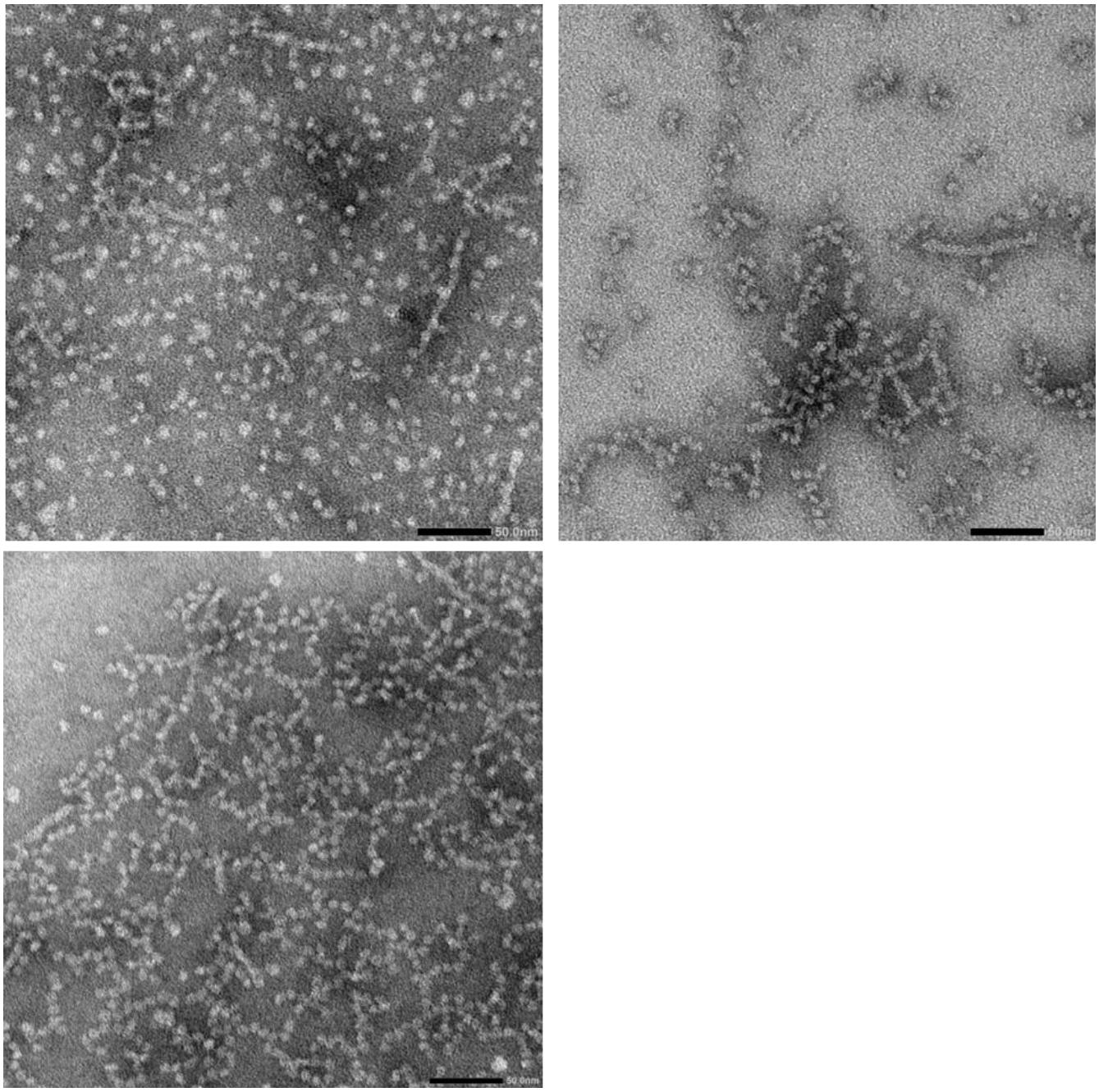

Figure S34. Representative negative stain TEM images (enlarged images) of **1** at pH 7.4 in the presence of 0.10 M NaCl after aging for 1 h at room temperature (25±1 ºC). Conditions: [**1**] = 0.05 mM, 10 mM HEPES buffer pH 7.4 containing 0.10 M NaCl and 0.5% (v/v) MeOH. It appears that sphere-like nanoparticles may partly join together. One of our hypotheses based on the TEM images is that the joined sphere-like nanoparticles may transit to the nanofibers. Scale bars: 50 nm.

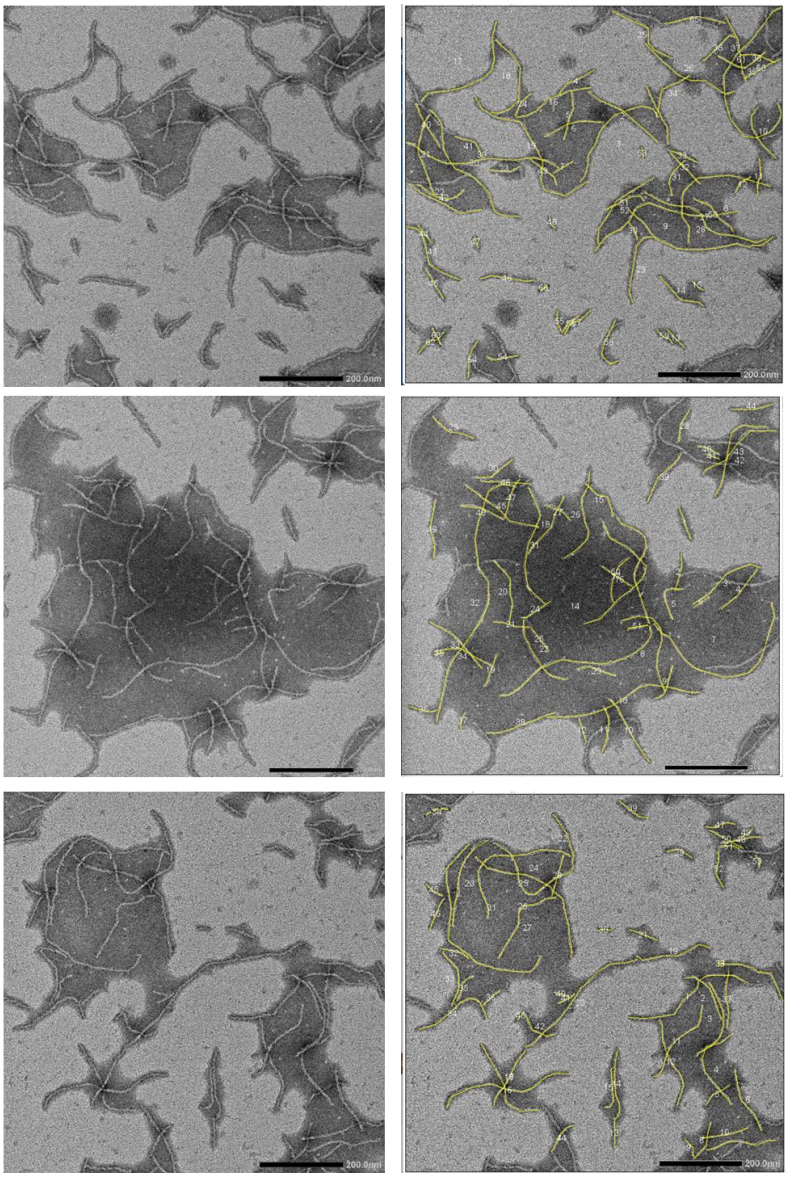

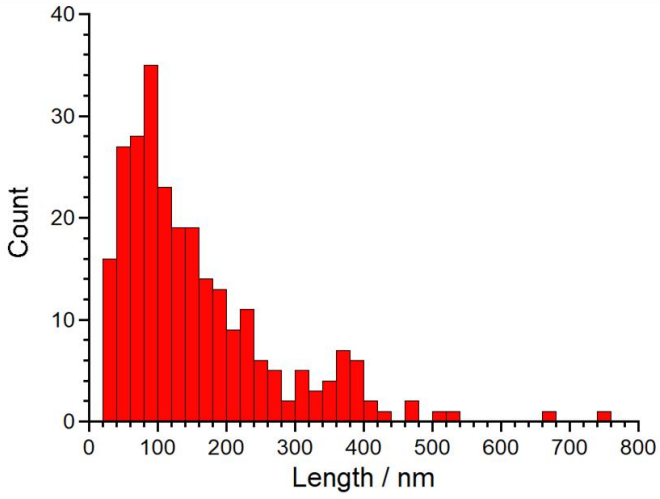

Figure S35. a)-c) Three representative TEM images (left) of **1** (0.05 mM) at pH 5.5 in the presence of 0.20 M NaCl after aging for 1 h at room temperature (25±1 °C), and the corresponding images were analyzed with the ImageJ software (right). Scale bars: 200 nm. d) The histogram of lengths was prepared using five TEM images (number of measured nanofibers: 261). Conditions: [**1**] = 0.05 mM, 10 mM MES buffer pH 5.5 containing 0.20 M NaCl and 0.5% (v/v) MeOH.

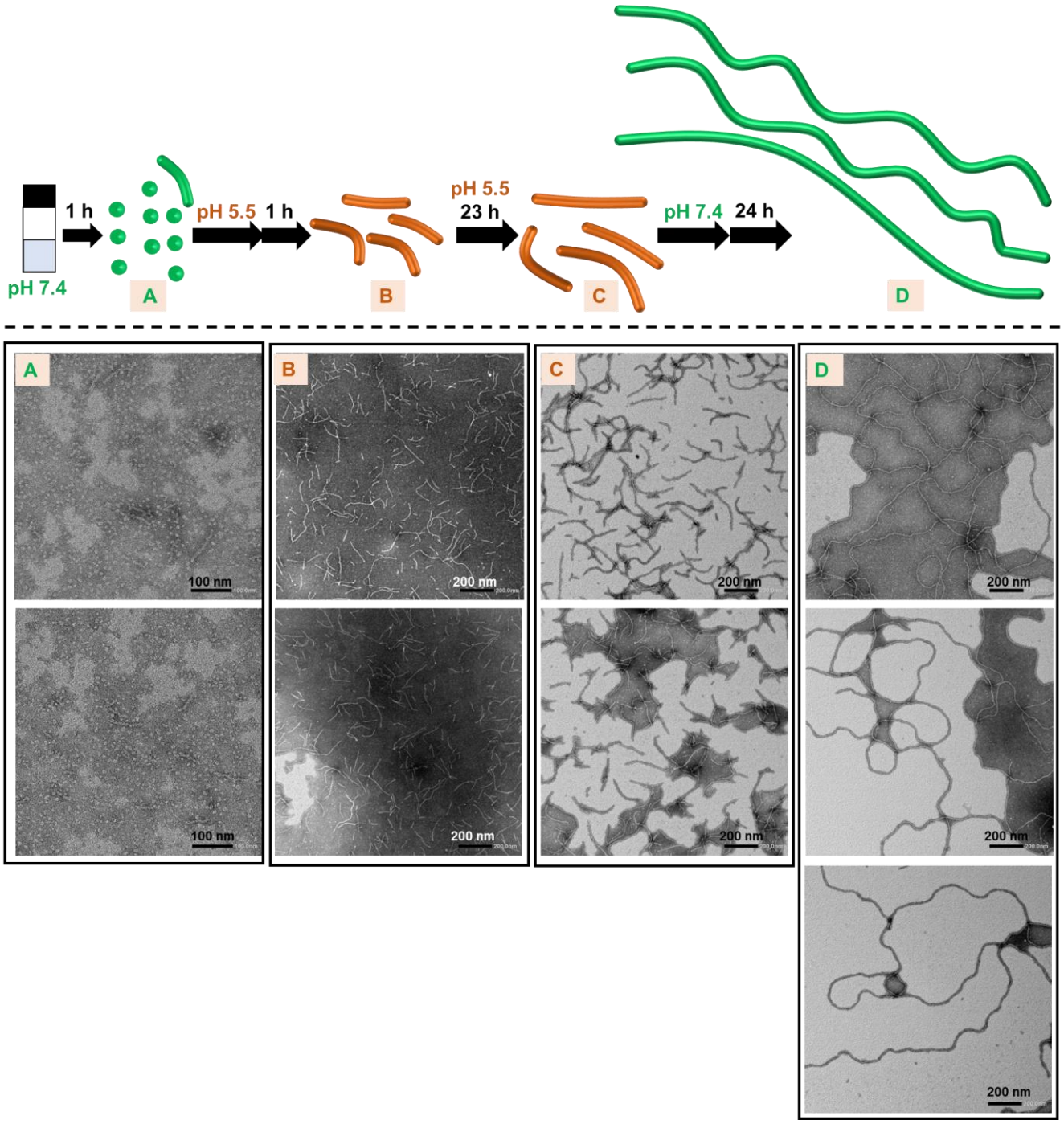

Figure S36. pH-responsive self-assembly behavior of **1** (0.05 mM) in 10 mM HEPES buffer (pH 7.4, 0.10 M NaCl) containing 0.5% (v/v) MeOH at 25 ºC (pH 7.4→5.5→7.4). The pH values were adjusted using HCl (0.5 M and 0.1 M) and NaOH (0.5 M and 0.1 M). Representative negative stain TEM images after aging for A) 1 h, after adjustment of pH to 5.5, then aging for B) 1 h and C) 24 h, D) after adjustment of pH to 7.4, then aging for 24 h.

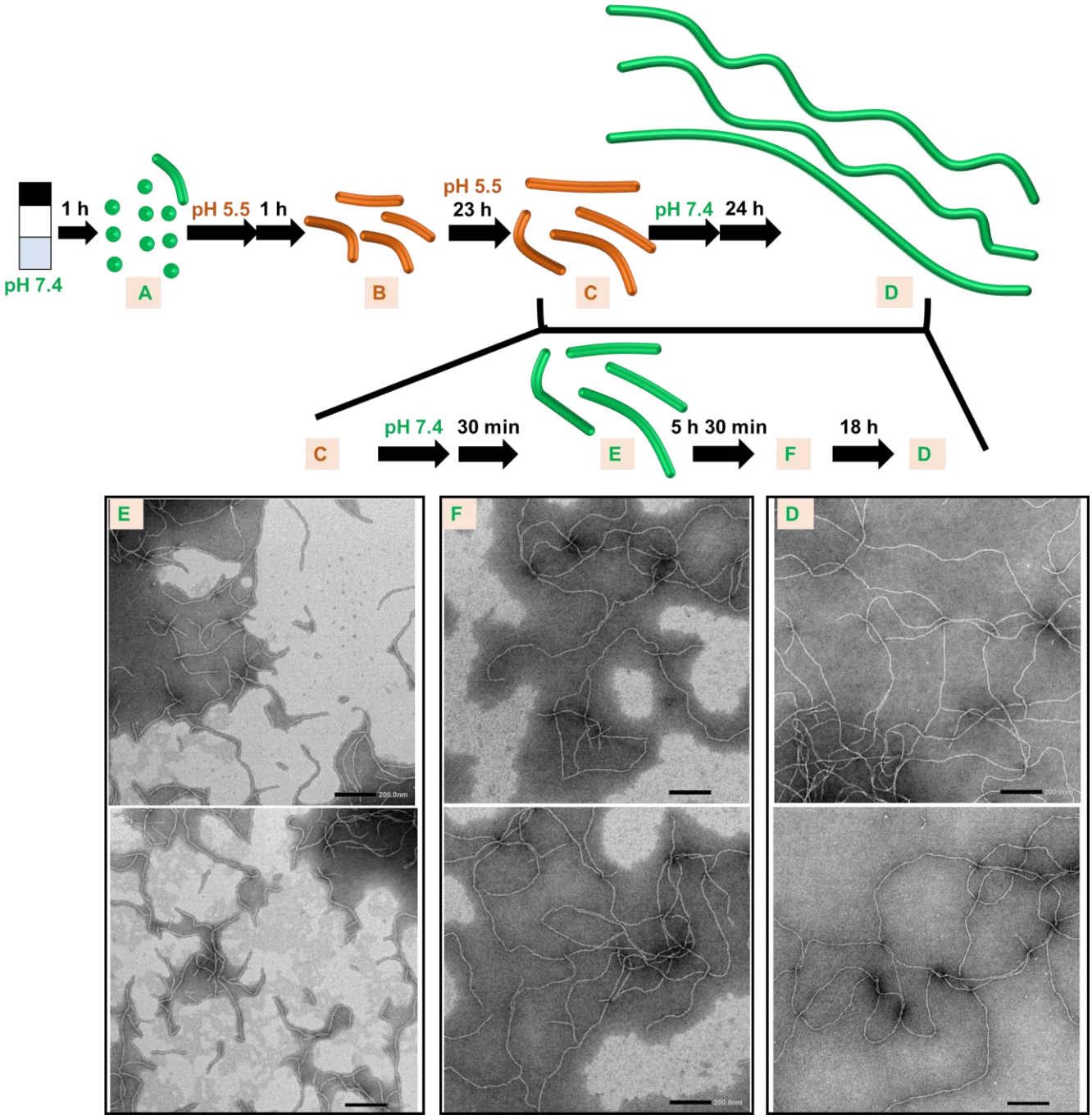

Figure S37. pH-responsive self-assembly behavior of **1** (0.05 mM) in 10 mM HEPES buffer (pH 7.4, 0.10 M NaCl) containing 0.5% (v/v) MeOH at 25 ºC (pH 7.4→5.5→7.4). The pH values were adjusted using HCl (0.5 M and 0.1 M) and NaOH (0.5 M and 0.1 M). The TEM observation was focused on after adjustment of pH from 5.5 to 7.4, and then aging for E) 30 min, F) 6 h and D) 24 h. Scale bars: 200 nm.

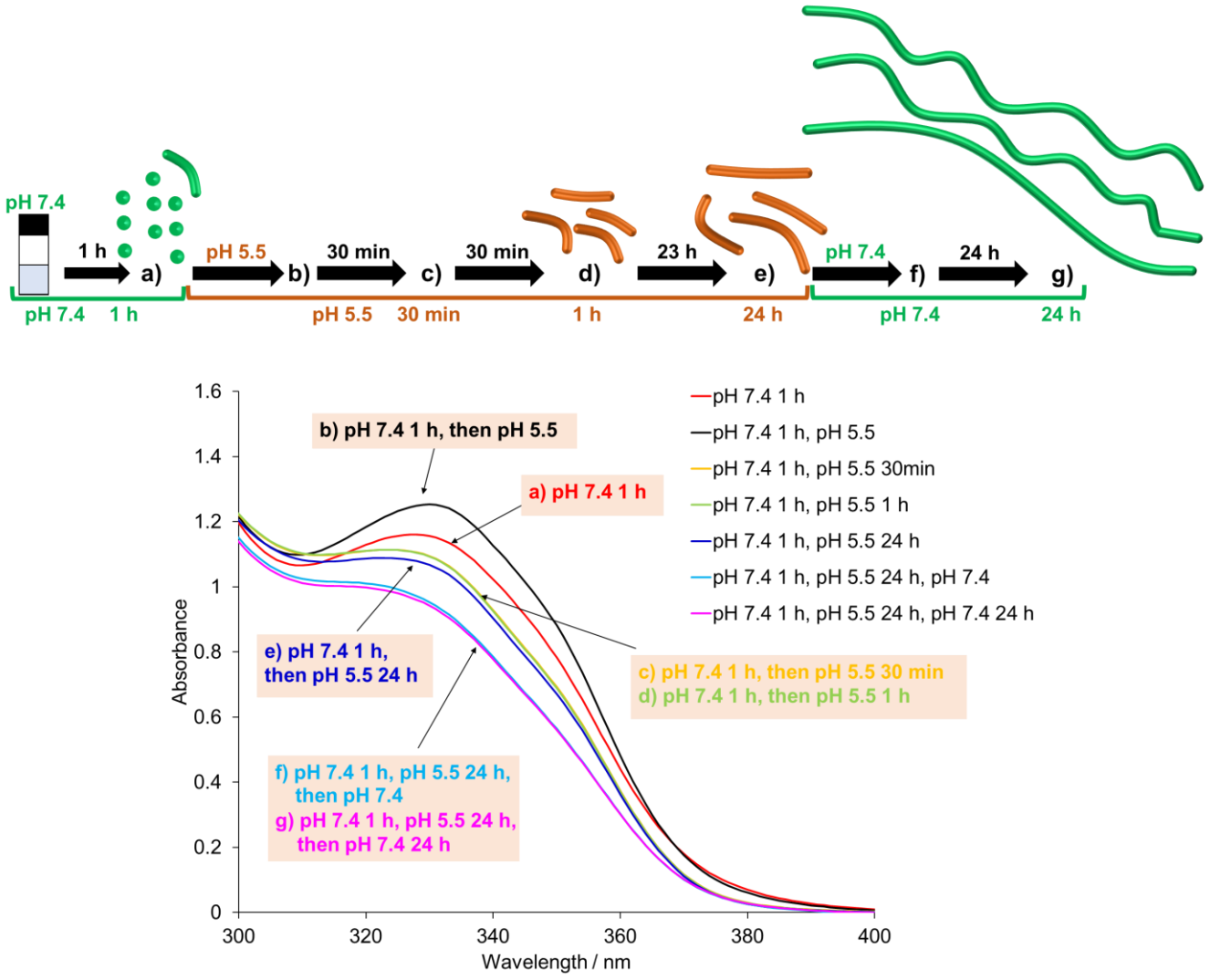

Figure S38. Change in UV-Vis absorption spectra based on the pH-responsive self-assembly behavior of **1**. Conditions: [**1**] = 50 μM, 10 mM HEPES buffer (pH 7.4, 0.10 M NaCl) containing 0.5% (v/v) MeOH at 25 °C. The pH values were adjusted using HCl (0.5 M and 0.1 M) and NaOH (0.5 M and 0.1 M).

a) → b); This spectral change suggests protonation of the 4-aminoquinoline moiety of **1** (monoprotonated form) in sphere-like nanoparticles by the pH change from 7.4 to 5.5.

b) → c), d); This spectral change suggests the transition from sphere-like nanoparticles to nanofibers at pH 5.5.

e) → f); This spectral change suggests deprotonation of the 4-aminoquinoline moiety in the nanofibers (i.e., from diprotonated form to monoprotonated form) because the pH of the sample solution returned to pH 7.4. Furthermore, when the pH was adjusted to 7.4, absorption spectrum of f) was found to correspond to nanofibers, rather than the sphere-like nanoparticles shown in spectrum of a).

f) → g); Since nanofibers were formed at f), the change in absorption spectra was negligible during aging because the growth of nanofibers is not reflected in the absorption spectral change.

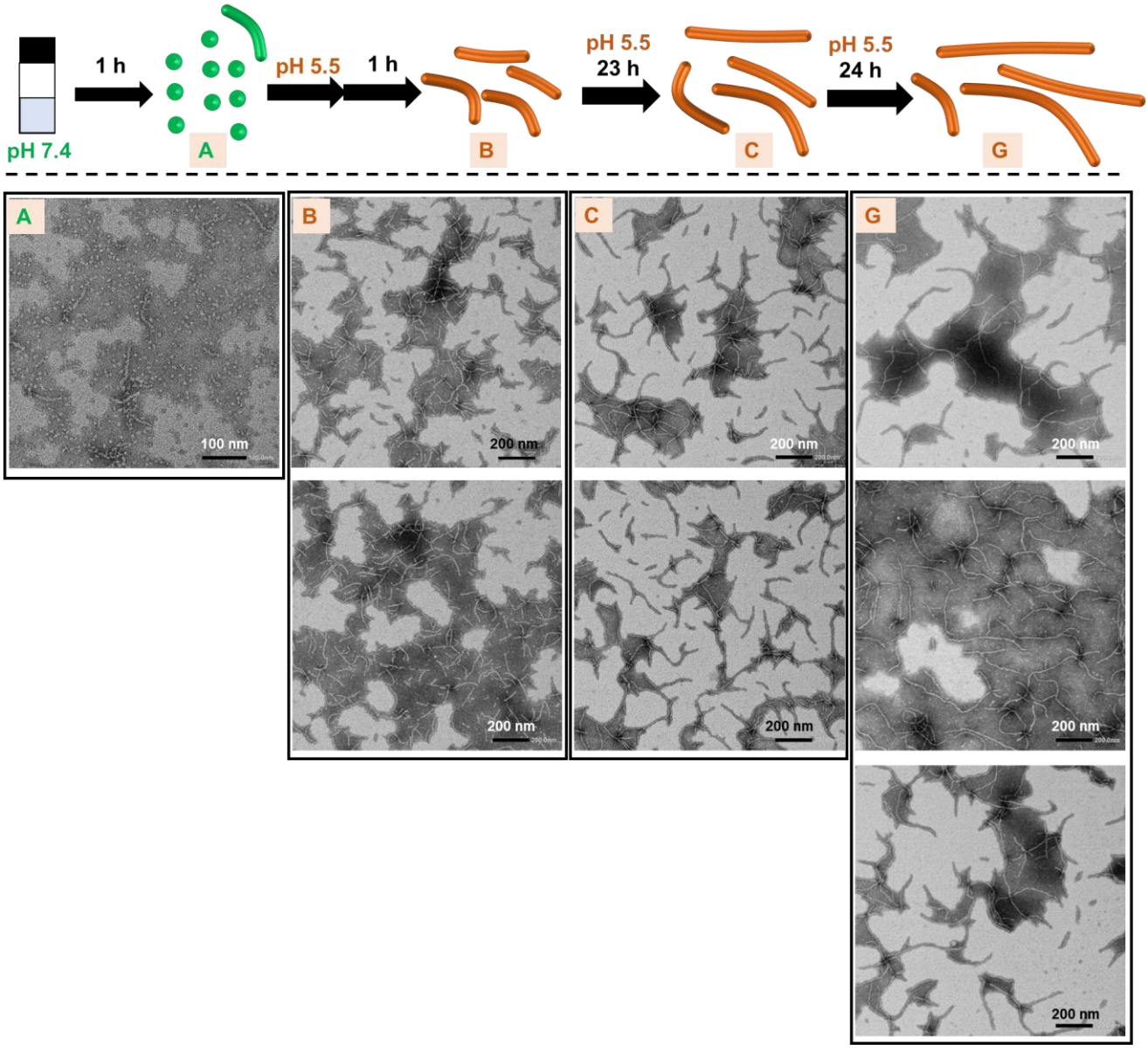

Figure S39. pH-responsive self-assembly behavior of **1** (0.05 mM) in 10 mM HEPES buffer (pH 7.4, 0.10 M NaCl) containing 0.5% (v/v) MeOH at 25 ºC (pH 7.4→5.5). Representative TEM images after aging for A) 1 h, after adjustment of pH to 5.5, then aging for B) 1 h, C) 24 h, and G) 48 h. The pH value was adjusted using HCl (0.5 M) and NaOH (0.1 M).

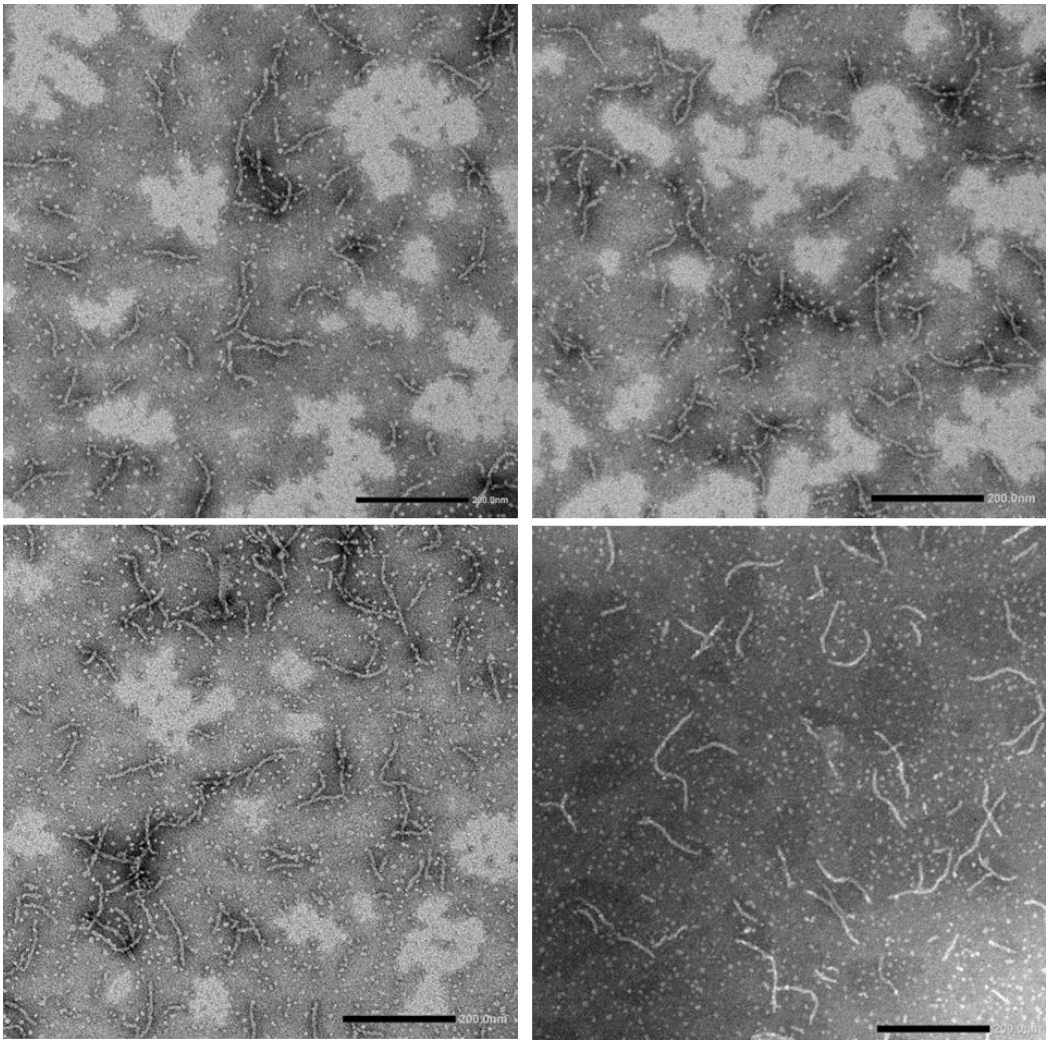

Figure S40. Representative negative stain TEM images of **1** at pH 7.4 in the presence of 0.10 M NaCl after aging for 2 h at room temperature (25±1 ºC). Conditions: [**1**] = 0.05 mM, 10 mM HEPES buffer pH 7.4 containing 0.10 M NaCl and 0.5% (v/v) MeOH. Scale bars: 200 nm.

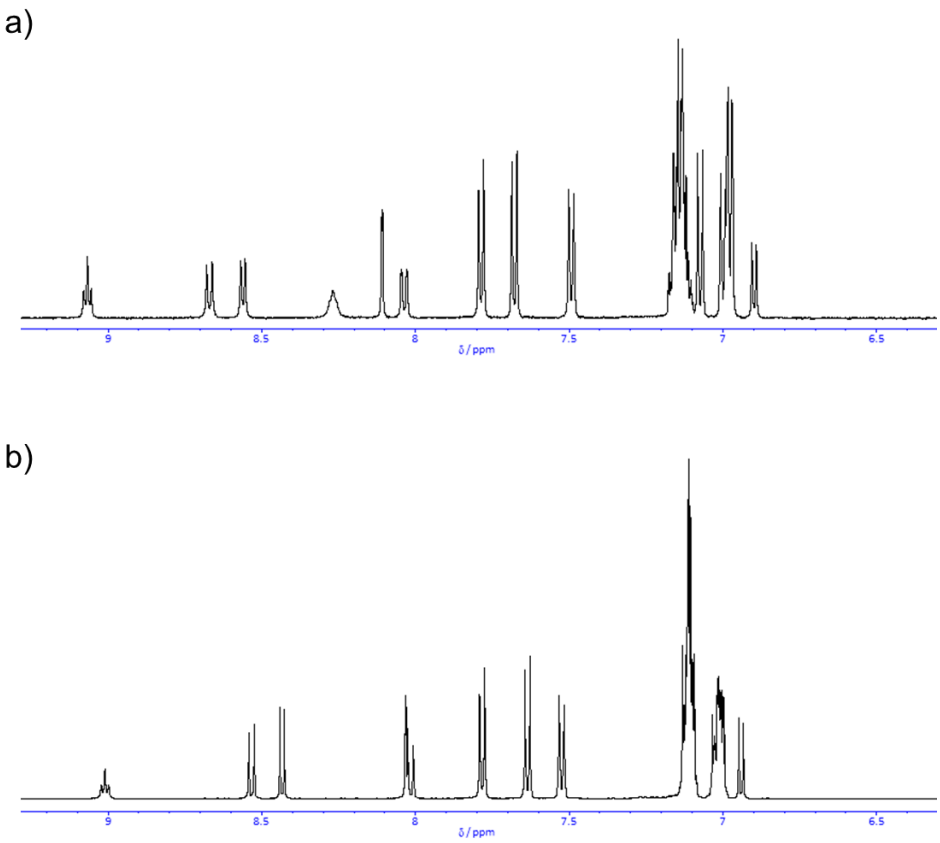

Figure S41. Partial ^{1}H NMR spectrum of a) **1**·2HCl (2.0 mM) in DMSO-d_6 and b) **1**·2HCl (10 mM) in CD_3OD.

References:

[S1] X. Liu, G. Liang, *Chem. Commun.* **2017**, *53*, 1037-1040.

[S2] Y. Hisamatsu, K. Otani, H. Takase, N. Umezawa, T. Higuchi, *Chem. Eur. J.* **2021**, *27*, 6489-6499.

[S3] J. Kubitschke, S. Javor, J. Rebek, Jr., *Chem. Commun.* **2012**, *48*, 9251-9253.

[S4] Y. Hisamatsu, N. Umezawa, H. Yagi, K. Kato, T. Higuchi, *Chem. Sci.* **2018**, *9*, 7455-7467.

[S5] D. Lombardo, G. Munao, P. Calandra, L. Pasqua, M. T. Caccamo, *Phys. Chem. Chem. Phys.* **2019**, *21*, 11983-11991.

^{1}H NMR spectrum ($CDCl_3$) of compound **S1**

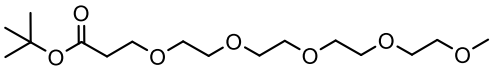

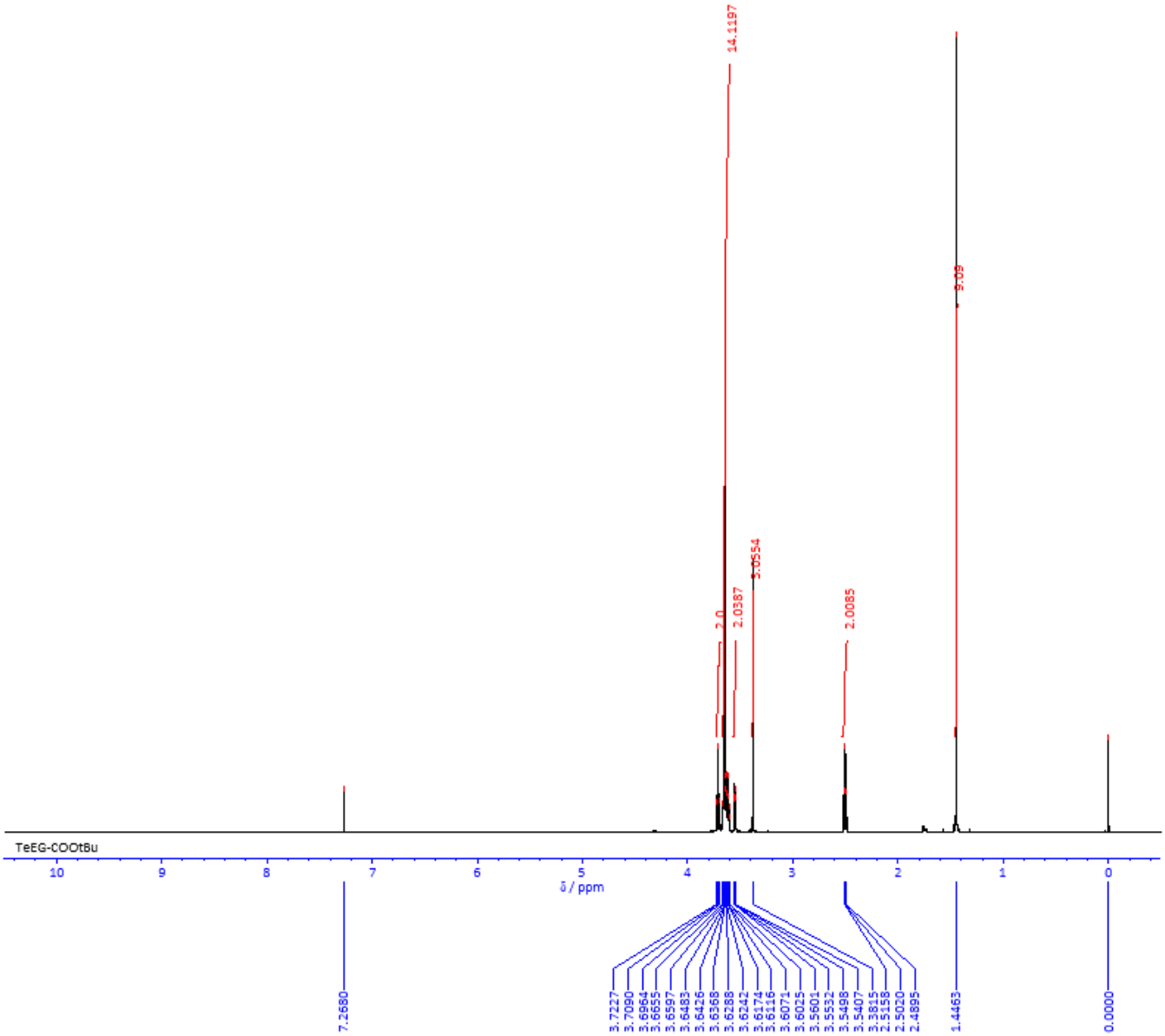

^{13}C NMR spectrum ($CDCl_3$) of compound **S1**

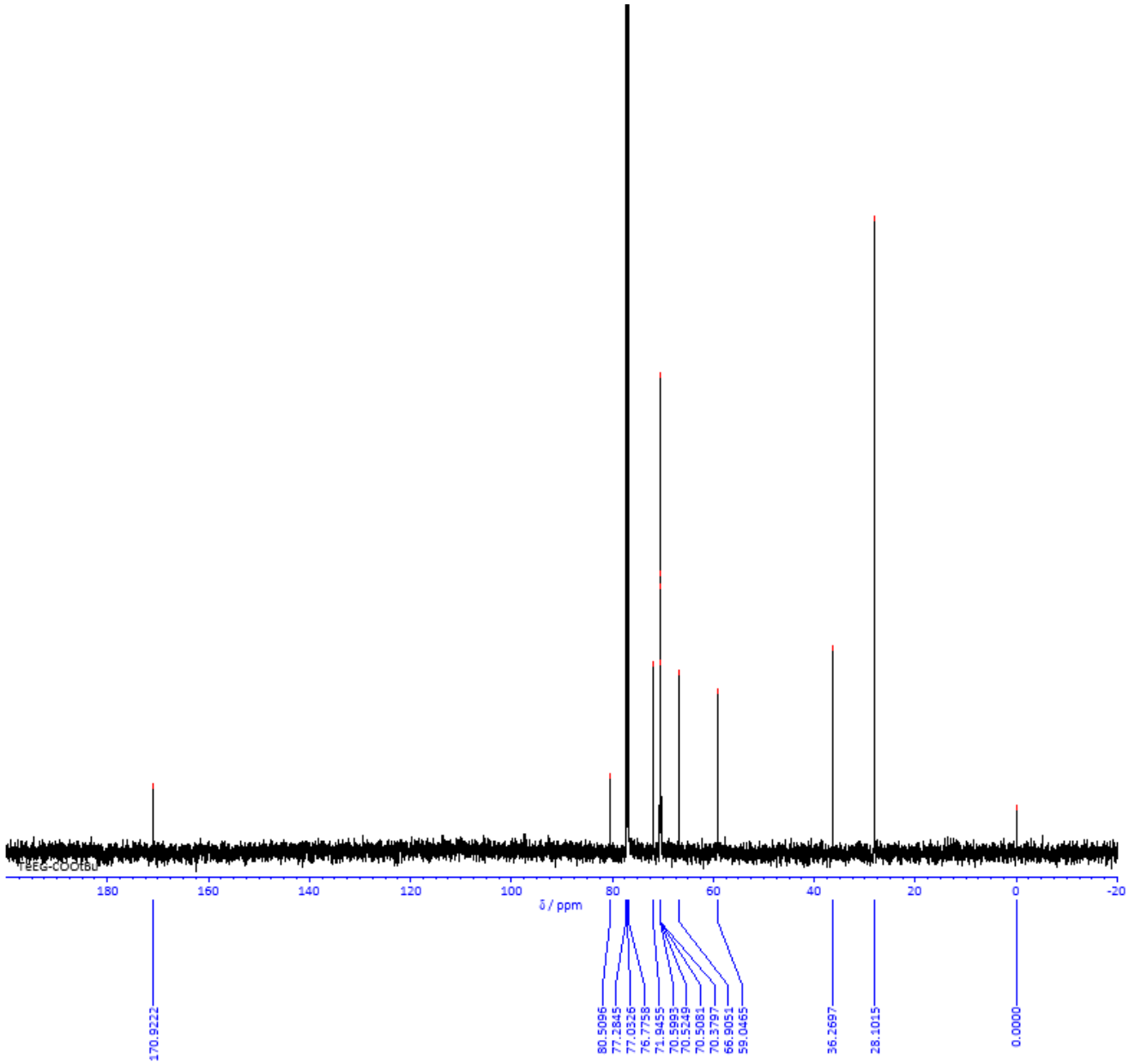

^{1}H NMR spectrum ($CDCl_3$) of compound **S3**

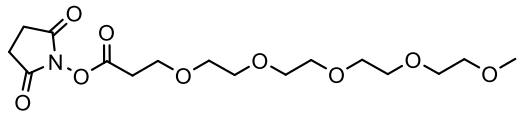

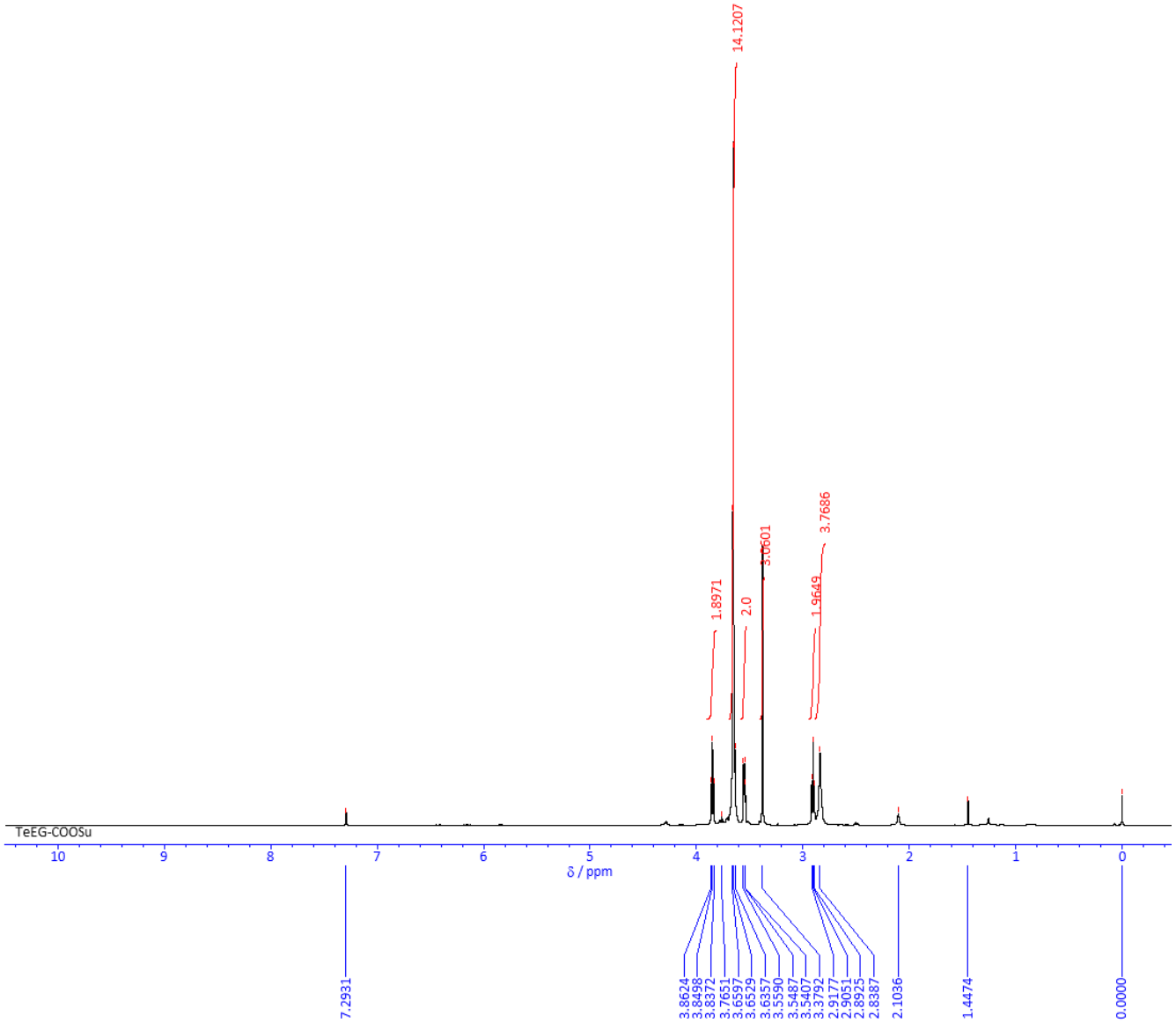

^{13}C NMR spectrum ($CDCl_3$) of compound **S3**

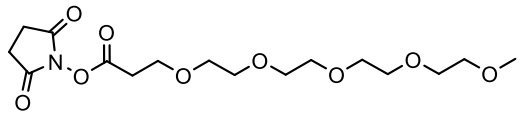

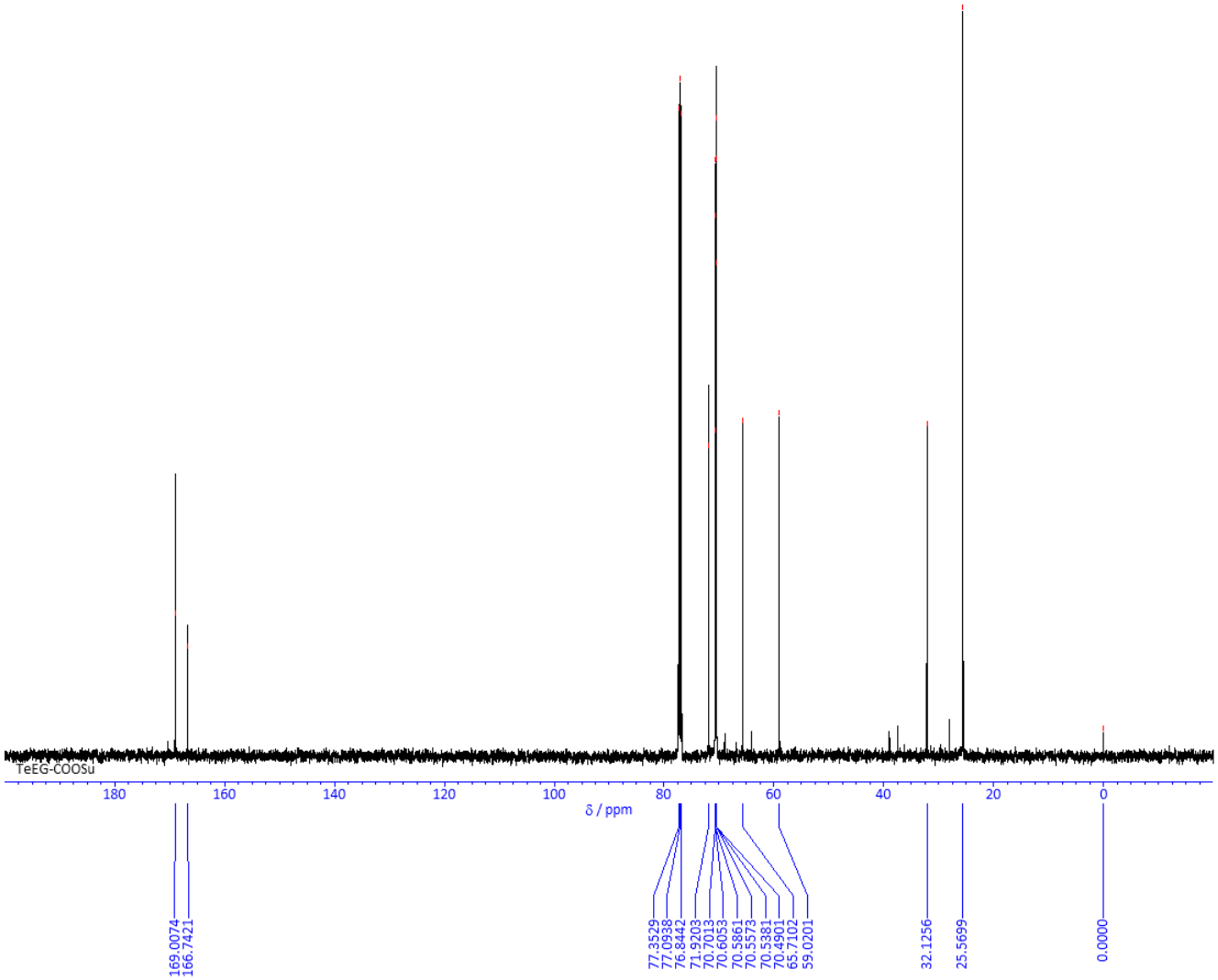

^{1}H NMR spectrum ($CDCl_3$) of compound **S5**

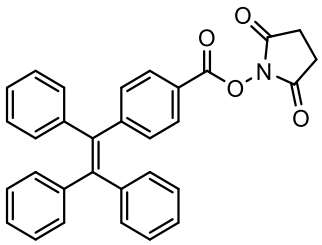

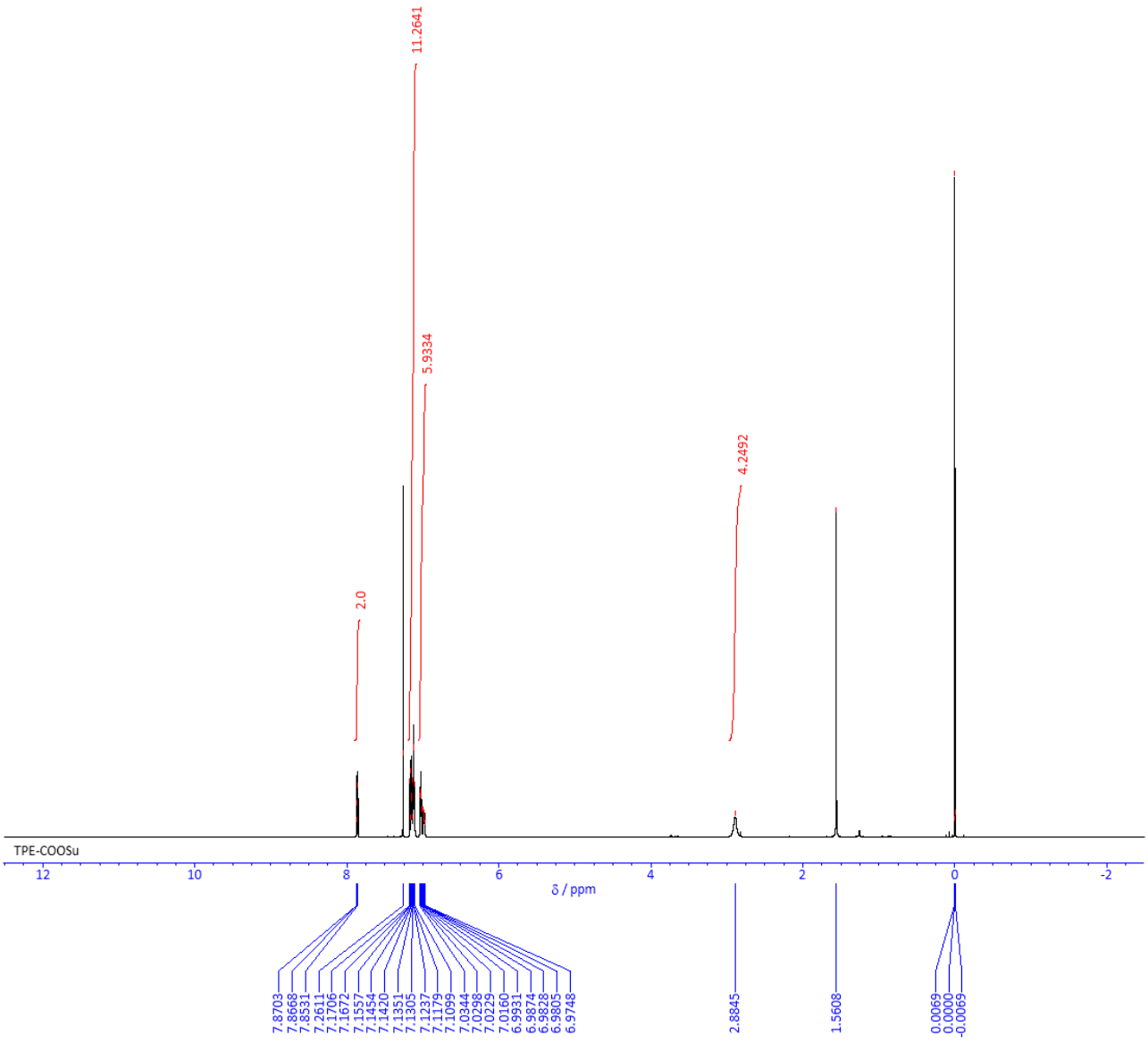

^{13}C NMR spectrum ($CDCl_3$) of compound **S5**

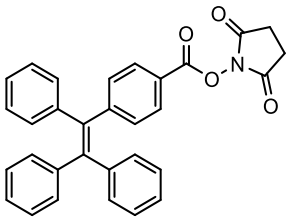

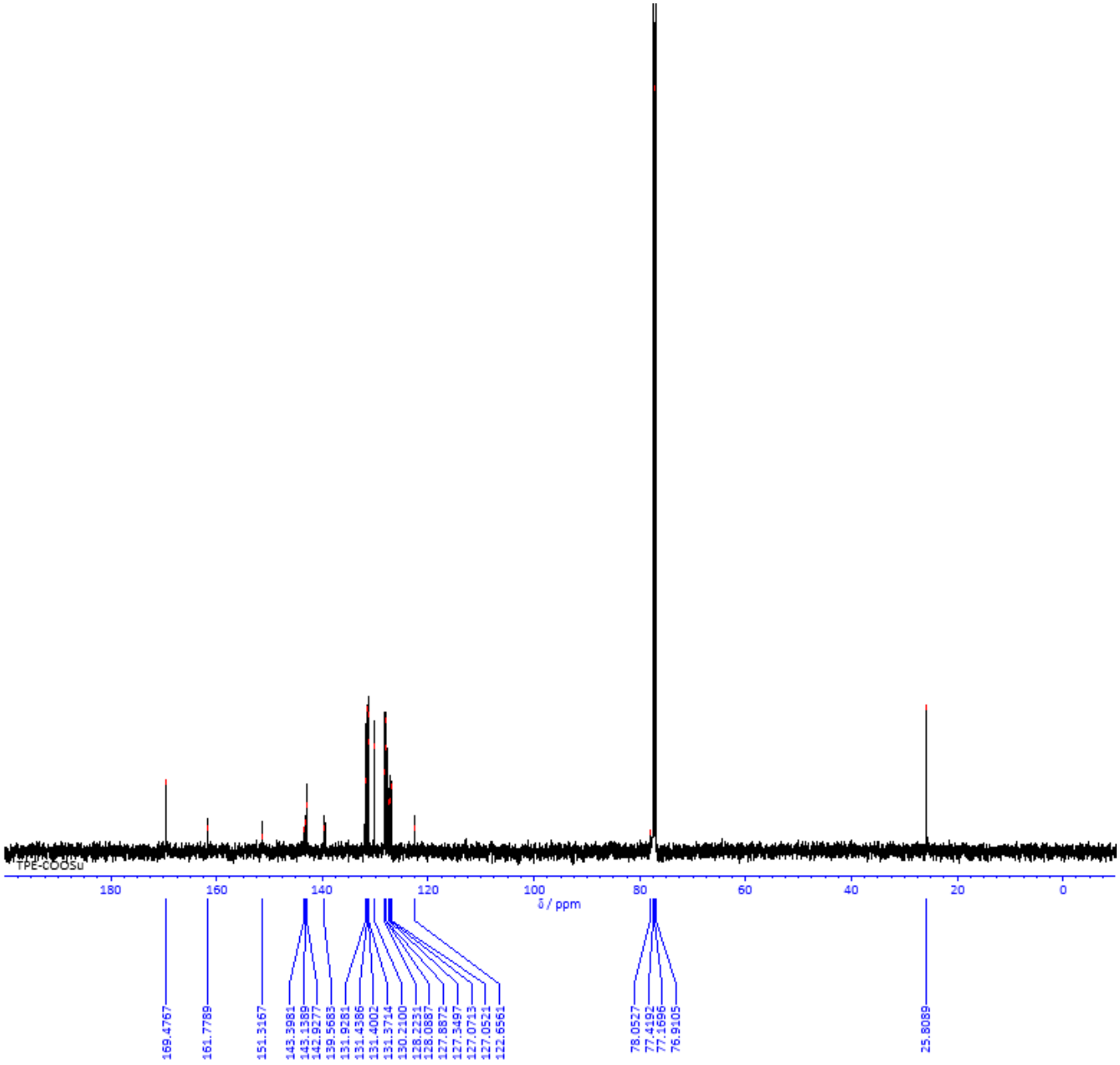

^{1}H NMR spectrum ($CDCl_3$) of compound **S7**

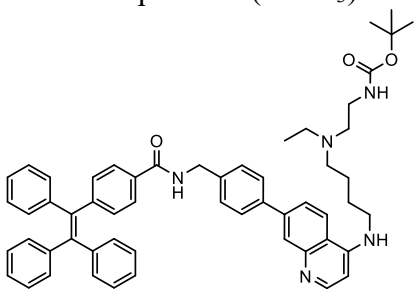

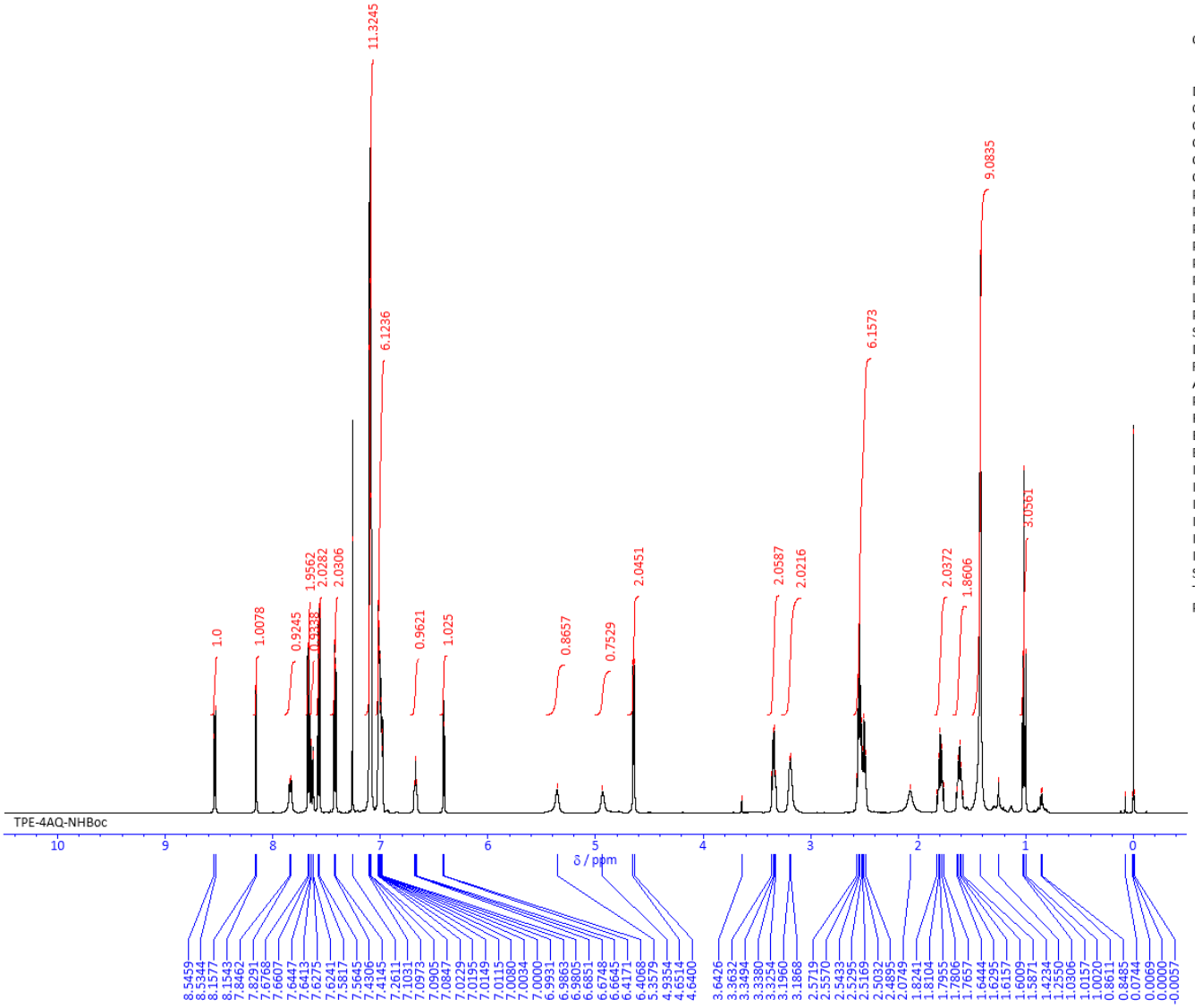

^{13}C NMR spectrum ($CDCl_3$) of compound **S7**

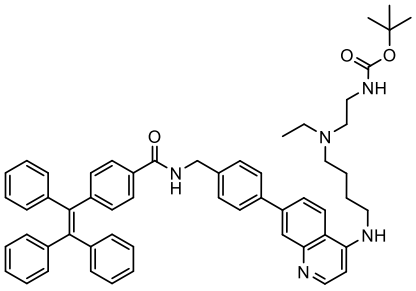

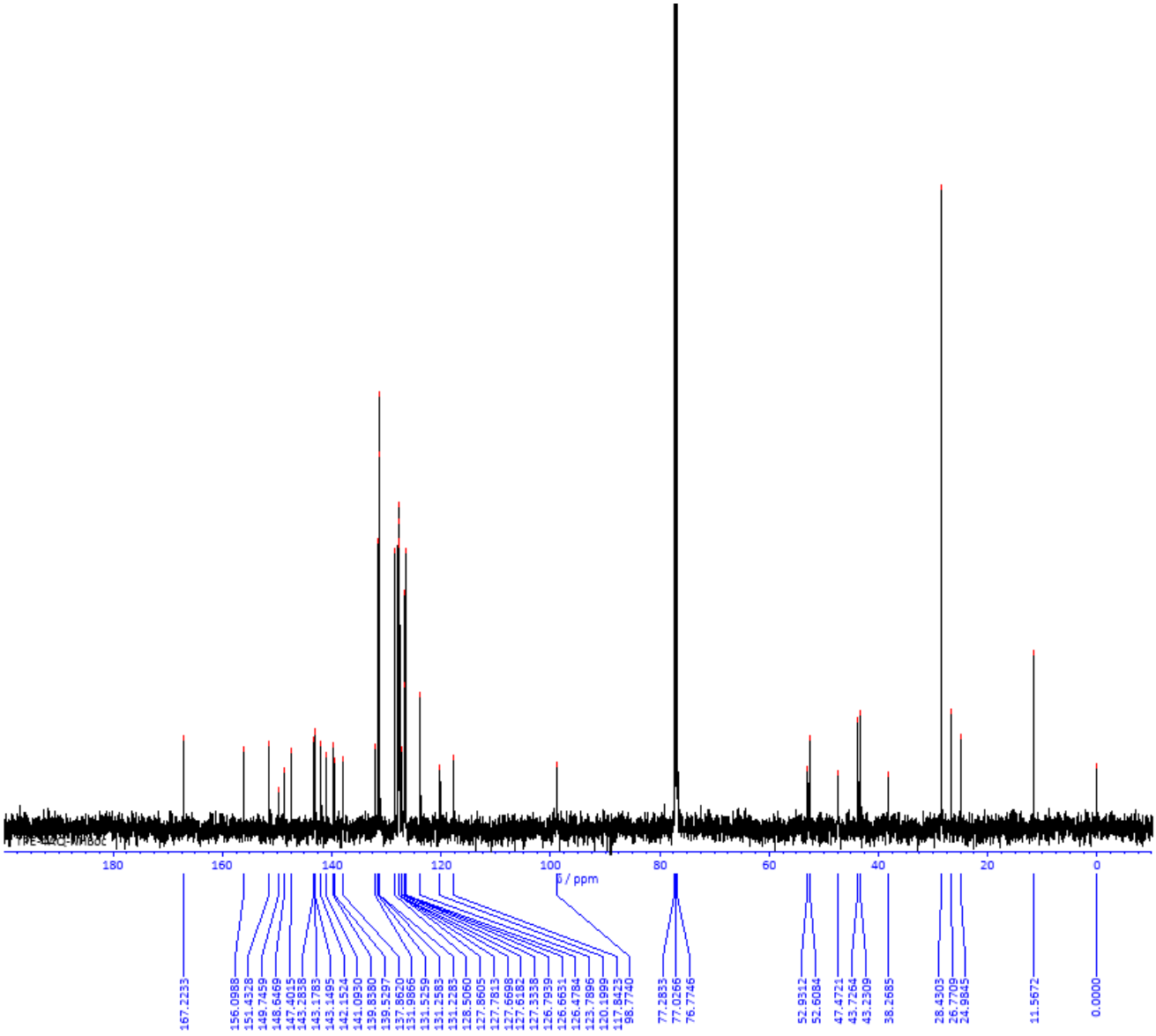

^{1}H NMR spectrum (CD_3OD) of compound **S8**·3TFA

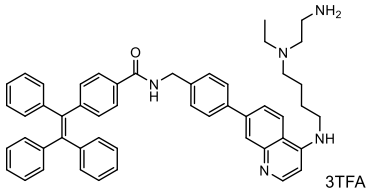

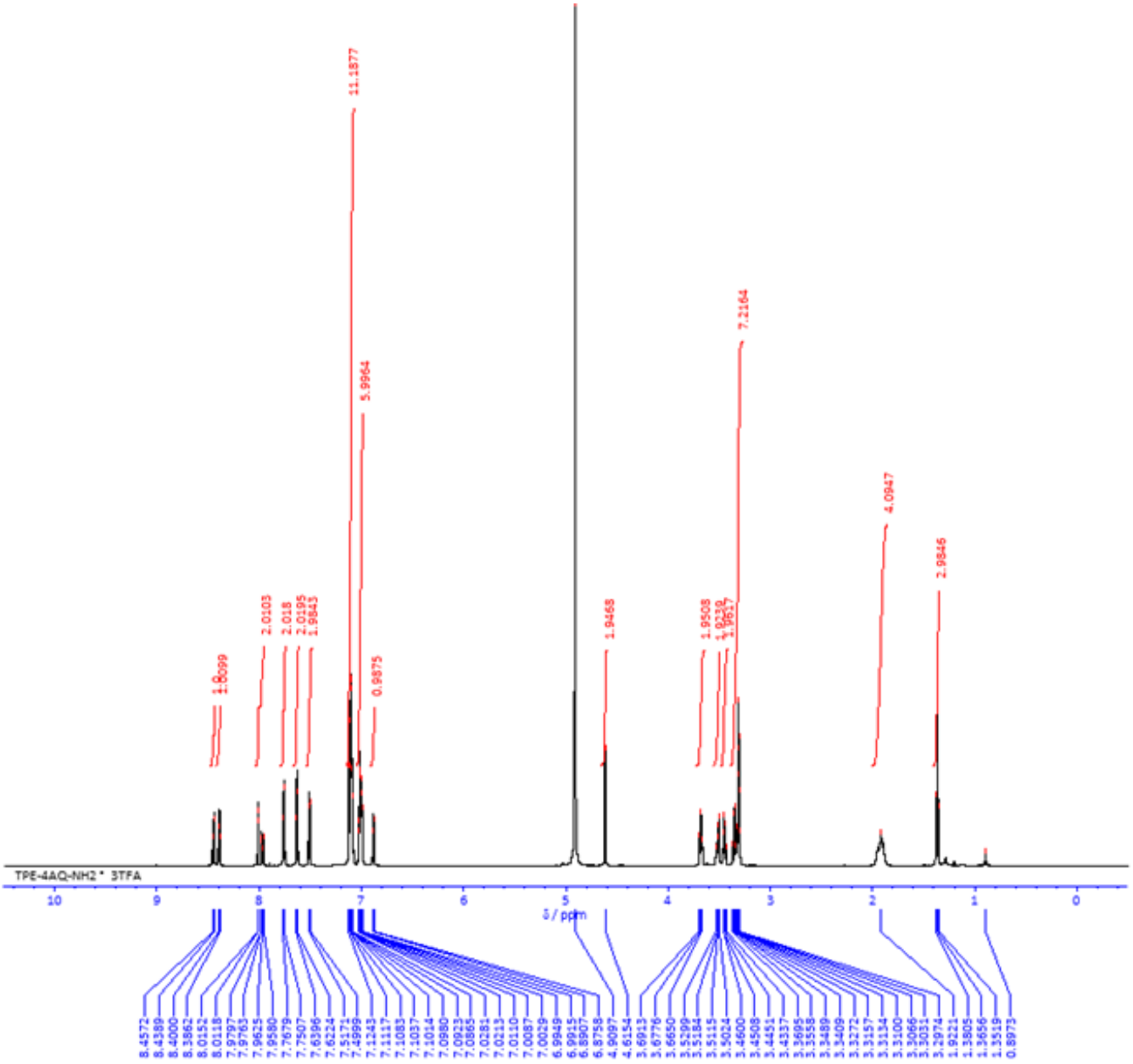

^{13}C NMR spectrum (CD_3OD) of compound **S8**·3TFA

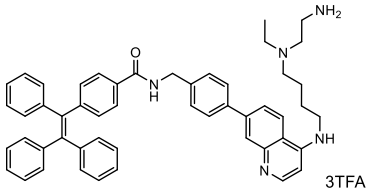

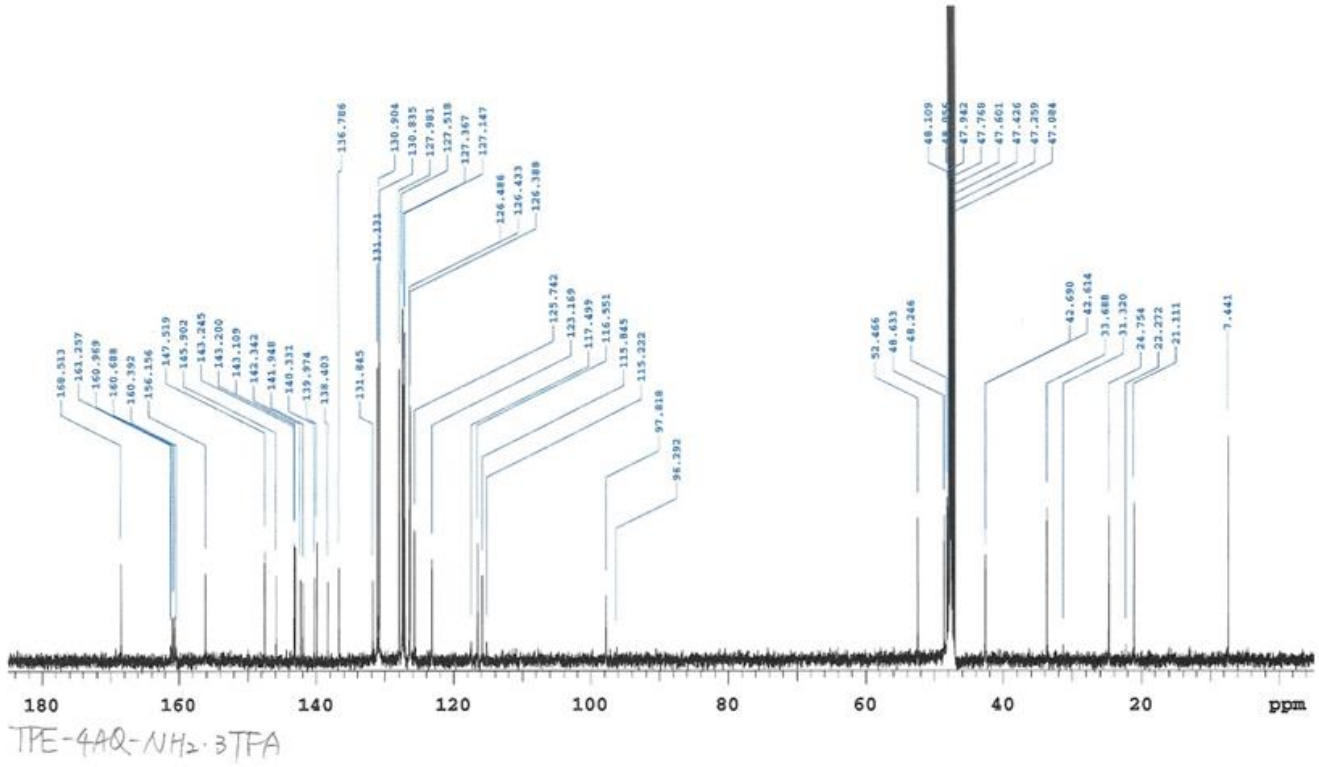

^{1}H NMR spectrum (CD_3OD) of compound **1**·2HCl

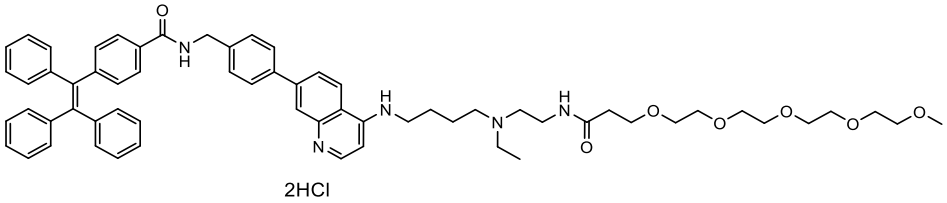

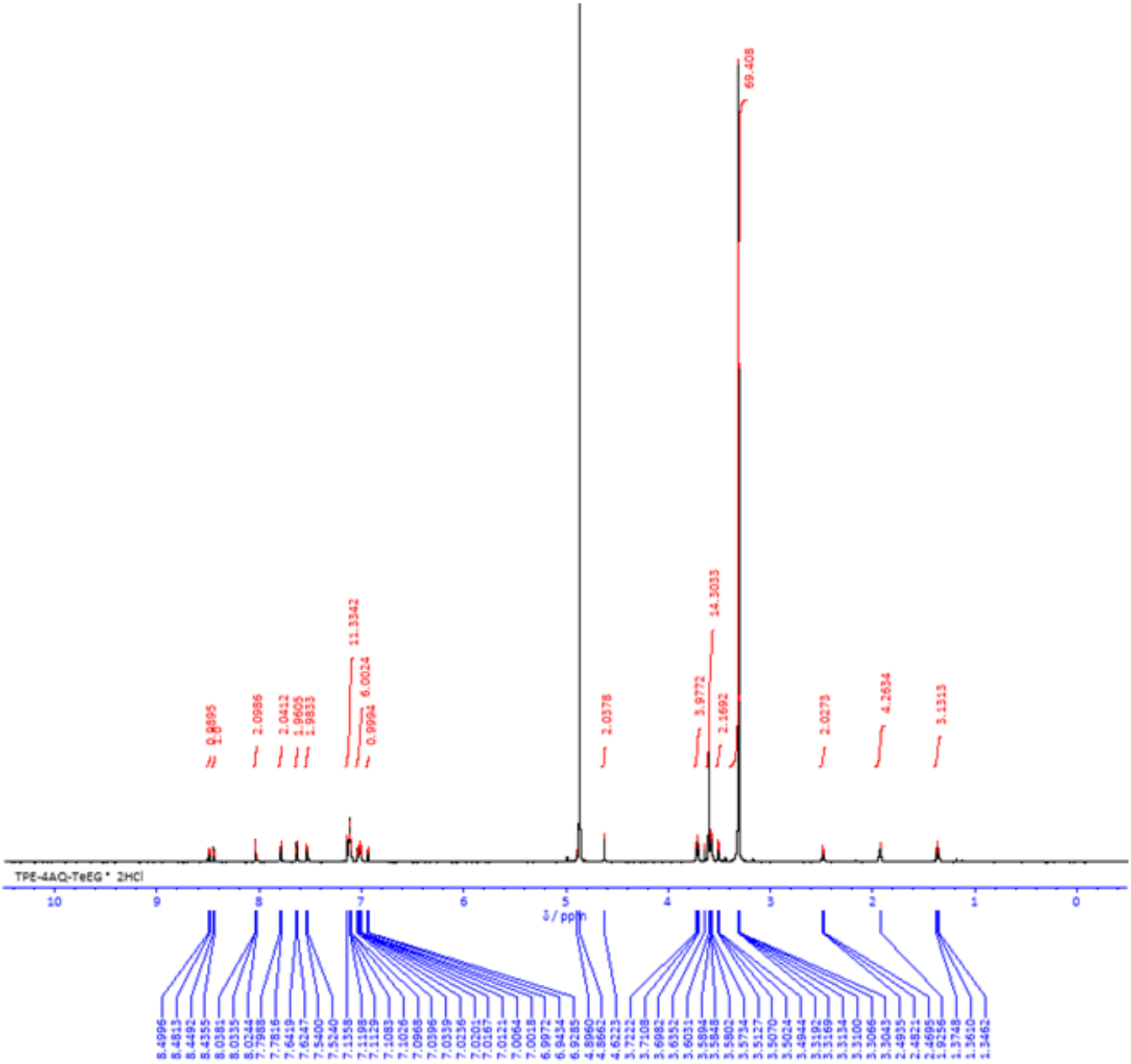

^{13}C NMR spectrum (CD_3OD) of compound **1**·2HCl

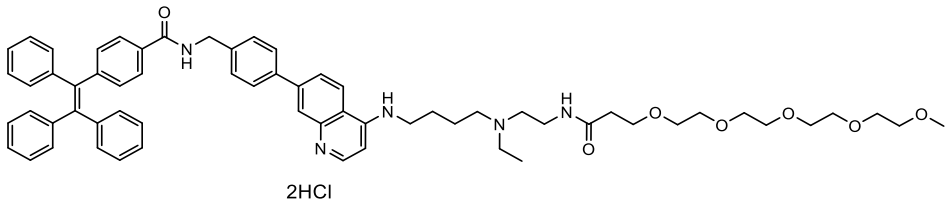

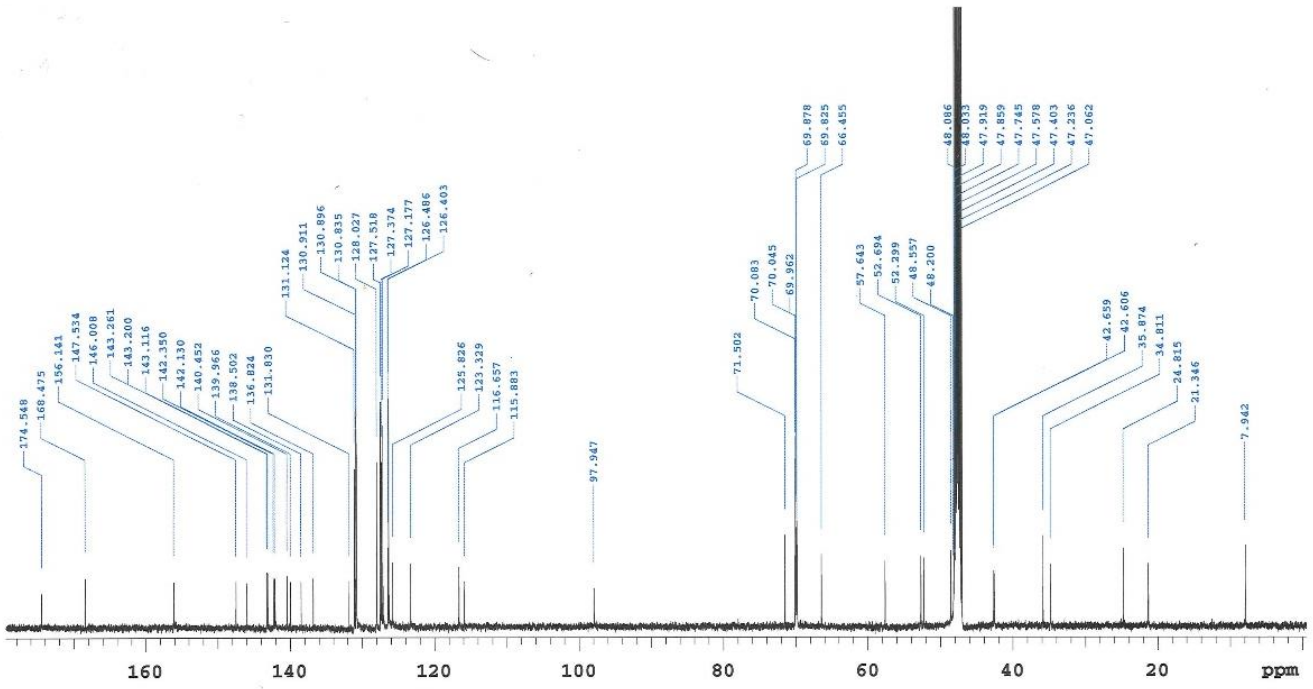

^{1}H NMR spectrum ($CDCl_3$) of compound **S10**

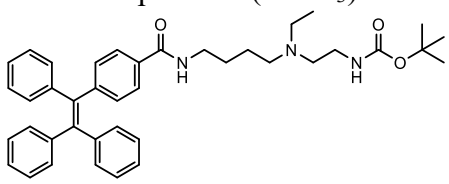

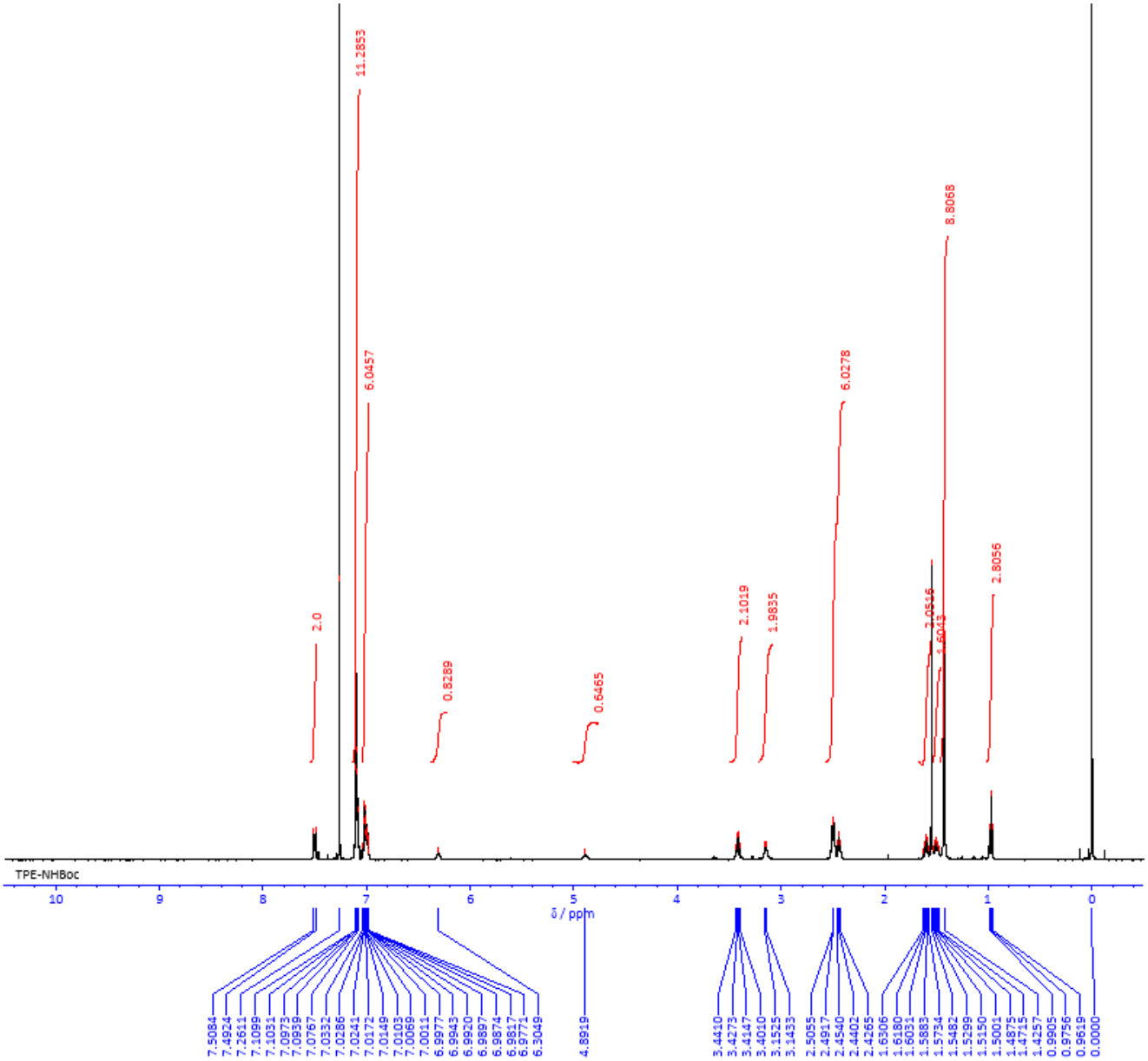

^{13}C NMR spectrum ($CDCl_3$) of compound **S10**

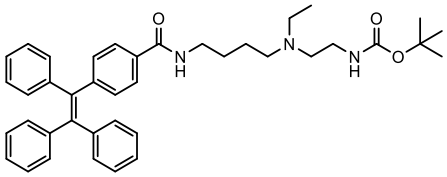

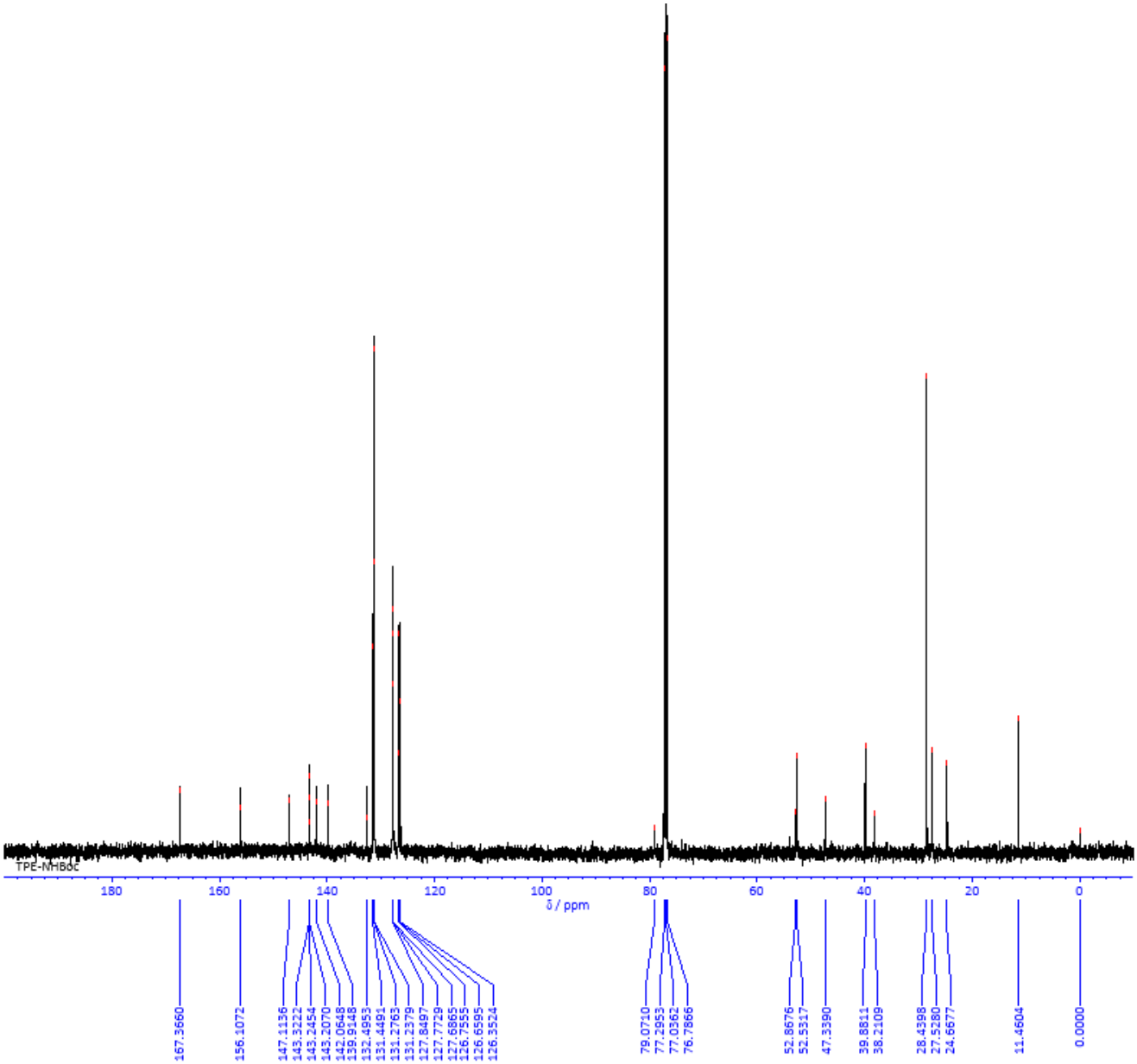

^{1}H NMR spectrum ($CDCl_3$) of compound **S11**

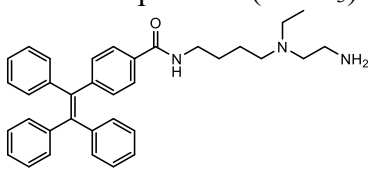

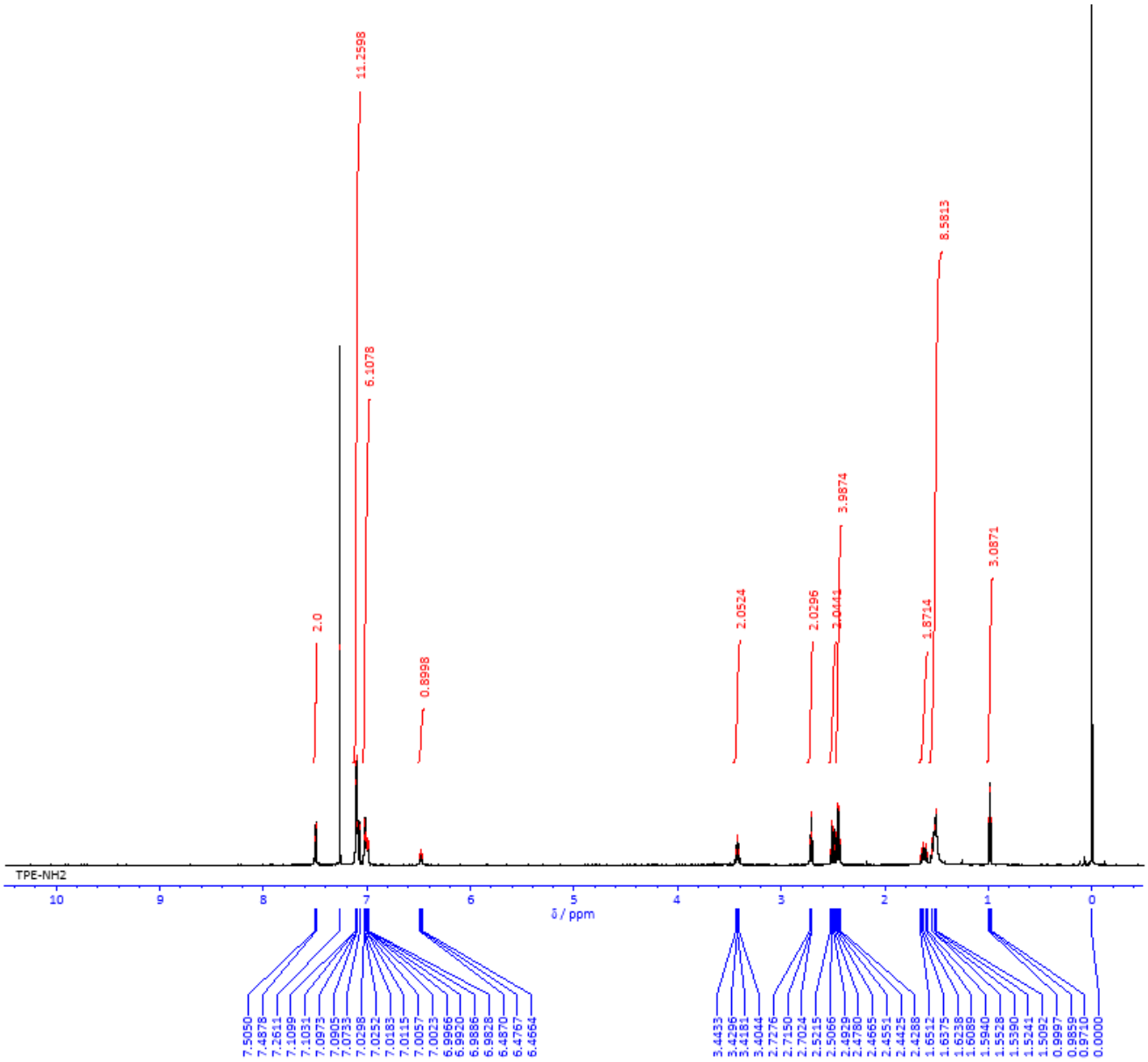

^{13}C NMR spectrum ($CDCl_3$) of compound **S11**

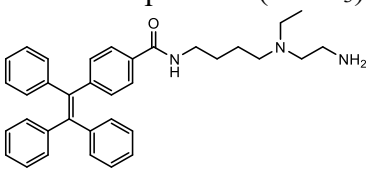

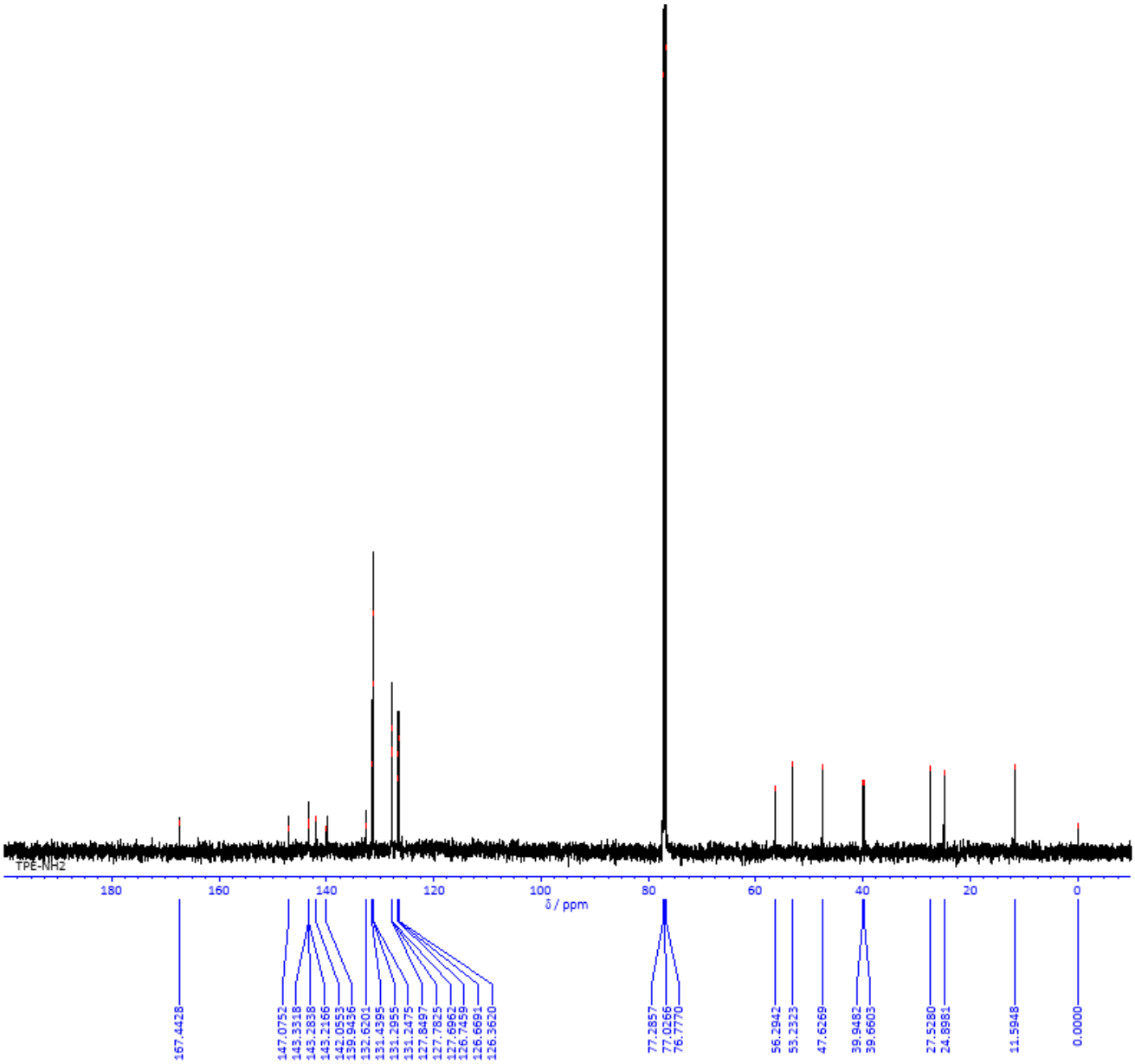

^{1}H NMR spectrum (CD_3OD) of compound **2**·HCl

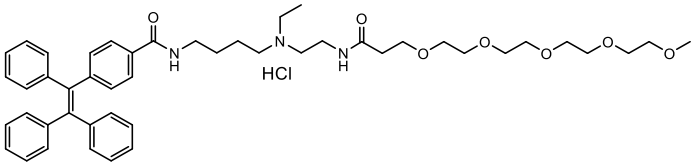

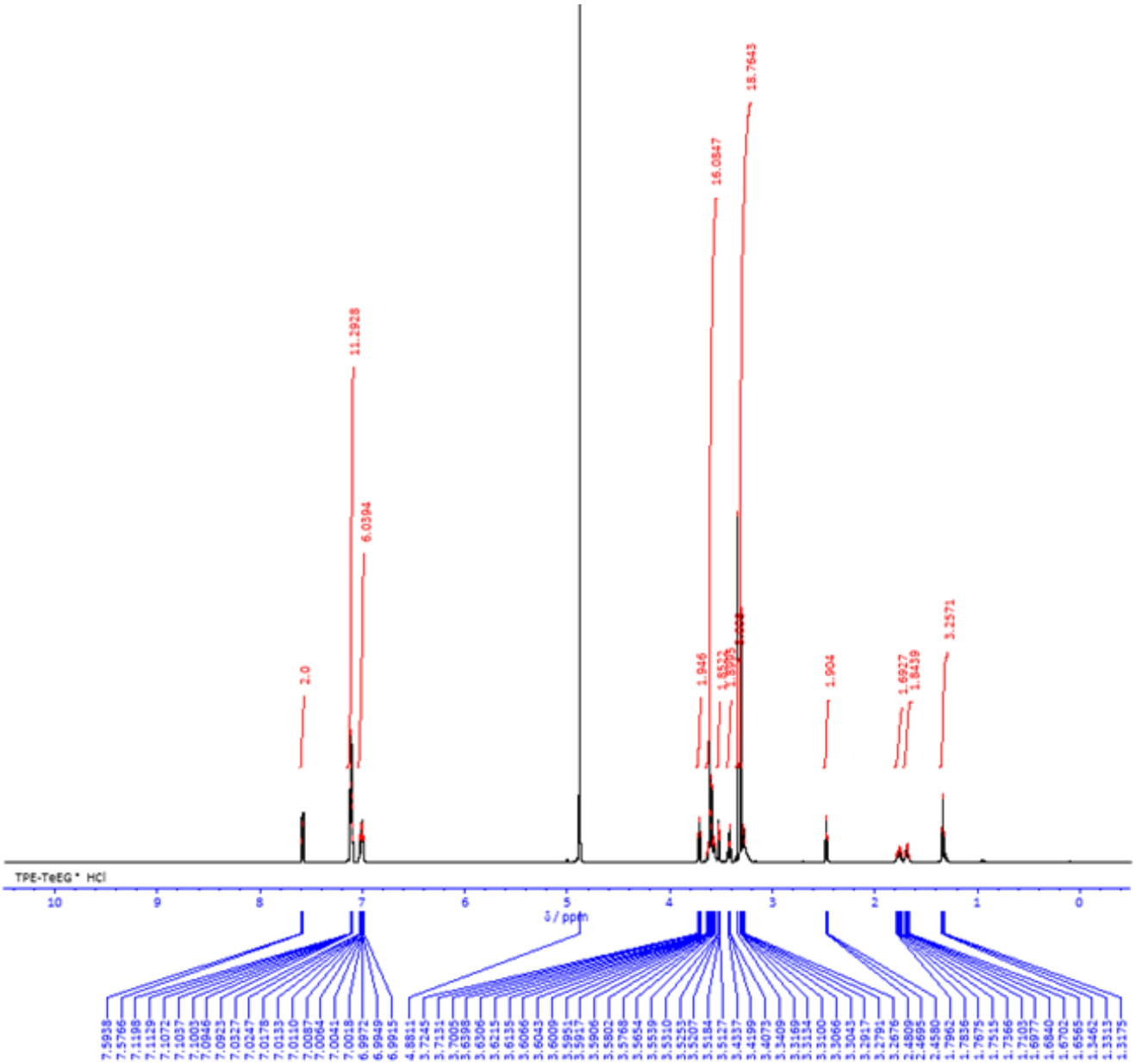

^{13}C NMR spectrum (CD_3OD) of compound **2**·HCl